EFFECTS OF NANOSILICA FILLER ON THE THERMAL AND MECHANICAL PROPERTIES OF AN EPOXY/AMINE RESIN SYSTEM

A Thesis by

Ritu Gurung
M.Sc., Tribhuvan University, Nepal 2005

Submitted to the Department of Chemistry
and the faculty of the Graduate School of
Wichita State University
in partial fulfillment of
the requirements for the degree of
Masters of Science

December 2011

EFFECTS OF NANOSILICA FILLER ON THERMAL AND MECHANICAL PROPERTIES OF AN EPOXY/AMINE RESIN SYSTEM

The following faculty members have examined the final copy of this thesis for form and content, and recommended that it be accepted in partial fulfillment of the requirement for the degree of Master of Science with a major in Chemistry.

_____

Late William T. K. Stevenson, Advisor

_____

David M. Eichhorn, Committee chair

_____

William C. Groutas, Committee member

_____

Dennis H. Burns, Committee member

_____

Suresh (Raju) Keshavanarayana, Committee member

ACKNOWLEDGEMENTS

I would like to thank my late advisor, Dr. William T. K. Stevenson for giving me the chance to work on a very interesting project. He had given me the freedom to explore on my own but his brilliant ideas and guidance never left me adrift. I am very grateful to my committee chair, Dr. David M. Eichhorn, who helped me academically and emotionally through the rough road to finish this thesis. I would like to show my gratitude to my committee members, Dr. William C. Groutas, Dr. Dennis H. Burns and Dr. Suresh Keshavanarayana who shared their knowledge and imparted significant assistance in finishing my research. I also thank the faculty and staff of the Chemistry Department at WSU for their guidance and support.

I am indebted to Ms. Archana Mishra and Mr. Navaneetha Krishnan Subbaiyan for their help in completing my thesis. I also would like to acknowledge Deepee, Swasti, Sanush, Nisha, Krishna and Surendra for their encouragement in persuing my master's degree.

I would like to express thanks to my lab-mates Rama, Janet, Anusha, Irish and Daniel for their assistance and friendship. I am also thankful to Dr. Kevin Langenwalter for proofreading my thesis.

I especially would like to thank my husband Yam Thapa for his endless love, patience and support. I also like to express my deep love to our precious daughter Yasaswi, for bringing happiness and excitement to my life.

Finally and most importantly, I owe my deepest gratitude to my parents, Mr. Tula Ram Gurung and Mrs. Mira Gurung and my siblings (Ishu, Anup, Amith and Nitu). Their support has been unconditional all these years; they have given up many things for me to be at WSU; they have cherished with me every great moment and supported me whenever I needed it.

ABSTRACT

The cure kinetics of an epoxy resin with surface modified silica filler (Nanopox F 400 resin) and without silica filler (DGEBA resin), cured with an amine curing agent, DDS at an N-H/epoxy molar ratio of 1.1:1 was studied by Dynamic Scanning Calorimetry in two basic modes; Dynamic temperature scanning and Isothermal temperature scanning. Dynamic temperature scanning analysis suggests that the addition of surface modified silica nanoparticles in the epoxy resin increases the rate of reaction by acting as a catalyst. The hydroxyl groups in silica nanoparticles catalyze the cure reaction by shifting the exothermic peak towards the lower temperature. Under dynamic temperature scanning, the glass transition temperature (T_g) was lower for the Nanopox F 400 system than the unfilled control system. The glass transition temperature and changes in the T_g found in DSC analysis were in line with TMA analysis and DMA analysis. Isothermal scanning analysis shows that the control system follows the Kamal autocatalytic model whereas Nanopox F 400 system follows the modified Kamal autocatalytic model. The model parameters were determined by a nonlinear multiple regression method.

The mechanical properties of Nanopox F 400 resin and control resin both cured with DDS at an N-H/epoxy molar ratio of 1.1:1 were examined by tensile testing. The tensile results showed increase in modulus and decrease in tensile strength for 40 wt. % surface modified Nanopox F 400 system compared to the control system. The effect of processing technique and silica content on the tensile properties of silica reinforced epoxy resin was further analyzed. The structure of Nanopox F 400 resin was characterized by FT-IR spectroscopy and ^{1}H NMR spectroscopy.

TABLE OF CONTENTS

TABLE OF CONTENTS (continued)

TABLE OF CONTENTS (continued)

LIST OF TABLES

Table Page

LIST OF TABLES (continued)

Table Page

LIST OF FIGURES

Figure Page

LIST OF FIGURES (continued)

Figure Page

LIST OF FIGURES (continued)

Figure Page

LIST OF FIGURES (continued)

Figure Page

LIST OF FIGURES (continued)

Figure Page

CHAPTER 1

INTRODUCTION

1.1 Introduction

Epoxy resin is one of the most widely used thermosetting resins. The epoxy group is a functional group which consists of an oxygen atom bonded to two carbon atoms in a three membered ring. Epoxy resins display low shrinkage on cure, good mechanical properties, and good chemical and electrical resistance; and are thus used in coatings, adhesives, castings and composite applications[1]. The major drawback in the use of epoxy resins is brittleness upon curing. Therefore, an improvement in toughness is desired. Epoxies are commonly modified by the inclusion of inorganic particulate fillers, such as silica, alumina, mica or talc [2-5]. These fillers are added to epoxy resins to improve resin stiffness, tensile strength and fracture toughness [6]. Zheng *et al*[7], for example, showed that the addition of 3 wt.% of silica nanoparticles increases tensile strength up to 115% and impact strength by 56%. Rosso *et al*[8], found that the addition of 5 vol.% of silica nanoparticles increases the tensile modulus by 20% and fracture toughness by 70%. A vast amount of experimentation has been performed to toughen the epoxy resin in recent years [6-13].

A Nanocomposite can contain an organic polymer base with inorganic filler, where the inorganic filler is nanosized. The organic polymer base is the continuous phase and cures around the inorganic filler [14].

The advantages of these composites are that they combine both the best features of the inorganic material (e.g., rigidity, thermal stability) and the organic polymer (e.g., flexibility,

ductility and processabilty). Unfortunately, the incorporation of inorganic fillers typically increases the pre cure viscosity which reduces the ease of processing [13-16].

The Epoxy/silica system is one of the most widely used organic-inorganic hybrid materials [7, 8, 10-12, 14, 17, 18]. Silica reinforcement increases mechanical properties such as modulus, tensile strength and fracture toughness of an epoxy resin. According to Hajji *et al*[19], nanocomposites can be prepared by various synthetic routes. The organic component can be introduced as:

i) a precursor, which can be a monomer or an oligomer

ii) a preformed linear polymer (in molten, solution, or emulsion states)

iii) a polymer network, physically (e.g., a semi crystalline linear polymer) or chemically (e.g., thermosets, elastomers) cross-linked.

The inorganic component can be introduced as:

i) a precursor (e.g. Tetra-ethyl-ortho-silicate or TEOS)

ii) Preformed nanoparticles (e.g. silica nanopowder).

There are three general methods to prepare polymer/silica nanocomposites according to the starting material and processing techniques:

i) Blending

ii) Sol-gel processes

iii) In-situ polymerization.

Blending:

The blending process is generally a simple mixing of silica nanoparticles into the polymer.

A sol-gel processes:

A sol-gel process is a novel reinforcement technique, which can generate reinforcing particles within the polymer matrix. The sol-gel reaction is carried out in the presence of organic molecules which are typically polymeric and contain functional groups to improve their bonding to the ceramic like phase. The sol-gel process can be viewed as a two-step network forming process, the first being the hydrolysis of a metal alkoxide and second consisting of a polycondensation reaction.

The sol-gel reaction of alkoxysilane can be described as follows:

Hydrolysis:

R= alkyl groups

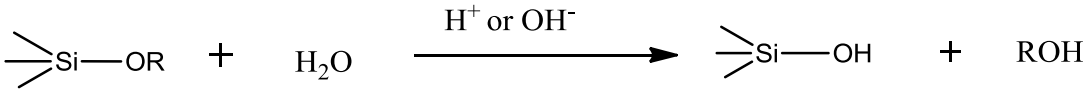

Polycondensation:

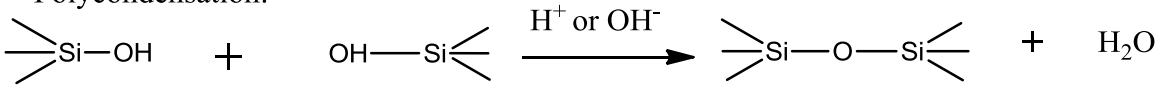

and/or

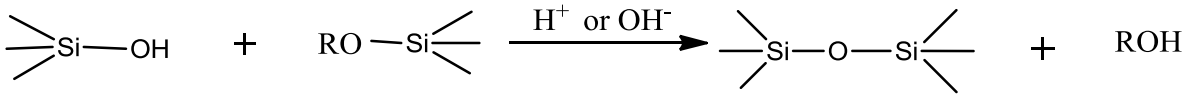

When the sol-gel reactions are complete, silica is obtained as summarized below.

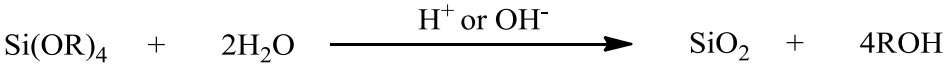

In-situ polymerization:

In the case of in-situ polymerization, nanosilica is dispersed in the monomers and polymerization of the monomers commences.

Structure of Silica:

Nanosilica consists of a three dimensional SiO_2 based cross-linked structure with –SiOH surface groups which are formed in a significant concentration during manufacture and which play a crucial role in forming hydrogen bonds with other particles leading to aggregation, as shown in Figure 1.1[20, 21]. These hydrogen bonds, though weak, hold individual silica particles together and the aggregates remain intact even under the best mixing conditions, unless stronger filler polymer interactions are present. Aggregation is to be avoided wherever possible.

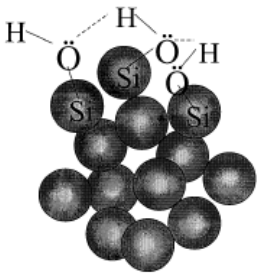

Figure 1.1. Schematic of aggregate formation between adjacent silica nanoparticles through hydrogen bonding among the silanol groups.

The differences in the properties of organic polymer and inorganic silica filler can often lead to aggregation of the filler. Therefore, the interfacial interactions between nanosilica and the epoxy resin, and the degree of dispersion of the nanometer-sized particles in the epoxy resin are the most decisive factors affecting the properties of the resulting materials. The incorporation of untreated silica nanoparticles into the epoxy matrix improves the polymer material but is not optimal due to the formation of aggregates during the curing process. A variety of methods have been used to enhance the compatibility between the polymer and nanosilica. The most frequently used method is to modify the surface of the silica nanoparticles, which can also improve the dispersion of nanosilica in the polymer matrix.

1.2. Surface modification of silica nanoparticles by a coupling agent:

The surface modification of silica nanoparticles by a coupling agent is the most frequently used method to enhance the compatibility between polymer (hydrophobic) and nanosilica filler (hydrophilic) and, therefore, to improve the dispersion of nanosilica in the polymer[13, 17, 22, 23].

Silane coupling agents are the most used type of modifying agent. They are generally represented by $RSiX_3$ as shown in Figure 1.2, where 'X' is a chloro, ethoxy or methoxy groups and 'R' is vinyl-, amino-, epoxy-, etc. An example of silane coupling agent is, 3-amino propyl triethoxy Silane (APTES) as shown in Figure 1. 3. The functional group 'X' reacts with hydroxyl groups on the SiO_2 surface and the 'R' group reacts with the polymer forming the covalent bond [18, 21] as shown in Figure 1.4.

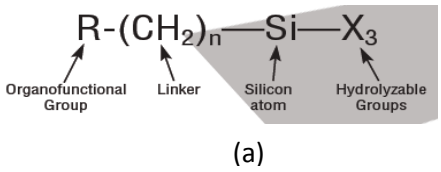

Figure 1.2. General formula of Silane coupling agent[24]

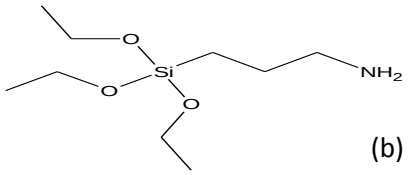

Figure 1.3. Structure of APTES.

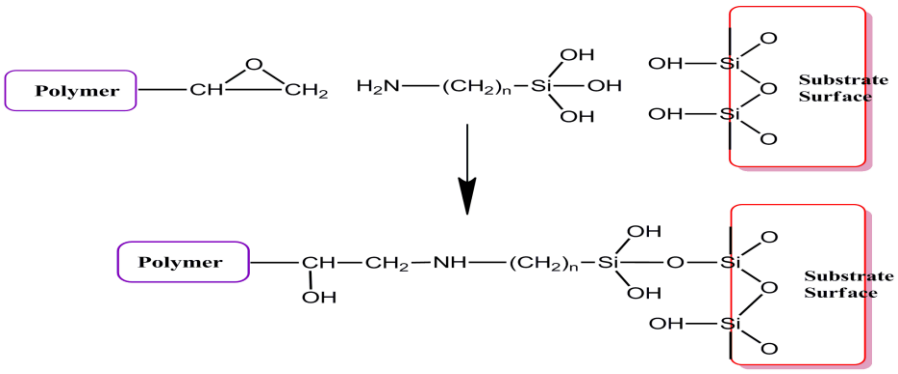

Figure 1.4.Linkers for surface attachment to inorganic particles and polymer[24].

With these modifications, the organic and inorganic networks are compatibilized. Such inter-linked networks are widely reported to offer improved mechanical properties [9, 12, 13, 15, 25, 26].

1.3. Reaction of Epoxy resin with Amine curative

The kinetics and curing mechanism of the epoxy- amine reaction has been analyzed extensively [27-33]. However, there is still a lack of complete understanding of the epoxy-amine reaction mechanism carried out in the presence of an inorganic filler (e.g. silica). Although, cured epoxy nanocomposites possess improved properties, the mechanisms responsible for these dramatic changes in properties are still under investigation[27] . Different factors may influence the curing process such as the temperature profile, time, epoxy/hardener ratio and the surface of the nanoparticles [34, 35].

The basic chemistry employed to cure epoxy resin is through the epoxide ring. The resin is cured or cross-linked by chemical reaction into a three-dimensional network by the use of a crosslinking agent or curing agent. Crosslinking agents function by reacting with, or causing the reaction of epoxide or hydroxyl groups in the epoxy resin. Curing occurs by a number of routes: for example, by homopolymerization, the reaction of an epoxy group with other epoxy groups or by the reaction of the epoxy and/or hydroxyl functionality with a reactive intermediate: or copolymerization with a curing agent. There are three major chemical types of curing agents employed in structural applications using epoxy resins; amines, acid anhydrides, and Lewis acids and bases. Among them, primary and secondary amines are the most widely used curing agents for engineering epoxy resins. Amine based curing agents were used in this study.

Ghaemy *et al*[36], proposed a reaction mechanism profile for a polymerizing silica/epoxy/amine system as summarized in Figure 1.5. He suggested that the hydroxyl groups on silica nanoparticles act as a catalyst for the reaction between the epoxide group and the primary or secondary amine groups. As would be expected, the presence of silica nanoparticles causes a decrease in the activation energy of cure and increases the rate constants for the cure reactions [36, 37]. Ghaemy's theory of lowered activation energy in the presence of inorganic nanoparticles is further supported by the work of Altmann *et al*[38] and Harsh *et al*[37].

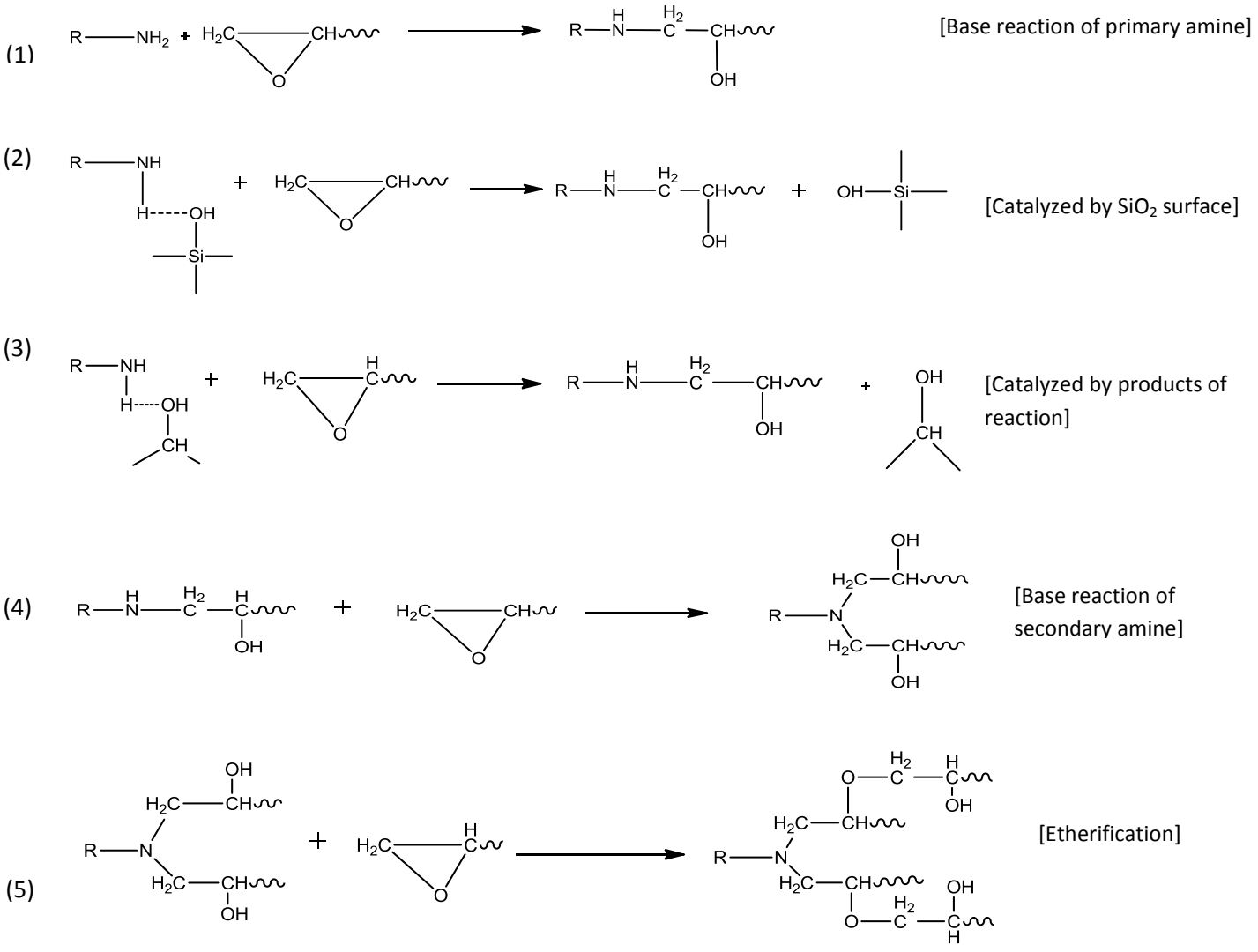

Figure 1.5. Major chemical reactions occurring in the polymerization of silica/epoxy/amines.

Reactions can be non-catalytic for example (1) and (4) or catalytic, reactions (2) and (3). Reactions between primary amines with epoxide groups yield secondary amines and hydroxyl groups, which, in turn yield tertiary amines and hydroxyl groups (similarly, for secondary amines and epoxies). The reaction between amine and epoxide groups can be catalyzed by hydroxyl groups present on the surface of nanosilica particles or produced during the epoxide ring opening reaction. Etherification reactions take place between the hydroxyl groups formed in (1) and (4) and any excess epoxy groups not consumed by reaction with amines [36, 37, 39].

The magnitudes of the rate constants for primary and secondary reactions of epoxies with amines are different. The ratio of the rate constants i.e., primary to secondary amines, has a strong effect on the cure process. There is no good agreement from the literature on values of the two rate constants except that k_1 (for reaction of epoxy with a primary amine) is greater than k_2 (for the reaction of epoxy with a secondary amine) [28].

The etherification reaction is known to occur at higher temperatures and advanced degrees of cure[40]. It may be considered insignificant at the early stages of the reaction and overall ,especially if the resin is formulated from either a stoichiometrically balanced mixture or with a small excess of amine. Most of the models proposed for the cure kinetics of epoxy resins disregard the etherification reaction and it seems to work well in most instances. The etherification reaction is shown to be significant when curing is done at higher temperatures in the presence of excess epoxy and especially at later stages of the curing process when most of the amines have reacted[41, 42].

1.4 Differential Scanning Calorimetry (DSC)

DSC is a thermoanalytical technique in which the difference in the amount of heat required to increase the temperature of a sample and reference is measured as a function of temperature. As it measures the heat flow to or from the reacting system, it is a very convenient tool to study the overall epoxy-amine cure reaction. The major advantages of using DSC are the small sample size and ease of data gathering. DSC also can be used to identify phase transitions such as the glass transition temperature, which can be correlated to the state of cure of the resin. Both the sample and reference pan are maintained at the same temperature throughout the experiment and increased at a constant rate. DSC can be operated in two basic modes (1) dynamic temperature scanning (2) isothermal temperature scanning.

The basic principle underlying DSC is that when the sample undergoes a physical transformation such as a phase transition, more or less heat will need to flow to it than to the reference pan to maintain both at the same temperature. Whether less or more heat must flow to the sample depends on whether the process is exothermic or endothermic. The cure of epoxy groups with amines is an exothermic process. A typical output from a DSC run in dynamic temperature scanning mode is shown in Figure 1.6[43]. The amount of heat associated with the transition (absorbed or released) can be determined by calibrating the instrument then by integrating the area between the curve and baseline. The total heat, Q_{total}, associated with the reaction or transition is equal to the area in the DSC trace as shown in equation (1)

$$Q_{total} = \int_{t_0}^{t_f} \left(\frac{dq}{dt} \right) dt \qquad (1)$$

Where (*dq/dt*) is the heat flow and t_f is the time at which the DSC signal goes back to the baseline. The degree of cure, α_t, at an intermediate time t can be calculated by integrating the heat flow up to that time t i.e., A with the following equation (2).

$$degree\ of\ cure,\ \alpha_t = \frac{\int_{t_0}^{t}\left(\frac{dq}{dt}\right)dt}{Q_{total}} = \frac{area\ A}{area\ A + area\ B} \qquad (2)$$

These data can be used to calculate the rate of cure by differentiating the normalized degree of cure with respect to time (dα/dt). Kinetic parameters are obtained when mathematical models are fitted into the experimental data generated from a DSC run.

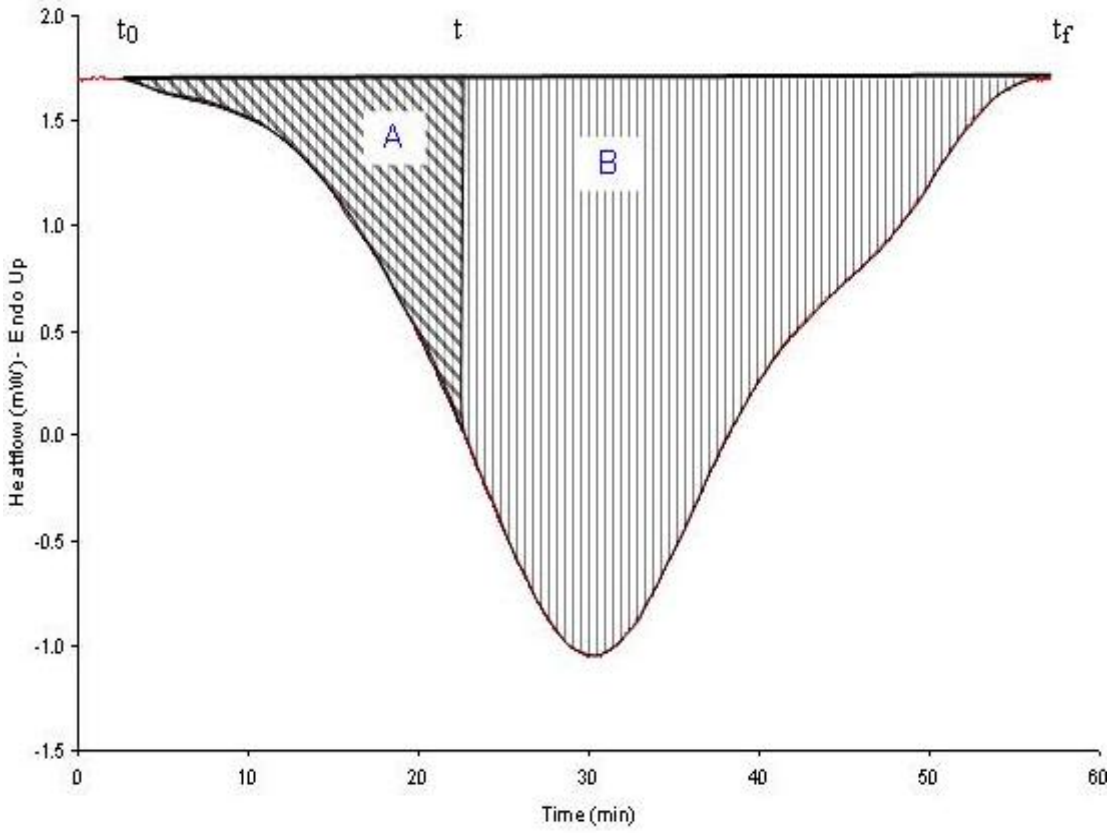

Figure 1.6. A typical DSC output in dynamic temperature scanning mode. The shaded area represents the amount of heat associated with the reaction or transition[44].

1.5. Cure kinetics

Analytical models have been developed in recent years to interpret the curing of organic matrix composites. Many studies have been conducted on the kinetics of cure reactions, and a variety of kinetic models have been used to relate the rate of chemical reactions to the time, temperature and extent of cure. A successful model contains knowledge of thermal, chemical, and physical properties of the material which affect the curing process. The most important aspect of the model is an accurate description of the cure kinetics [45-50].

In general, kinetic models fall into two main categories: 1) a phenomenological model; and 2) a mechanistic model. A phenomenological model [50-56] captures the main features of the reaction kinetics ignoring the details of how individual species react with each other. A mechanistic model [28, 32, 33, 40, 42, 53] is based on a detailed analysis of the chemical reactions that are involved in the cure reaction. Hence, mechanistic models are better for prediction and interpretation of the reaction. However, due to the complexity of thermosetting reactions, phenomenological models are preferred when studying cure processes. With better sensitivity and design, DSC has often been used to formulate and check theoretical and empirical kinetic models, and to calculate parameters included in the model.

The general formula for the reaction rate according to a phenomenological model is,

$$\text{rate of reaction} = \frac{d\alpha}{dt} = k f(\alpha) \qquad (3)$$

Where α is the fractional conversion of the reactive group (degree of cure, from 0 to 1), t is the reaction time, k is a time-dependent reaction rate constant and $f(\alpha)$ is some function of the degree of cure.

The rate constant, k, is usually considered to have an Arrhenius type temperature dependence:

$$\mathbf{k} = \mathbf{A}\mathbf{e}^{\left(\frac{-\mathbf{E}_a}{\mathbf{RT}}\right)} \qquad (4)$$

Where *A* is the frequency factor, *R* is the universal gas constant (8.314 J/mol.K), $E_{a.}$ is the activation energy of reaction and *T* is the absolute temperature in Kelvin.

The rate of reaction usually decreases as the chemical reaction progresses and eventually becomes zero, as the reaction comes near to completion, or if it becomes impossible for the reacting groups to find each other (vitrification). The polymerization of epoxy with amines exhibits autocatalysis at the beginning of the reaction, as hydroxyl groups so formed catalyze succeeding reactions. In the absence of vitrification, the degree of cure will be equal to unity at the completion of the reaction so the functional form of $f(\alpha)$ can be written as[46] ,

$$f(\alpha) = g(\alpha)(1-\alpha)^n \qquad (5)$$

Where $g(\alpha)$ is an experimentally derived function and *n* is the kinetic exponent. Assuming $g(\alpha)$ to be equal to 1, equation (5) becomes the simplest kinetic model (*an n^{th} order kinetic model*). This has been used to model the cure of thermoset resins [46, 54].

An n^{th} *model* cannot describe the progress of the entire reaction because several simultaneous reactions occur during the cure process and the maximum rate of reaction occurs later in the reaction rather than at the very beginning of the reaction. Thus, the n^{th} *model* fails to account for autocatalysis which is a very significant phenomenon in an epoxy-amine cure. If the resin vitrifies before the completion of the reaction, the maximum achievable degree of cure (α_f) will be less than unity. Equation (5) thus becomes;

$$f(\alpha) = g(\alpha)(\alpha_f - \alpha)^n \qquad (6)$$

α = Degree of cure

α_f = Maximum achievable degree of cure

Different expressions have been used by various investigators to describe the cure kinetics of epoxy-amine systems. For example, Horie *et al*[57] in 1970 proposed an expression to model the cure kinetics by assuming that the secondary amine formed in the reaction shows the same degree of reactivity toward the epoxy group as the primary amine initially present. The expression then becomes,

$$\frac{d\alpha}{dt} = (k_1 + k_2\alpha)(1-\alpha)(B-\alpha) \qquad (7)$$

Where k_1 is the rate constant for the reaction catalyzed by groups initially present in the resin and k_2 is the rate constant for the reaction as catalyzed by newly formed groups and which represents the influence of the reaction products on the rate of reaction. *B* is the initial ratio of the number of amine N-H bonds to the number of epoxide groups (a measure of stoichiometric balance). Equation 7 was used by Loos *et al*[49] to describe the cure kinetics of Hercules 3501-6 epoxy resin.

Equation 7 takes into account the autocatalytic nature of the epoxy amine reaction but it does not take into account the etherification reaction which is possible when insufficient amine curative is added. In order to model cases where the Horie equation is inadequate, Kamal and co-workers developed the following semi-empirical model,

$$\frac{d\alpha}{dt} = k\alpha^m(\alpha_f - \alpha)^n \qquad (8)$$

According to this model, equation (8), the rate of reaction is zero at the start of the reaction, when $\alpha^m \rightarrow 0$, increases up to maximum value and then decreases as the reaction comes to

completion or vitrification. Realistically, the initial rate of reaction may not be zero as the reactants can also be converted into products by catalysis using functional groups initially present in the resin. Kamal *et al* [55], developed the following more general model

$$\frac{d\alpha}{dt} = \left(k_1 + k_2\alpha^m\right)(\alpha_f - \alpha)^n \qquad (9)$$

Where α_f is the maximum degree of cure at the isothermal cure temperature with $0 < \alpha_f \leq 1$.

k_1 describes the rate constant of the uncatalyzed reaction of order *n.*

k_2 is the rate constant of the autocatalysed reaction of order *m*.

The introduction of the variable exponents *m* and *n* usually makes it possible to obtain a good fit to experimental data, and this application has found wide successful application for both epoxy and polyester systems[27, 37, 46, 47, 49, 52]

Various groups have used different forms of the Kamal model to describe the cure kinetics of epoxy resins. In our research, the Kamal model 1 (equation 9) appears to describe the cure kinetics of the neat epoxy-amine resin system (control resin). However, cure of the silica/epoxy/amine was completely different. When experimental data are fitted to the Kamal model 1(equation-9) to compute the four parameters, k_1, k_2, m, n by using a non-linear multiple regression method, anomalous results are obtained.

To describe the curing kinetics of silica/epoxy/amine system, a modified Kamal autocatalytic model was used, which is summarized below.

$$\frac{d\alpha}{dt} = k\alpha^m(1-\alpha)^n \qquad (10)$$

The modified Kamal autocatalytic model was found to describe the cure of silica filler containing resin. Shanyi Du *et al*[58]investigated the cure kinetics of silica/epoxy/amine system cure kinetics and demonstrated that the modified autocatalytic model was able to describe the curing kinetics of silica/epoxy/amine system.

CHAPTER 2

EXPERIMENTAL

2.1 Introduction

The neat epoxy resin used in this research was a standard mid performance Diglycidyl ether of bisphenol-A resin (DGEBA, Figure 2.1) supplied by Aldrich chemical company. Silica containing epoxy resin, Nanopox F 400 resin, was obtained commercially from Nanoresins AG, Germany. Nanopox F 400 resin was prepared by the sol gel method and contains 40 wt. % surface modified silica nanoparticle (average particle size 20 nm) in DGEBA epoxy resin. The influence of silica on the thermal and mechanical properties of the epoxy resin was studied by Dynamic Scanning Calorimetry (DSC), Thermal Mechanical Analysis (TMA), Dynamic Mechanical Analysis (DMA), Tensile Testing and Fracture Toughness testing.

The preparation of Nanopox F 400 resin constituted a "trade secret" that the supplier would not divulge. Hence, we prepared our own silica modified epoxy resin system (hereafter refereed as Homemade resin) by simply blending epoxy resin with silica nanopowder to further investigate the influence of preparation technique on the tensile properties of modified silica containing epoxy resin. The influence of curing agent/resin ratio and silica content on the tensile properties of epoxy resin were also studied. Silica nanopowder (Aerosil 200, 10-20nm in diameter) obtained from Aldrich chemical company was added to the base DGEBA resin after surface modification. The surface of the silica nanopowder was chemically modified by 3-aminopropyltriethoxysilane coupling agent (Figure 2.2), supplied by Aldrich chemical company.

4, 4'-diaminodiphenylsulfone (DDS, Figure 2.3) was used as a common curing agent obtained from Fisher Scientific. The level of curing agent incorporation was based on a calculation using the amine equivalent weight of the DDS and the epoxy equivalent weight of the epoxy resin.

Solvents such as acetone, ethanol, acetic acid and disposables such as NaCl plates were received from the Aldrich chemical company.

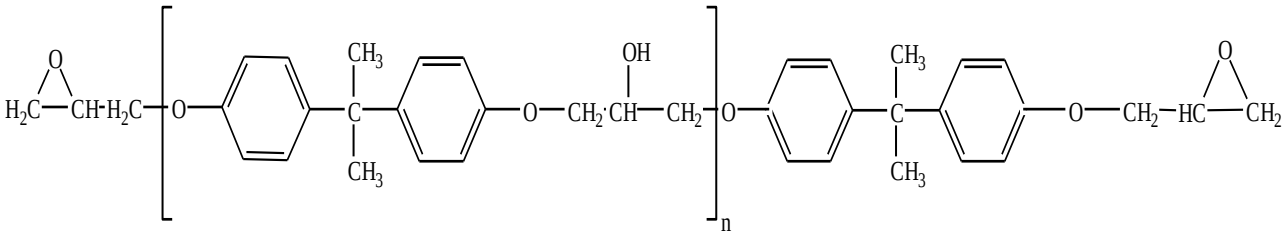

Figure 2.1. Diglycidyl ether of bisphenol A (DGEBA), n= 0 (monomer), n=1 (dimer) etc.

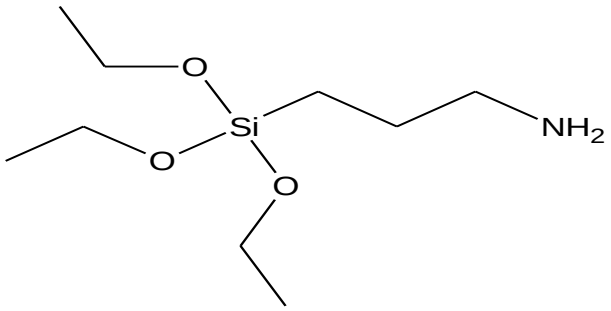

Figure 2.2. 3-Aminopropyltriethoxysilane

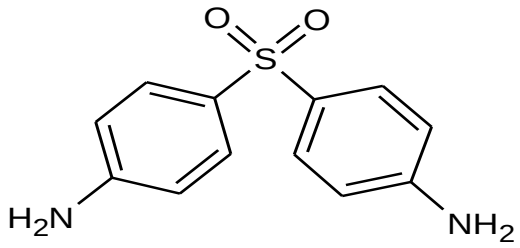

Figure 2.3. 4, 4'-Diaminodiphenylsulfone

2.2 Processing

2.2.1 Preparation of Silica/Epoxy/Amine nanocomposite from Nanopox F 400 resin

The appropriate amount Nanopox F 400 resin was placed in a fast freeze dry flask and placed in an oil bath at 50°C. The DDS was first dissolved in 100 % acetone then added slowly to the resin with continuous mechanical stirring until a homogenous mixture was observed. Vacuum was then applied and the bath temperature was gradually increased up to 100°C. Upon complete removal of acetone, a clear solution was obtained. For the DSC experiments, aluminum pans were filled with 5-10 mg resin mixture (solvent removed) and hermetically sealed. The same procedure was applied for the sample preparation of the control resin (DGEBA +DDS). The stoichiometric ratio of epoxy resin to curing agent was 1:1.1 for the DSC measurements.

The samples for mechanical testing were made by pouring the solvent-removed resin mixture into mould release-coated dog-bone shaped moulds which were preheated at 140°. The mixture was cured in these moulds at 140 °C for 2 hours followed by 200 °C for 2 hours in a digitally controlled forced air programmed oven. The edges of these cured dog bone tensile samples were sanded down using fine aluminum oxide sandpaper to remove imperfections, and were used for tensile testing. For the tensile testing, the stoichiometric ratio of epoxy resin to curing agent was adjusted to 1:0.9; 1:1 and 1:1.1 to help measure the influence of stoichiometry on properties after cure.

The compact tension specimens were prepared using the same procedure as stated for the dog-bone shaped tensile specimens. Plates were made by casting and then cut into 3.05 cm x 3.81cm x 2.5cm rectangles according to Ting and Cottington [59]. A sharp razor blade was used to initiate a crack before specimens were fractured.

For DMA and TMA measurements, cured samples of the control resin and Nanopox F 400 cured with DDS were sent to the National Institute of Aviation Research (NIAR) for testing.

2.2.2 Preparation of surface treated Nanosilica particles for the homemade nanocomposite

To an appropriate amount of silane coupling agent, 95% ethanol was added with a few drops of acetic acid to achieve a pH of 3-5. The mixture was stirred for 1-2 minutes. Next, the appropriate amount of silica nanopowder (10-20nm) was introduced into the beaker and the reaction mixture was stirred for 10-15 minutes in a high shear mixer. The reaction mixture was transferred to a round bottom flask and the ethanol solvent was evaporated using a Rotovap for about 20 minutes. Throughout this process, the temperature was maintained at 50 °C. The modified silica was dried in a vacuum oven for 20 minutes. The surface treated silica nanopowder was then ground and further stored in a jar for the preparation of homemade nanocomposites.

2.2.3 Preparation of the homemade nanocomposite samples for the tensile testing

Epoxy resin, DGEBA, was placed in a freeze dry flask in an oil bath at 50°C and surface treated silica (different wt %) was then added with continuous stirring. The mixture was then stirred for 10 minutes using a high shear mixer to obtain a homogenously dispersed solution. DDS, the curing agent was dissolved in acetone and added to the reaction mixture. Vacuum was then applied and the temperature was gradually increased to 100°C with high shear mechanical stirring in an oil bath. Upon complete solvent removal, a clear solution was obtained. Steel moulds with 1/8” spacers were used to cure the resin. Moulds were treated with mould release agent and pre warmed to 140°C. The warm resin was poured into the mould and cured for 2 hours at 140 °C followed by 4 hours at 200 °C in a digitally controlled forced air oven. The

edges of these cured dog bone tensile samples were sanded down using fine aluminum oxide sandpaper to remove imperfections, and were used for tensile testing.

2.3 Analytical Techniques

2.3.1 Nuclear Magnetic Resonance (NMR) Spectroscopy

A Varian 300 MHz NMR spectrometer was used to obtain proton NMR spectra. Non overlapping peaks of the spectrum were used to quantify the structural units in the epoxy nanoresin. Approximately 0.1 mg of uncured material was dissolved in 1 ml of deuterated acetone and then analyzed by ^{1}H NMR Spectroscopy.

2.3.2 Fourier Transform Infrared (FT-IR) Spectroscopy

A Thermo Nicolet Avatar FTIR spectrometer was used to obtain FT-IR spectra of uncured Nanopox F 400 resin and unfilled control resin as liquid films on sodium chloride salt plates. This technique was used to obtain insight into functional groups present in the epoxy nanoresin. About 1 mg of sample was dissolved in an appropriate amount of acetone then deposited onto a salt plate for analysis after evaporation of the solvent. The samples were subjected to a minimum of 128 scans to produce a good signal-to-noise ratio.

2.3.3 Dynamic Scanning Calorimetry (DSC)

A differential scanning calorimeter (TA Instruments DSC Q2000) was used to monitor the heat flow during dynamic and isothermal scans under a nitrogen flow of 50 ml/min. Samples of 5-10 mg were sealed in hermetic pans and heated from 30 °C to 300 °C at variable heating rates (4 °C/min to 15 °C/min) for the dynamic scanning tests. The epoxy resin and its nanocomposites were considered completely cured at 300 °C because the residual heat of cure

tends to zero. The cured sample was cooled down to 30 °C and then rescanned up to 300 °C at 10 °C/min to obtain the ultimate glass transition temperature (T_g).

Isothermal experiments were conducted from 140 °C to 200 °C with an increment of 10 °C. The sample was placed in the DSC at 30 °C; the temperature was then quickly ramped up to the isothermal temperature at 30 °C/min and held there for 60 minutes. The sample was cooled rapidly to 30 °C and reheated up to 300 °C at 3 °C/min to determine any residual exotherm.

2.3.4. Dynamic Mechanical Analysis (DMA)

Viscoelastic properties of cured polymer were studied by Dynamic Mechanical Analysis or DMA. A sinusoidal force (stress, σ) is applied and the resulting displacement (strain, ε) is measured. The storage modulus and loss modulus can be determined as a function of temperature or time as the polymer is deformed under the oscillating force. The shear elastic modulus (G') is used to determine the stiffness of the material. The shear loss modulus (G") sheds light on the viscous damping and energy dissipation properties of the material. DMA is also used to determine the glass transition temperature or α transition of a material.

DMA tests were performed at NIAR using a TA DMA Q800 in three point bend mode. Cured resin was cut into samples about 2.5 cm x 0.6 cm x 0.3 cm (~1 x 0.25 x 0.1 in^3) and tested using oscillating amplitude of 10 μm. Samples were subjected to programmed heating at temperatures ranging from 75 °C to 280 °C. The test fixture was a 20 mm 3-point bend clamp operated at a fixed frequency of 1 Hz. The storage and loss moduli were measured as functions of temperature. From the tanδ versus temperature plots, the α-relaxation temperature (or T_g) was determined.

2.3.5 Thermal Mechanical Analysis

Thermomechanical analysis (TMA) is one of the simpler characterization techniques in the field of thermal analysis. With TMA, the dimensional properties of a sample are measured as the sample is heated, cooled or held under isothermal conditions. TMA offers a higher degree of sensitivity than DSC for the detection of the softening temperature of highly filled or highly cross-linked materials, such as composites. TMA was employed for the detection of Tg in conjunction with DSC. The probe used here for the TMA experiment was a penetration probe. When performing measurements with the penetration probe, loading is added to the probe so that it moves down through the material as it softens.

TMA tests were performed by NIAR laboratories using a TMA Q400 where the cured resin sample was subjected to a sharp probe with a load of 0.5 N under nitrogen atmosphere. The temperature was ramped from 100 ^{o}C to 280 ^{o}C at a rate of 5 ^{o}C/min. Results were plotted analyzed using the TA Universal Analysis 2000 and Microsoft Excel programs.

2.3.6 Mechanical Testing

2.3.6.1 Tensile Testing (ASTM D 638)

Tensile testing is the most fundamental type of mechanical testing method used to determine the stiffness and strength of a material. The sample is pulled by a tensile load at a constant rate until it fractures. A curve will result relating sample stress to sample strain, as shown in Figure 2.4. Nominal, tensile stress (σ_n) is a force per unit area of the original cross section of the test length. Tensile strain (ε) is defined as the fractional change in length over the minimum diameter portion of the sample. The point of failure is of much interest and the stress is called ultimate strength (σ_u) of the material.

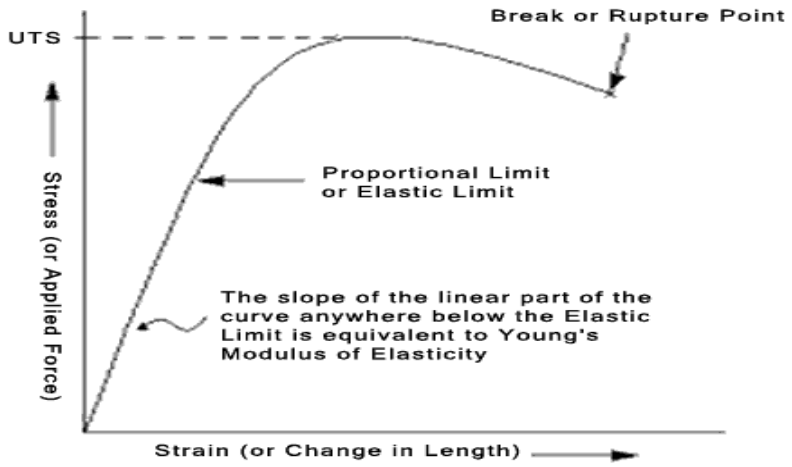

Figure 2.4. The stress-strain curve from a tensile test of a material able to yield [59].

The initial portion of the test reveals a linear relationship between the applied force (load) and the elongation of the material which obeys Hooke's Law i.e. where the stress to strain is proportional to strain,

$$\frac{\Delta\sigma}{\Delta\epsilon} = E \tag{22}$$

Where 'E' is the slope of the line in the linear elastic region and called the "Modulus of Elasticity" or "Young's Modulus". The modulus of elasticity is a measure of the stiffness of the material, but it only applies to the linear elastic region of the curve. If a specimen is loaded to within this linear region, it will return to its undeformed state if the load is removed.

The ASTM D638 test method covers the determination of the tensile properties of reinforced and unreinforced plastics in the form of standard dog bone-shaped tensile specimens when tested under defined conditions (Figure 2.5). The tensile tests were performed using an Instron tensile tester. Five to six dog bone shaped tensile specimens were prepared for both the control resin and the silica/ epoxy nanocomposites. The edges of the specimens were sanded down with an aluminum oxide sand paper to remove any imperfections. The width and thickness of each specimen were measured with a vernier caliper. An MTS ElectroMechanical Tester was

used to stretch the specimens at a fixed rate. A clip-on strain gauge was used to measure displacement/strain. The tensile test was performed at a crosshead speed of 5 mm/min [0.2 inch/min]. The machine was automatically stopped as soon as breakage occurred. The test was monitored by a computer program and output data was obtained as a load versus displacement. Stress (σ) was calculated by dividing the force at each point by the cross-sectional area of the narrowest section of the specimen. Strain (ε) was calculated by measuring the extension of a clip on 1 inch extensometer.

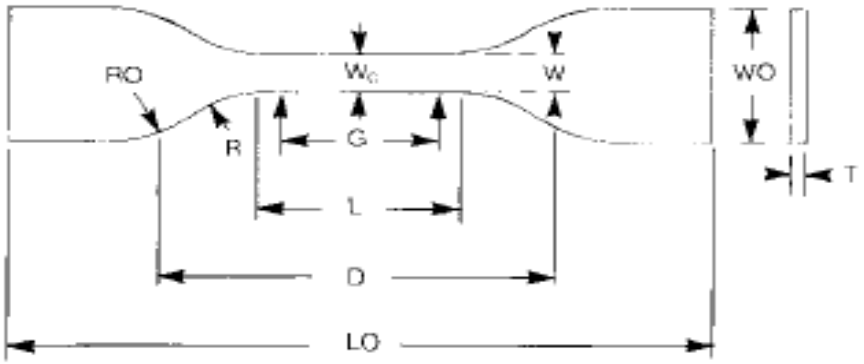

Figure 2.5. Tensile test specimens[59].

Table 2.1. Dimensions and nominal values in mm (inch) of the tensile test specimen.

Dimensions	Nominal Values mm (in)
W = width of narrow section	6 (0.25)
L= length of narrow section	57(2.25)
WO = width overall, min	19 (0.75)
LO = length overall, min	183 (7.2)
G = Gage length	50 (1.00)
D = Distance between grips	135(5.3)
R = Radius of fillet	76 (3)

CHAPTER 3

RESULTS AND DISCUSSION

3.1 Properties and Characterization

The properties of nanocomposites are a strong function of composition, the size of the particles and interfacial interactions. The interfacial interactions between the polymer and silica (which depends on the preparative procedure) strongly affect the mechanical and thermal properties of the nanocomposite. The internal surfaces (interfaces) are critical in determining the properties of nanofilled materials since 10-20 nm silica nanoparticles have a high surface area-to-volume ratio. This high surface area-to-volume ratio means that for the same particle loading, nanocomposite will possess a much greater interfacial area than a microcomposite. This interfacial area accounting for a significant volume fraction of the polymer surrounding the particle, is affected by the particle surface, and has properties different from the bulk polymer.

Infra-Red (IR) spectroscopy and Proton Nuclear Magnetic Resonance (NMR) Spectroscopy were used as techniques of characterization to understand structure-property relationships in the nanocomposite.

3.1.1 Infra Red Spectroscopy

The chemical characterization of a commercially available, high performance (40 wt. %) surface modified silica containing epoxy nanocomposite procured by the sol-gel technique (Nanopox F 400 resin), was performed using Infra-Red (IR) spectroscopy.

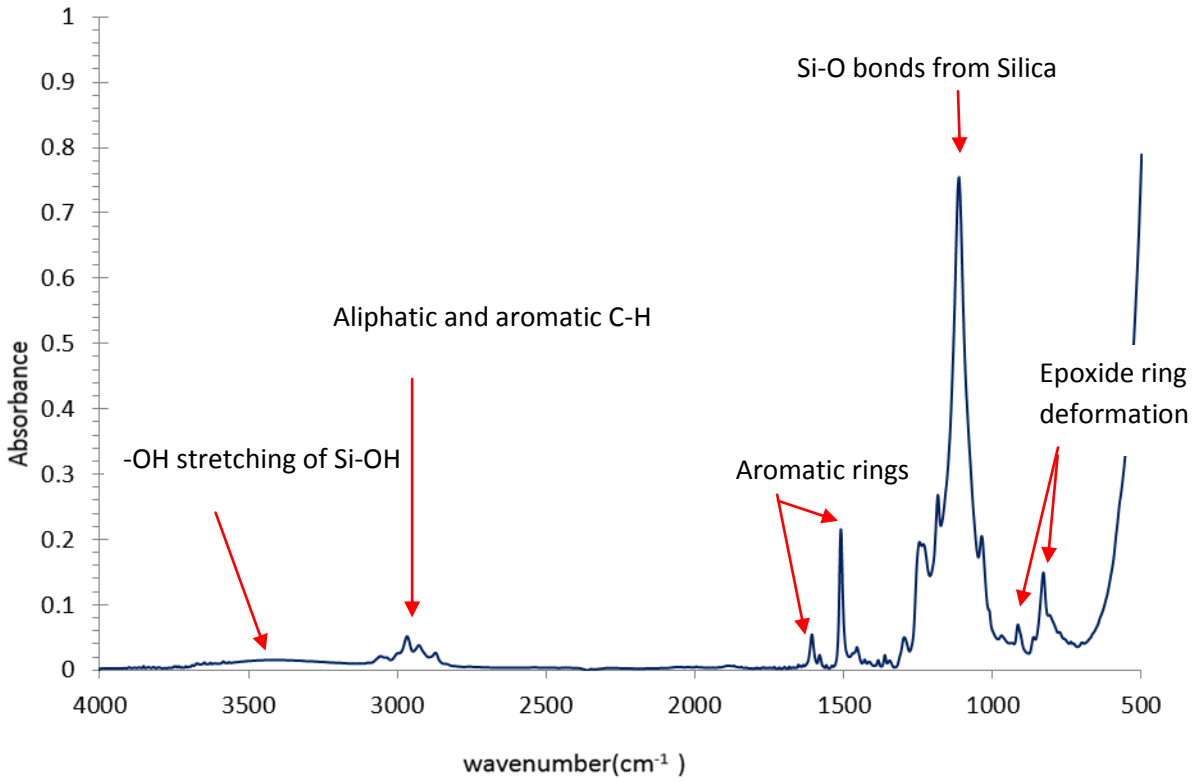

Figure 3.1. IR spectrum of Nanopox F 400 resin on a NaCl plate after acetone solvent removal.

The IR spectrum of Nanopox F 400 resin is shown in Figure 3.1. Absorbances are labeled by comparison with the Infrared spectra of reference compounds and by simple principles of IR absorbance spectroscopy. The broad and strong absorbance at 1000-1200 cm^{-1} confirmed the presence of silicon-oxide filler. More specifically, the presence of silica is marked by the strong absorbance at 1110 cm^{-1} due to Si-O-Si asymmetric stretching. The other characteristic peak is the broad one around (3100-3600 cm^{-1}) due to Si-OH bond stretching as shown in an expanded spectrum below (Figure 3.2).

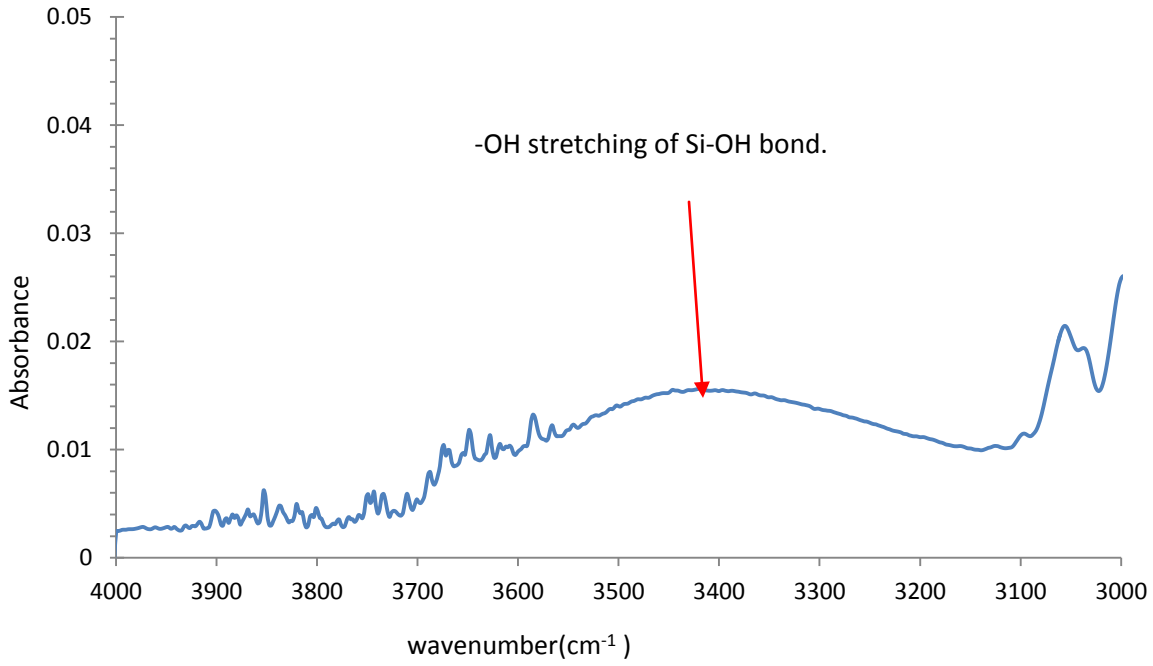

Figure 3.2. Infra-red spectrum of Nanopox F 400 resin expanded view from 3000 cm^{-1} to 4000 cm^{-1}.

The small shoulders at 1180 cm^{-1} and 1232 cm^{-1} correspond to symmetric and asymmetric C-O stretching as shown in Figure 3.3. The epoxies groups produce distinctive peaks at 915 cm^{-1} due to epoxide ring deformation. The sharp peak at 1509 cm^{-1} corresponds to generic carbon-carbon stretching in the aromatic ring. The broad peak above and below 3000 cm^{-1} corresponds to the aromatic C-H stretching and aliphatic C-H stretching respectively.

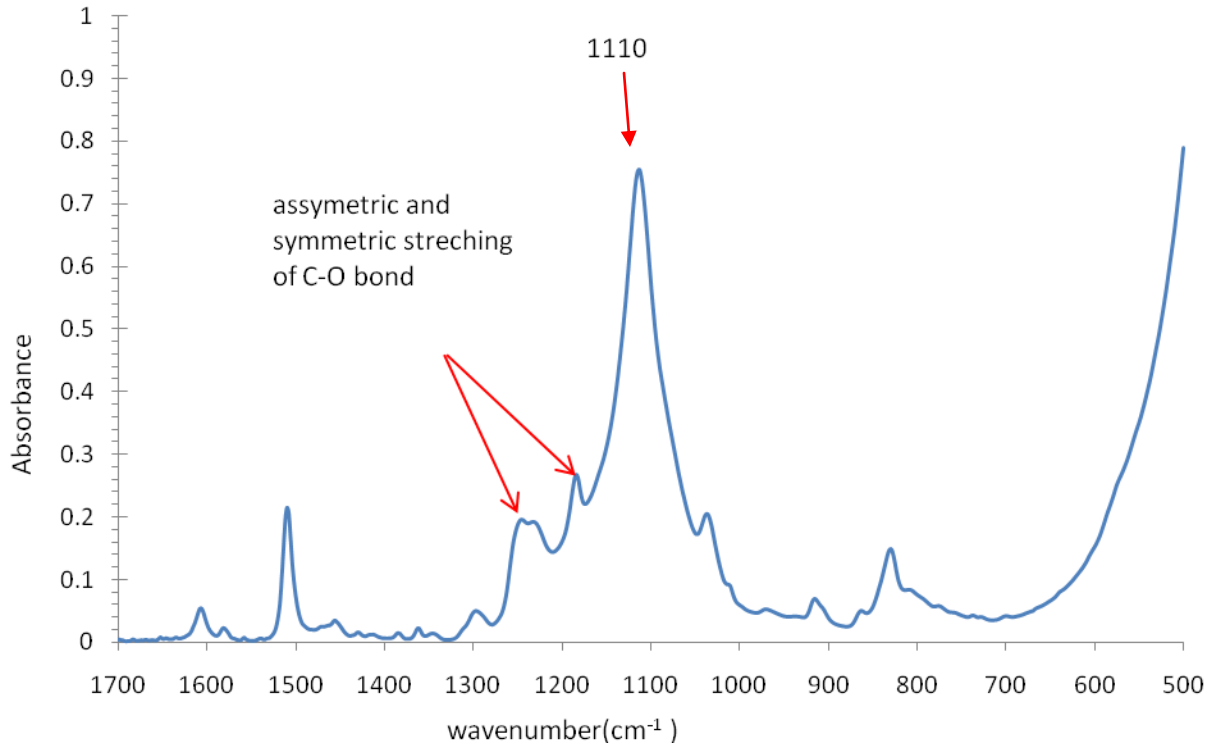

Figure 3.3. Infra-red spectrum of Nanopox F 400 resin expanded view from 500 cm^{-1} to 1700 cm^{-1}.

3.1.2 Proton Nuclear Magnetic Resonance Spectroscopy

Characterization of Nanopox F 400 resin was also performed using proton nuclear magnetic resonance (NMR) spectroscopy. The proton NMR spectra of pure Diglycidyl ether of Bisphenol-A **(**DGEBA) and Nanopox F 400 resin are shown in Figure 3.4 and Figure 3.5. NMR signals were identified by comparing with the signals generated using ACDLABS (9.0) software and by comparing with the spectrum of unfilled DGEBA resin. Deuterated acetone solvent was used when modeling the DGEBA spectrum using ACD software.

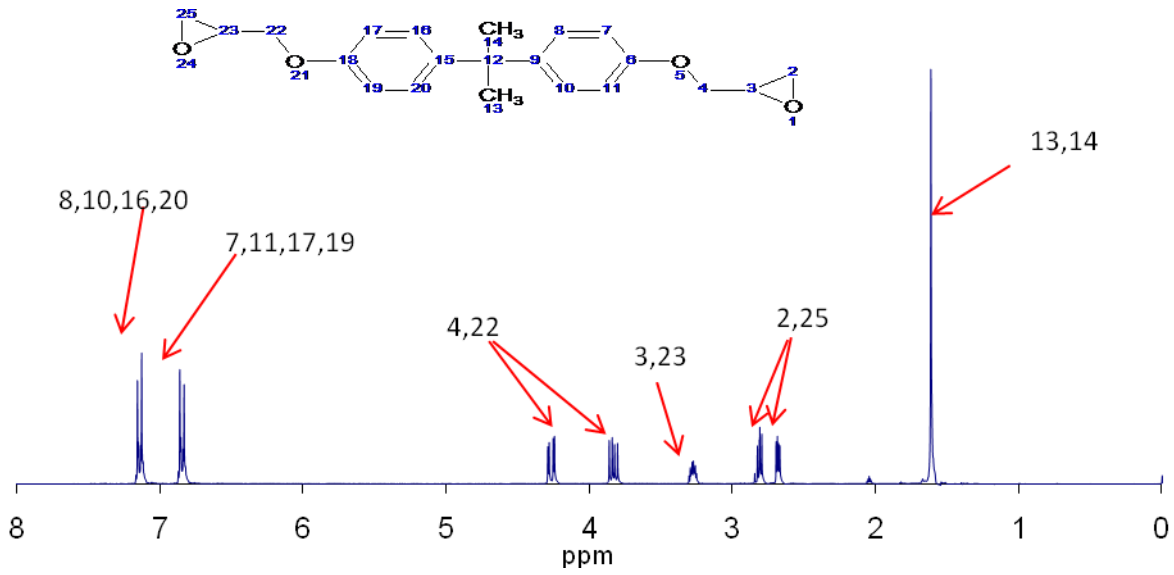

Figure 3.4. ^{1}H NMR spectrum of an uncured and unfilled DGEBA resin dissolved in d_6 acetone.

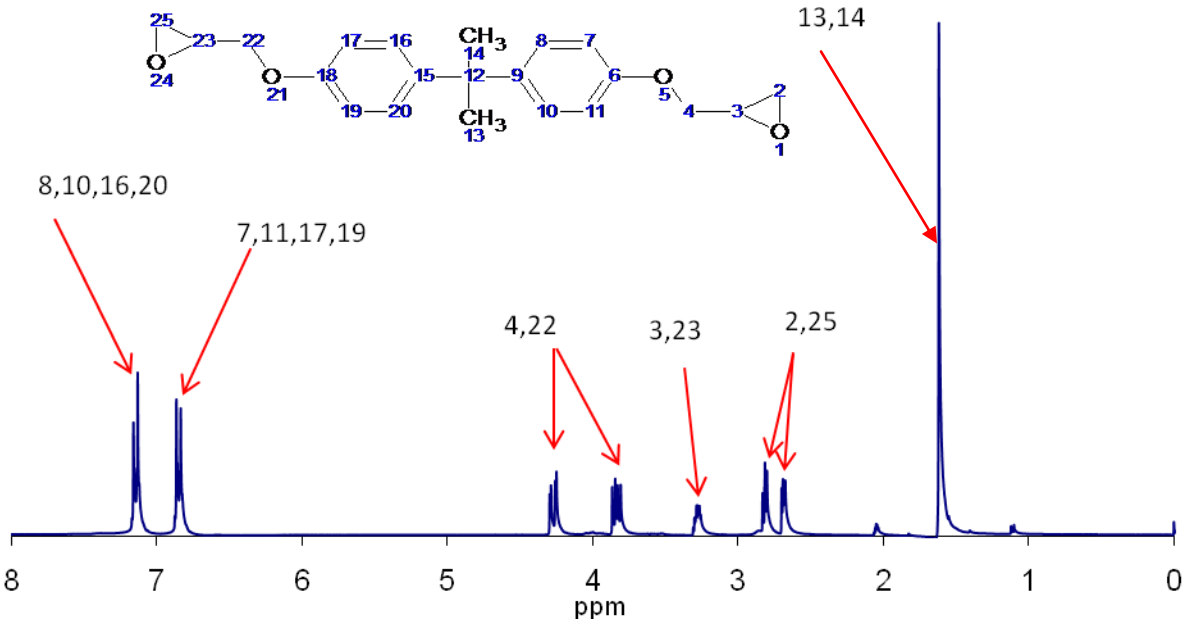

Figure 3.5. Identification of DGEBA epoxy resin in an uncured Nanopox F 400 resin dissolved in d_6 acetone. (DGEBA: Diglycidyl ether of Bisphenol-A)

Chemical shifts generated using ACD software and chemical shifts for proton NMR spectra of DGEBA resin and Nanopox F 400 resin are tabulated in Table 3.1.

Table 3.1. Assignment of carbon numbers and chemical shifts for proton NMR spectra of DGEBA resin and Nanopox F 400 resin.

Carbon numbers designated for DGEBA	Chemical shift generated by ACD software in ppm for DGEBA resin	Chemical shift observed for DGEBA resin in ppm	Chemical shift observed for Nanopox F 400 resin in ppm
13,14	1.24	1.61	1.62
2,25	2.52	2.68	2.68
2,25	2.68	2.82	2.81
3,23	3.1	3.27	3.28
4,22	3.74	3.83	3.83
4,22	4.17	4.27	4.27
7,11,17,19	6.75	6.85	6.85
8,10,16,20	7.17	7.14	7.14

The spectra of pure DGEBA resin and Nanopox F 400 resin show common peaks except peaks at 2.9 ppm and 1.1 ppm (Figure 3.5) because Nanopox F 400 resin contains 40 wt. % of surface modified silica nanoparticles, the peak at 2.9 ppm, a singlet, represents the hydrogen atom linked to a hydroxyl group of silica filler as shown in an expanded spectrum (Figure 3.6). The region between 1-1.5 ppm is expanded in Figure 3.7 to highlight the two peaks at 1.10 ppm and 1.11 ppm which are possibly due to the $–CH_2$ groups associated with Si atom of the surface modifying agent present in Nanopox F 400 resin.

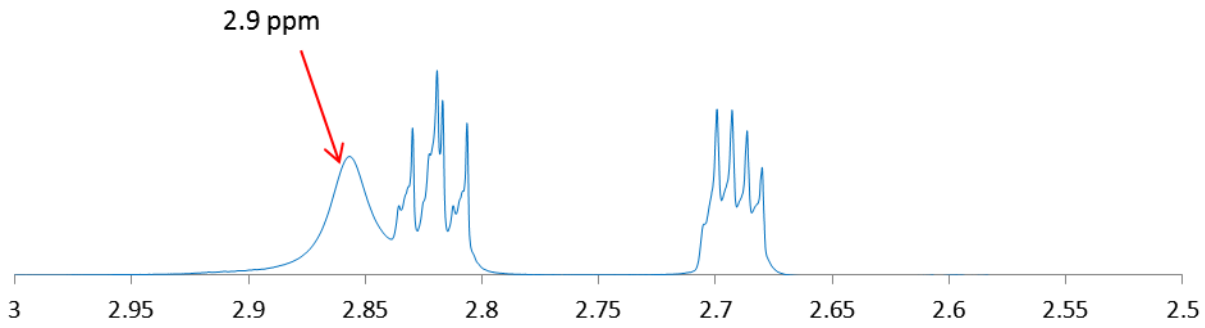

Figure 3.6. ^{1}H NMR plot of Nanopox F 400 resin expanded from 2.5 to 3 ppm.

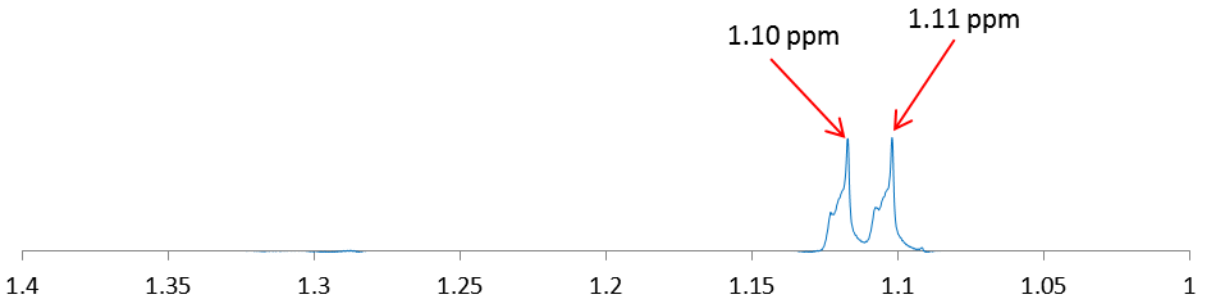

Figure 3.7. ^{1}H NMR plot of Nanopox F 400 resin expanded from 1 to 1.5 ppm.

3.2 Thermal Analysis

3.2.1 Dynamic Temperature Cure

The cure kinetics of epoxy resin was studied by Differential Scanning Calorimetry (DSC). Epoxy-amine mixtures with and without SiO_2 nanoparticles were studied to compare the cure kinetics of epoxy resin with and without silica filler. The epoxy resin without silica filler is labeled as the control resin, which is pure Diglycidyl ether of Bisphenol-A (DGEBA) resin cured with an little molar excess of Diamino Diphenyl Sulphone (DDS) i.e. N-H/epoxy ratio of 1.1:1.The epoxy resin with surface modified SiO_2 nanoparticles is hereafter referred to as Nanopox F 400 resin, and contains 40 wt. % silica nanoparticles in DGEBA prepared via a sol-gel technique, cured with DDS with an N-H/epoxy ratio 1.1:1.

The control resin was ramped from 30 °C to an end temperature of about 350 °C at various heating rates. A representative programmed DSC trace of the control resin, at a heating rate of 3 °C/min, is reproduced in Figure 3.8.1. After a first scan, the DSC cell was re-cooled to room temperature at a cooling rate of 30 °C/min and re-heated to 300 °C at a standard heating rate of 10 °C/min to measure the ultimate glass transition temperature (T_g) as shown in Figure 3.8.2. The absence of a residual exotherm in the second scan affirmed that the cure reaction was completed during the first scan. A similar exotherm were produced by Nanopox F 400 as reproduced in Figure 3.9.

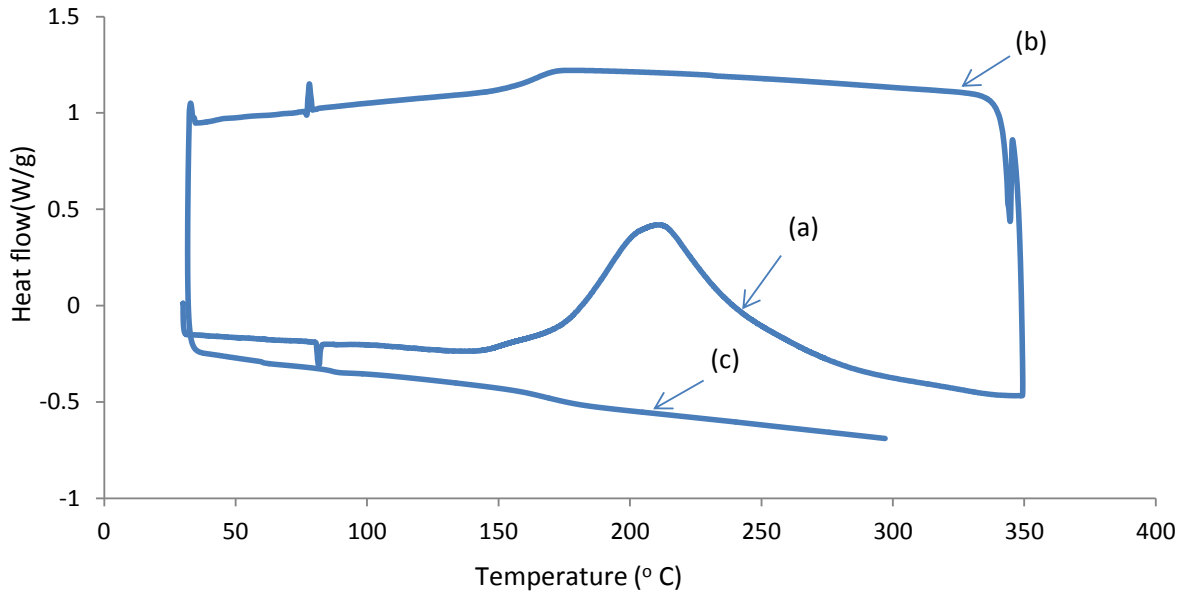

Figure 3.8.1. An exotherm generated from dynamic temperature scanning of the control resin cured with DDS curative at 4 °C/min from 30 °C to 300 °C (a), re-cooled to 30 °C (b) and re-heated to 300 °C (c).

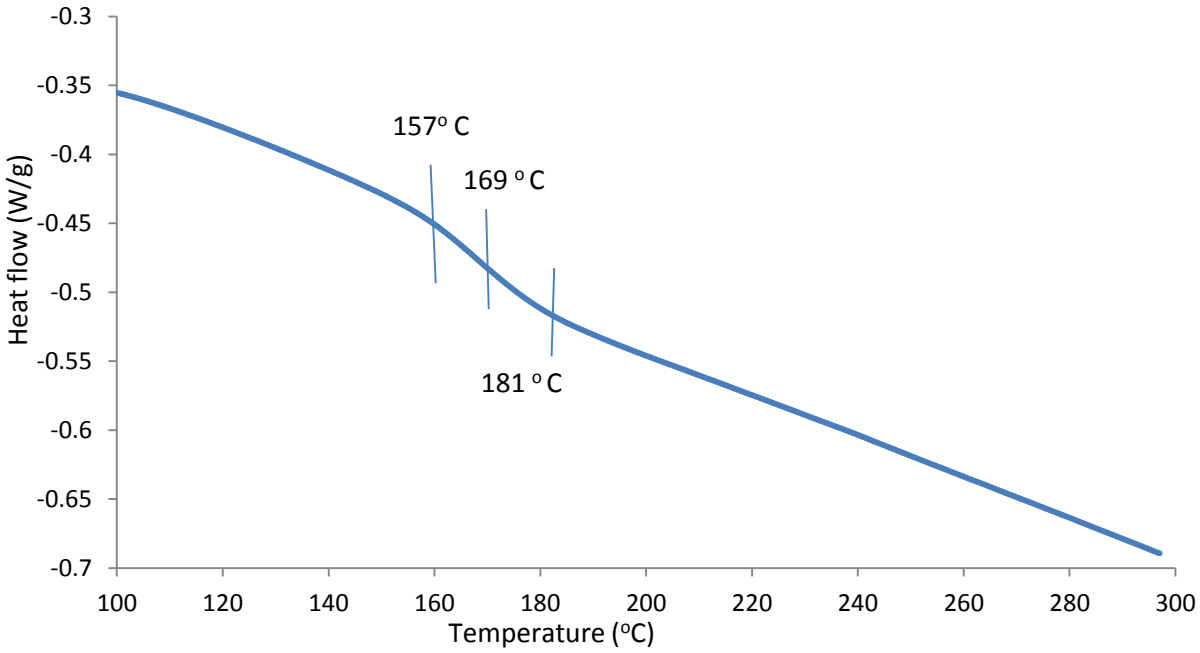

Figure 3.8.2. DSC trace from the rescan of the control resin previously cured with DDS curative from 30°C to 300 °C at 10 °C/min [(c) in Figure 3.8.1]. (The ultimate glass transition temperature, T_g =169 °C)

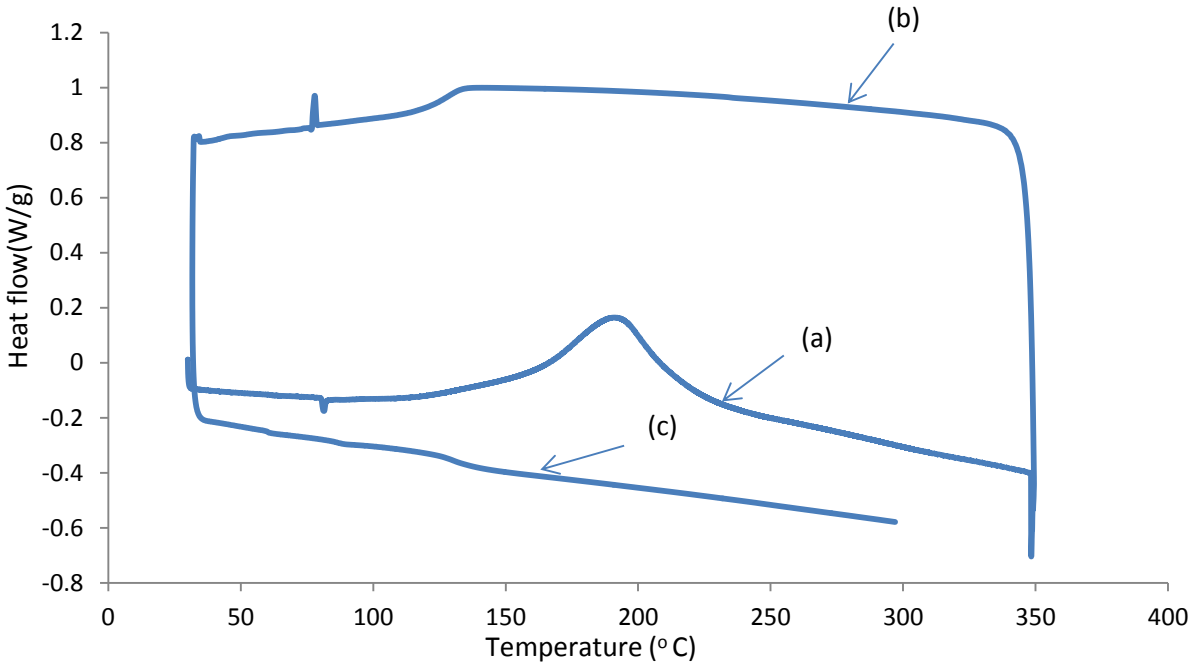

Figure 3.9. An exotherm generated from dynamic temperature scanning of Nanopox F 400 resin cured with DDS curative at 4 °C/min from 30 °C to 300 °C (a), re-cooled to 30 °C (b) and re-heated to 300 °C (c).

Data generated from dynamic temperature scanning was used to construct plots for the degree of cure (α) as a function of temperature over a range of heating rates from 4 °C/min to 15 °C/min. A summary of plots of α vs. T obtained for the control resin is shown in Figure 3.10.

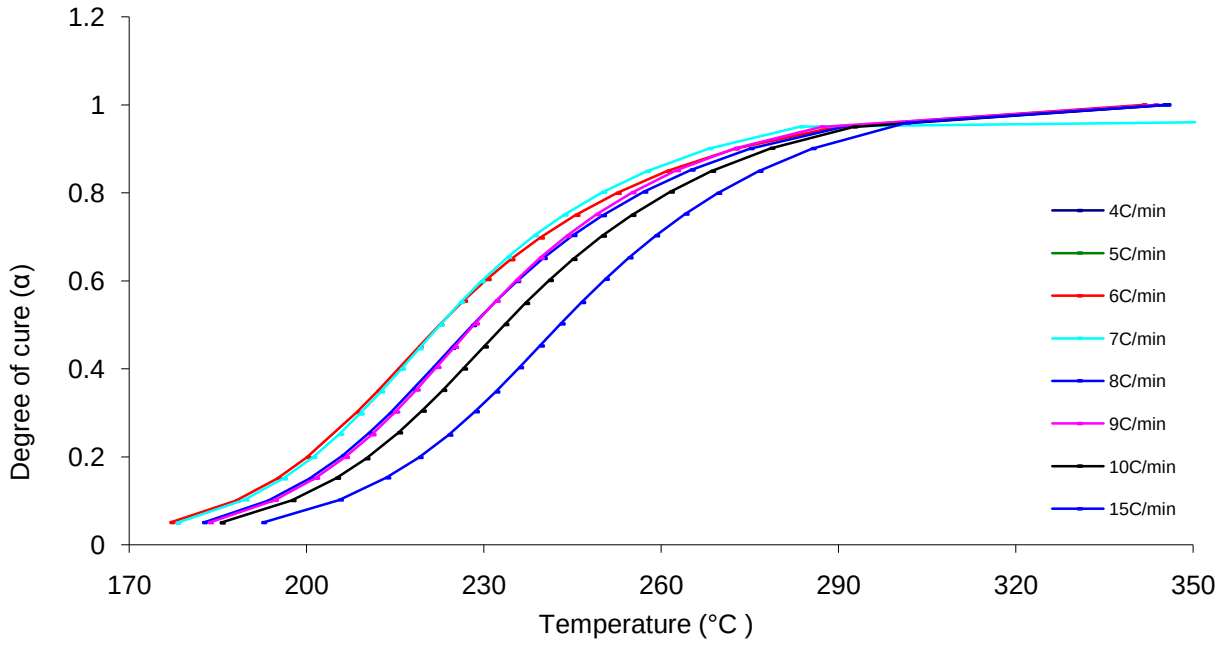

Figure 3.10 Summary of degree of cure (α) vs temperature (^{o}C) for the control resin cured at different heating rates with DDS curative.

This plot (Figure 3.10) indicates that the cure reaction shifts to higher temperatures at higher heating rates, see Figure 3.11, as is usually the case.

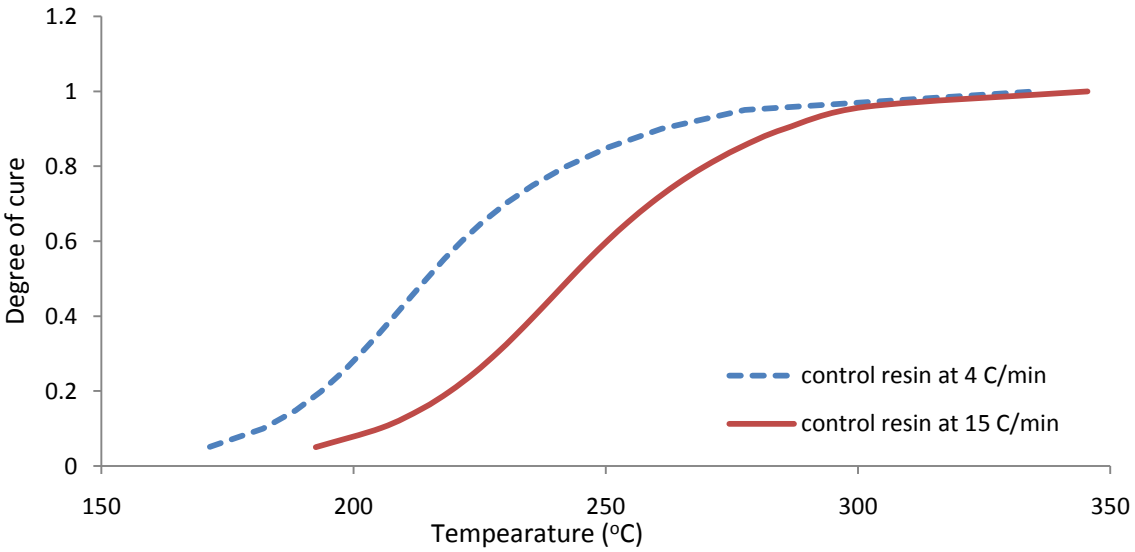

Figure 3.11. A comparison of the degree of cure profiles of the control resin cured with DDS curative at 4 ^{o}C/min and 15 ^{o}C/min heating rates.

This behavior happens because at slower heating rates, the molecules have sufficient time to unravel, rearrange themselves and react. However, at faster heating rates molecules are not given sufficient time to react during the time frame of the experiment and therefore appear to need to be heated to higher temperatures in order to react.

Similar plots were constructed for Nanopox F 400 resin cured with DDS curative. Again, plots of degree of cure as a function of temperature at different heating rates (4 ^{o}C/min to 15 ^{o}C/min) were constructed as shown in Figure 3.12.

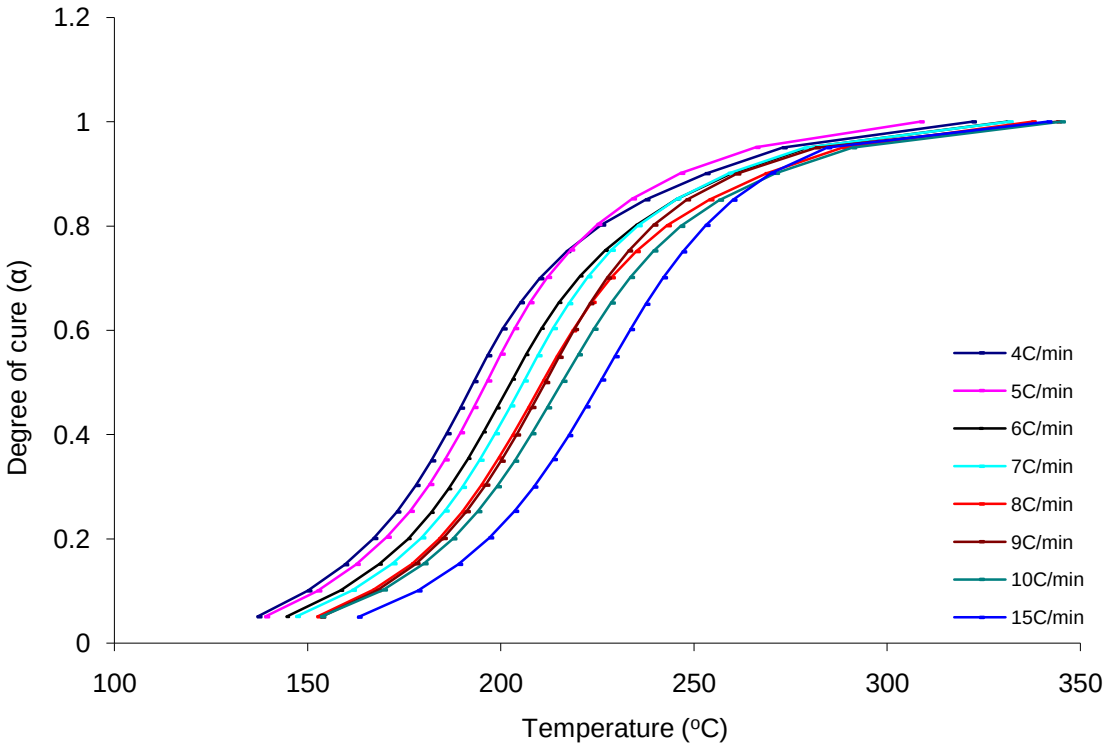

Figure 3.12. Summary of degree of cure (α) vs temperature (^{o}C) for Nanopox F 400 resin cured with DDS curative.

As expected, the cure apparently shifts to higher temperatures as the heating rate increases. For example, Figure 3.13 compares the degree of cure versus temperature of Nanopox F 400 resin at 4 ^{o}C/min heating rate and 15 ^{o}C/min heating rate. At the lower heating rates of 4 ^{o}C/min, cure

started at 140 °C and was completed at 325 °C. However, at the higher heating rates of 15 °C/min, cure shifted towards higher tempearatures starting at 160 °C and completing at 335 °C.

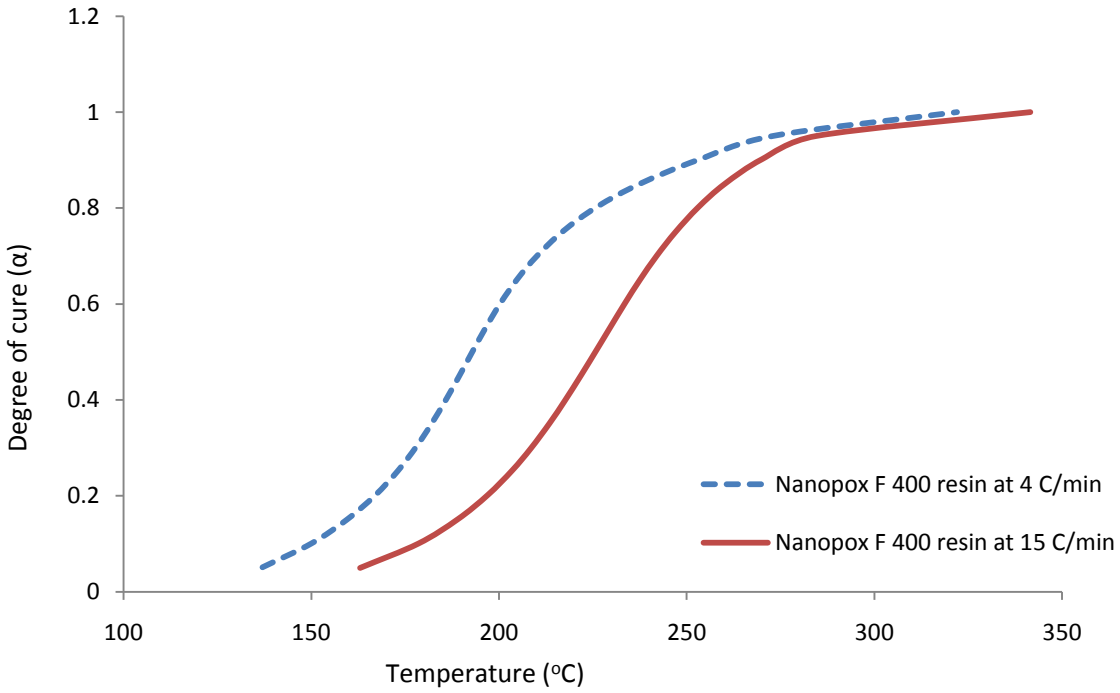

Figure 3.13. A comparison of the degree of cure profiles of Nanopox F 400 resin cured with DDS curative at 4 °C/min and 15 °C/min heating rate.

It is noticed that the curing started early and completed at lower temperature in Nanopox F 400 resin than the control resin (see Figure 3.14. a and Figure 3.14.b). However, it is observed that the beginning cure temperature is signifiantly lower for Nanopox F 400 resin than for the control resin when comparing two different heating rates of the control resin and Nanopox F 400 resin as shown in Figure 3.14.a and Figure 3.14.b. In other words, at lower temperatures, Nanopox F 400 based resin is activated toward cure over the control resin.

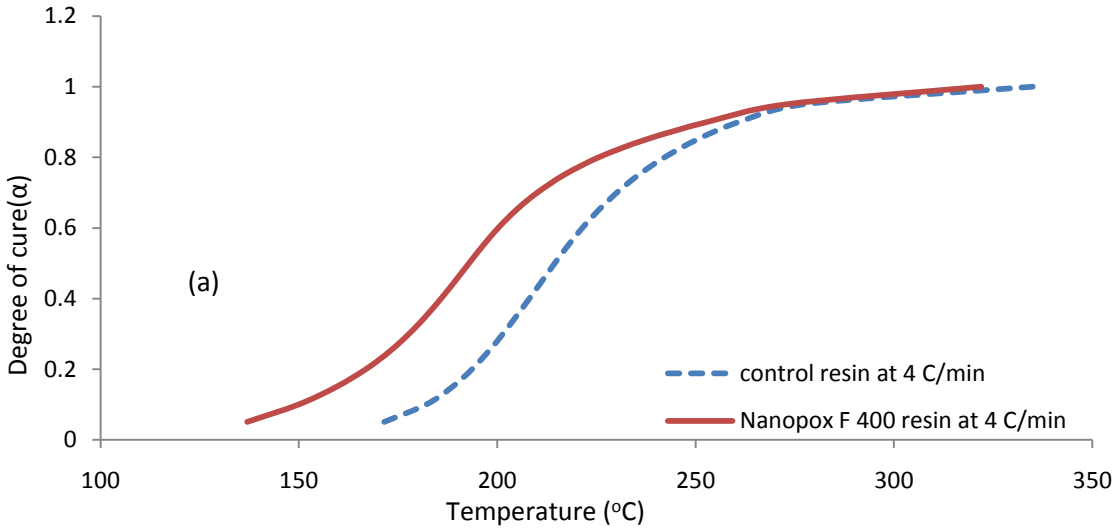

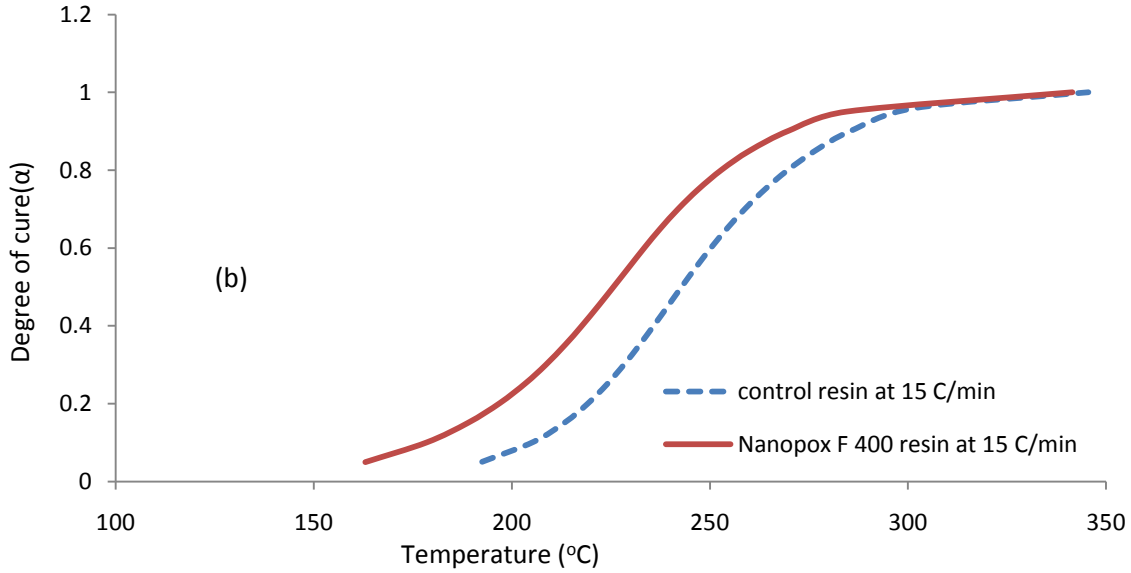

Figure 3.14.(a) &(b) A comparison of α vs.T of the control resin and Nanopox F 400 resin cured with DDS curative at 4 ^{o}C/min (a) and 15 ^{o}C/min (b) heating rates.

The acceleration of Nanopox F 400 resin cure at the beginning of cure is attributed to a catalytic effect of the hydroxyl groups present and the silica filler surface on the reaction between the epoxide group and primary, then secondary amine groups in the DDS curative.

Figure 3.15 compares the ultimate T_g of the control resin and Nanopox F 400 cured over a range of heating rates. The measured ultimate T_g's were unaffected by the rate of programmed warm up during the previous cure cycle and were averaged at 173± 6°C for the control resin and 130 ±2°C for the Nanopox F 400 resin over all the heating rates. The measured Tg is a function of heating rate during rescan. For this reason, all T_g's were recorded at a heating rate of 10^oC/min.

From Figure 3.15, it is seen that the ultimate T_g of Nanopox F 400 resin system is lower than the control resin. This is due to presence of surface modified silica filler in Nanopox F 400 resin, which might result in chain mobility assisting the large-scale segmental motion in the Nanopox F 400 resin. However, in general, the presence of micron sized silica filler should raise the overall T_g [60].

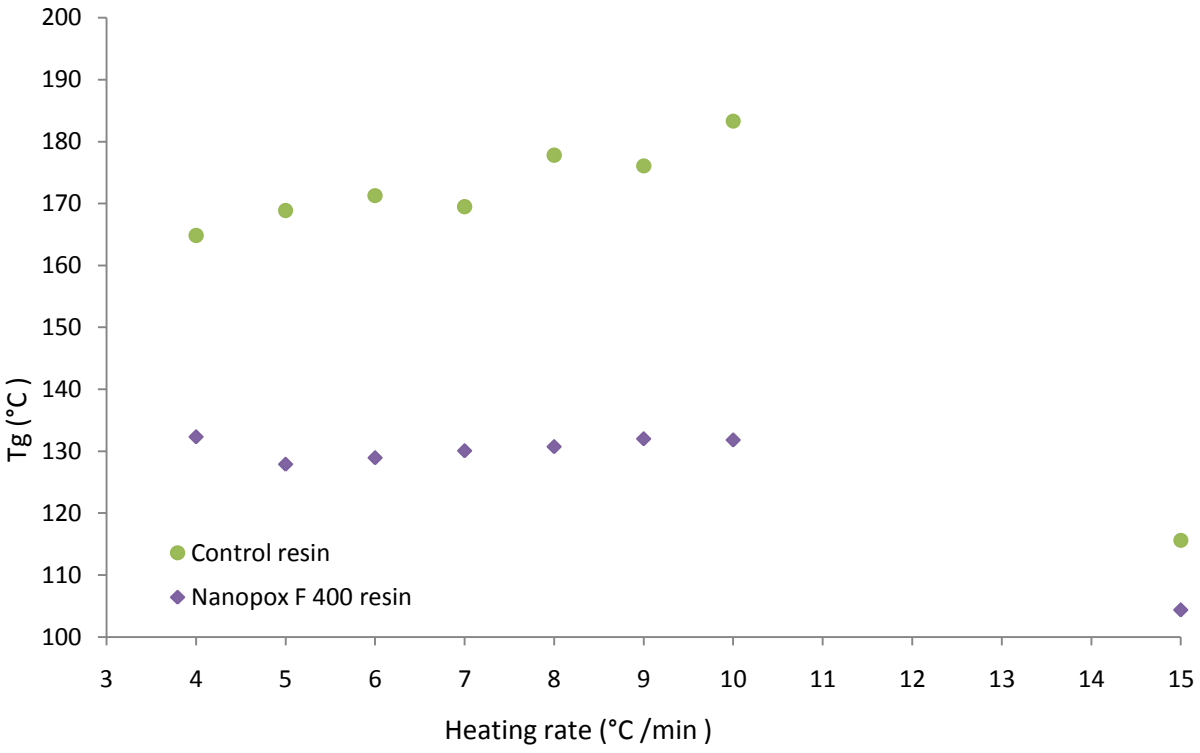

Figure 3.15. Ultimate glass transition temperatures, (T_g ^oC) of the control resin and Nanopox F 400 resin both cured with DDS curative over a range of heating rates.

The total heat of reaction is determined by time integration of the heat flow as a function of heating rate for the control resin and Nanopox F 400 resin. Nanopox F 400 resin contains 60 % by weight of resin and 40 % by weight of silica filler. Since control resin has 100 % by weight of resin, thus, Nanopox F 400 resin data were normalized to 100% by weight of resin using a normalization factor of 1.49. The normalized Nanopox F 400 resin data provides a route for the direct comparison of the heat of reaction of the control resin and Nanopox F 400 resin as shown in Figure 3.16. It can be seen that the total heat of reaction of Nanopox F 400 resin is similar to the apparent heat of reaction measured for the control resin at different heating rates (4 ^{o}C/min to 15 ^{o}C/min). It indicates that the silica filler influences the cure but did not contribute any heat of reaction during the cure reaction of Nanopox F 400 resin and DDS curative.

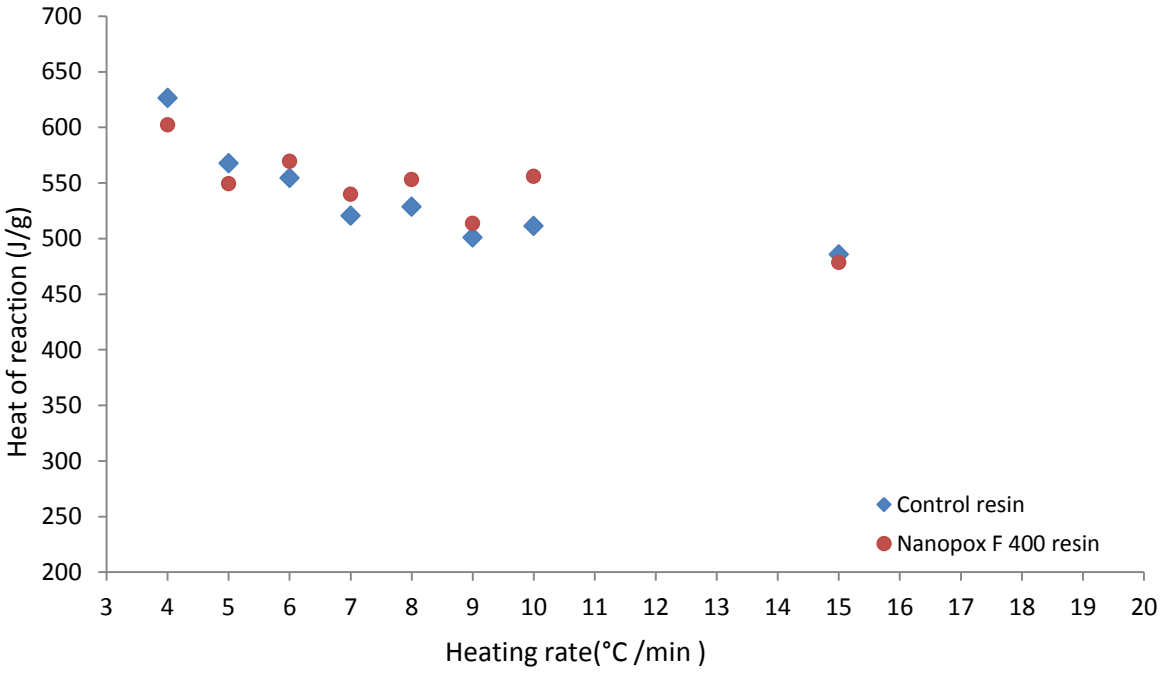

Figure 3.16. Total heat of reaction as a function of heating rates for the control resin and Nanopox F 400 resin (Normalized to 100 % resin) cured with DDS curative at an N-H/epoxy molar ratio of 1.1:1.

The rate of cure (dα/dt) is subsequently calculated by differentiating a graph of degree of cure (α) vs. time using origin 8.0 software. Figure 3.17 summarizes rate of cure vs. temperature plots obtained for the control resin cured with DDS curative at heating rates of 4 ^{o}C/min to 15 ^{o}C/min.

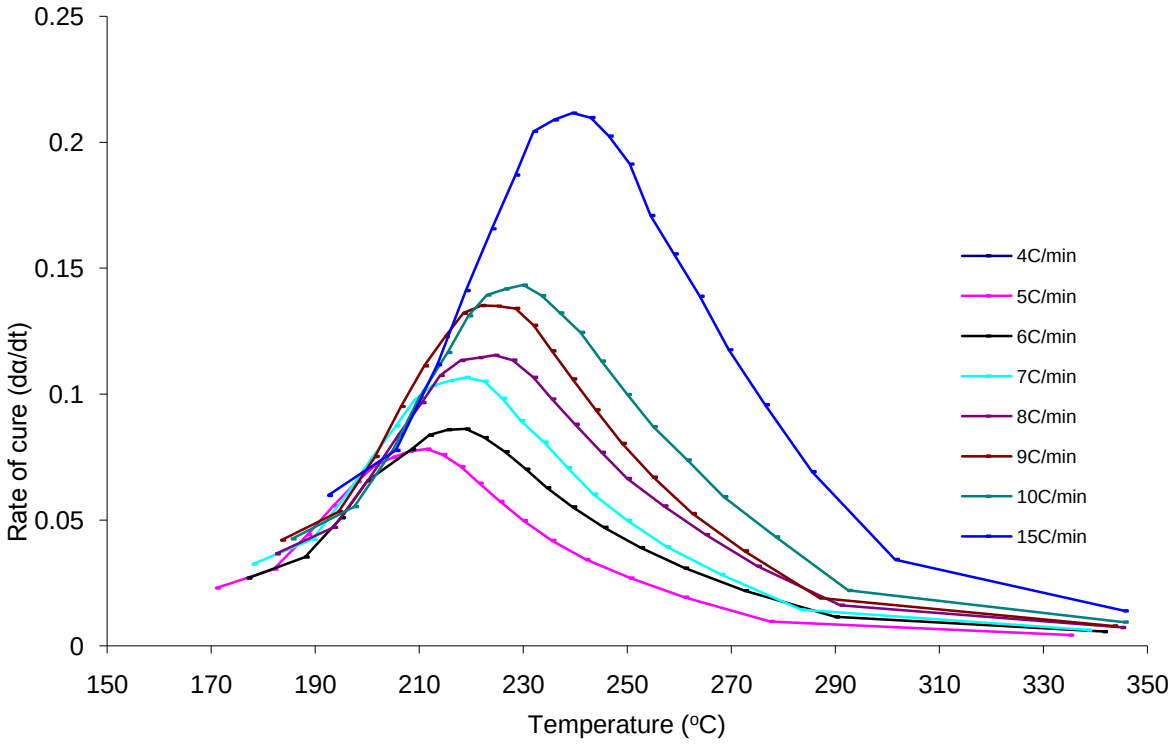

Figure 3.17. Summary of rate of cure (dα/dt) vs. temperature (T) for the control resin cured with DDS curative at heating rates of 4 ^{o}C/min to 15 ^{o}C/min.

It is observed that the apparent rate of cure increases as the heating rate is increased. There is a relative shift of the maximum rate of cure toward higher temperature with an increase in the heating rate.

Figure 3.18 summarizes the rate of cure as a function of temperature for Nanopox F 400 resin cured with DDS curative at heating rates ranging from 4 ^{o}C/min to 15 ^{o}C/min. As before, the rate of cure increases as the heating rate is increased. The temperature at which the highest cure rate is achieved also increases with increasing heating rate. The curing begins at nearly 170

^{o}C in the control resin whereas curing is started at around 130 ^{o}C in Nanopox F 400 resin for all the heating rates (Figure 3.17 & 3.18). As mentioned earlier, we believe a catalytic action of the hydroxyl groups in the silica filler is responsible for the acceleration of the cure reaction of Nanopox F 400 resin with amine curative at early temperatures.

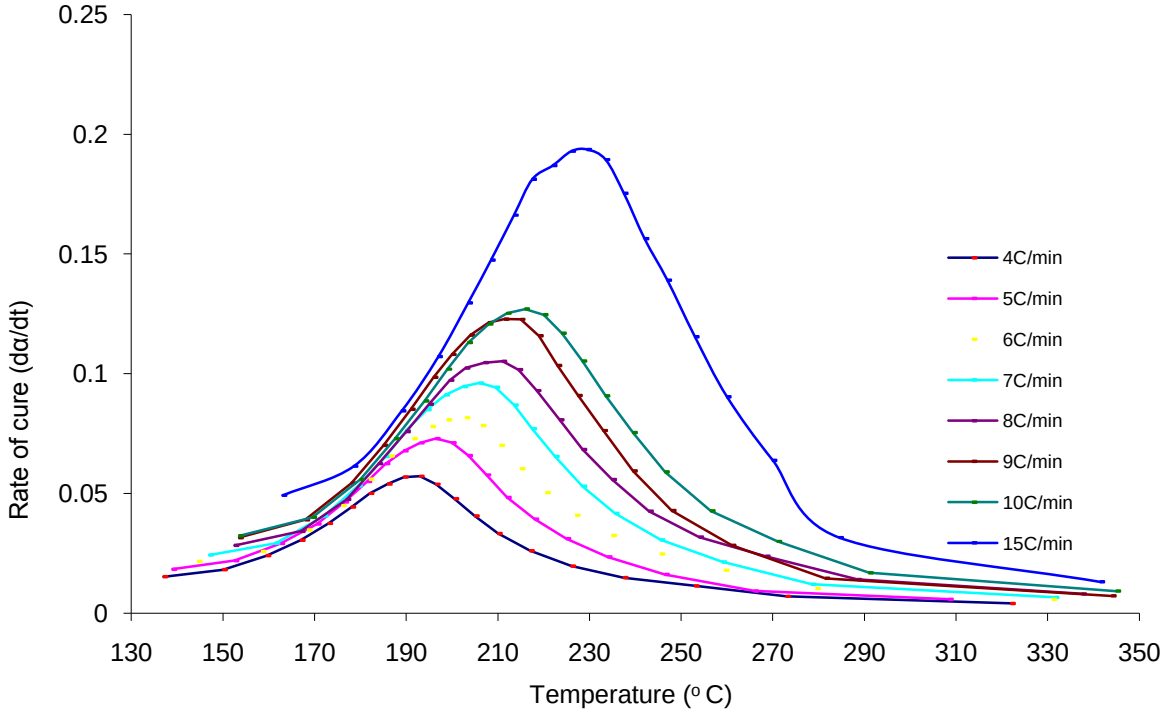

Figure 3.18.Summary of rate of cure (dα/dt) vs. temperature (T) for Nanopox F 400 resin cured with DDS curative at heating rates of 4 ^{o}C/min to 15 ^{o}C/min.

The apparent activation energy (E_a) can be measured for a resin cure reaction as a function of the degree of cure (α). This activation energy can yield insight into changes in the mechanism of cure. As the cure reaction proceeds, the reaction medium changes –it becomes more polar due to the creation of hydroxyl functionality, and becomes more viscous due to the buildup of crosslink density. As the viscosity of the resin builds up, it becomes more difficult for the functional groups to find each other, hence the apparent increases in E_a or apparent activation

energy. A plot of E_a Vs. α for the control resin and Nanopox F 400 resin were constructed by using information summarized in Figures 3.17 and 3.18.

The generic rate law equation for resin cure can be stated as

$$d\alpha/dt = k\ F(\alpha) \tag{3.1}$$

where α is the extent of cure, and k is the Arrhenius rate constant which is defined as

$$k = A \exp \{-E_a/RT\} \tag{3.2}$$

with A as the pre-exponential shape factor, E_a as the activation energy, R as the gas constant, and T as the temperature in degrees Kelvin.

Substituting the value of K from equation (3.2) in equation (3.1) and taking logarithms yields

$$\ln \{d\alpha/dt\} = \ln \{ A\ F(\alpha)\} - \{E_a / R\} \{1/T\} \tag{3.3}$$

This equation relates the rate of cure (dα/dt) to degree of cure (α) and temperature (T).

F(α) is an empirical function that defines the relationship between cure rate and the concentrations and chemical environment of functional groups in the resin. F(α) is complicated and difficult to measure and it changes with α. However, we can arrive at values of E_a without specifically determining F(α), by plotting ln(dα/dt) vs. (1/T) for a fixed value of α, so that lnA and lnF(α) can be made constant.

The apparent E_a was determined from equation (3.3) at a fixed value of α. By measuring ln(dα/dt) and T at a fixed value of α and at a defined heating rate. Therefore, the value of ln{A F(α)} is, therefore, made a constant. Data was collected for a range of fixed values of α (from α = 0.05 to α = 0.95) over a range of heating rates. By plotting ln(dα/dt) as y and 1/T as x, we generated linear graphs with a gradient equal to $-E_a/R$ and an intercept equal to ln{A F(α) }, from which E_a was calculated, for example α=0.05 as shown in Figure 3.19.a for the control resin and Figure 3.19.b for the Nanopox F 400 resin. The plots for all measured values of E_a at a

different degree of cure for the control resin and Nanopox F 400 resin can be found in the Appendices A and B. Good linearity was achieved in all the cases, as quantized by R^2.

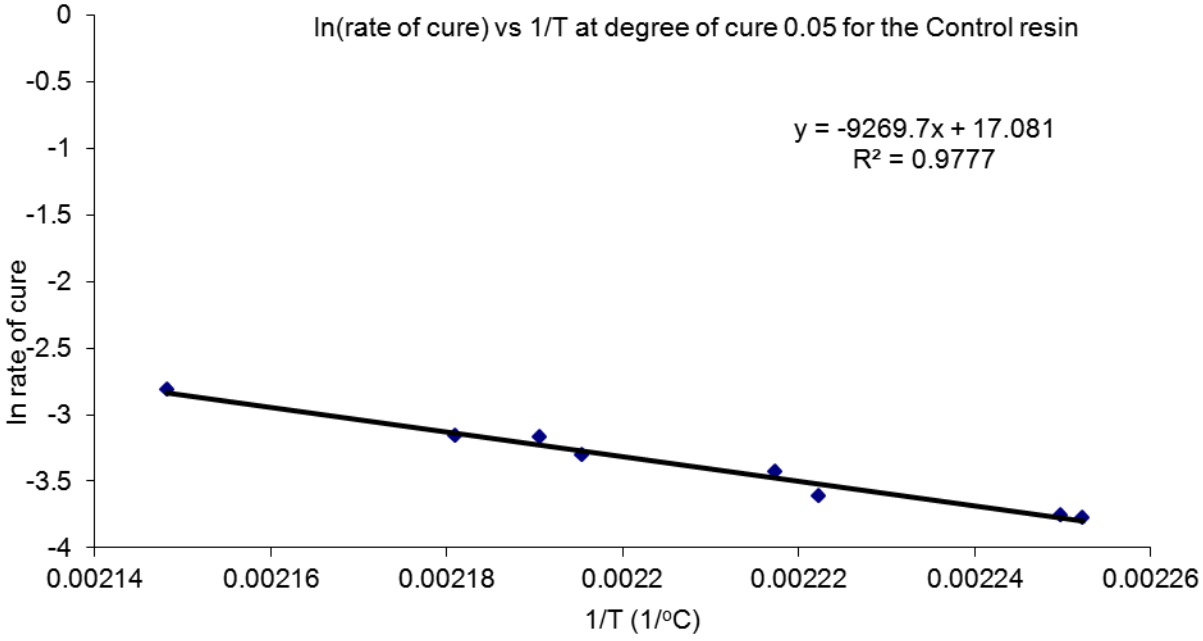

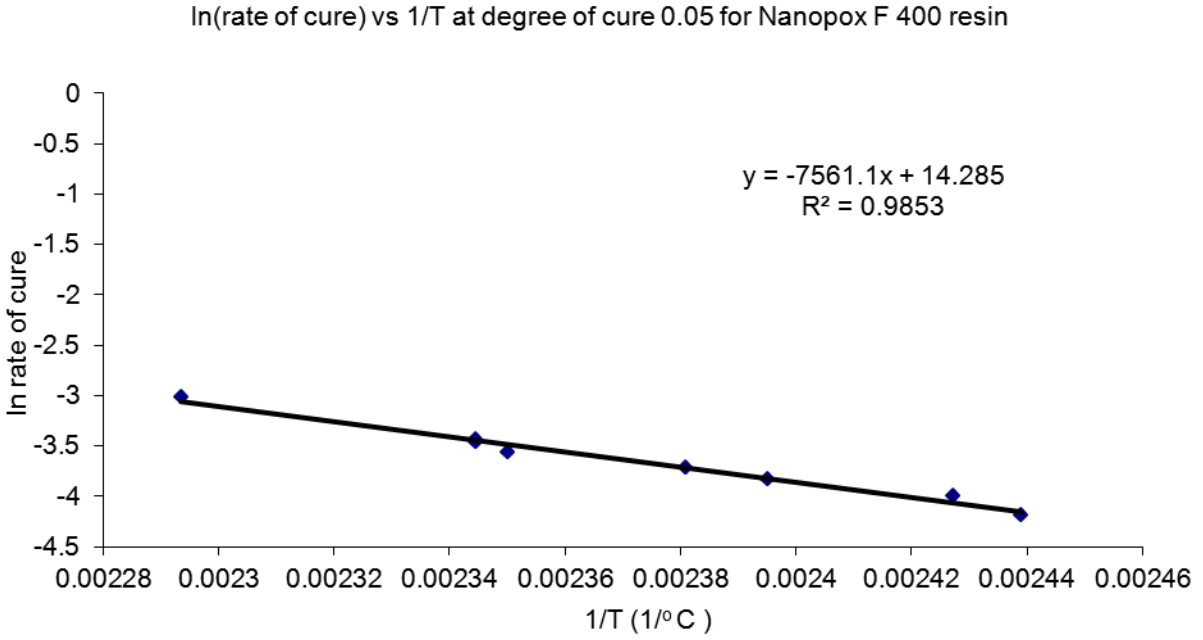

Figure 3.19.(a). Example plot of ln (dα/dt) versus 1/T for the control resin, cured to a fixed degree of cure α = 0.05**. (b)** Example plot of ln (dα/dt) versus 1/T for Nanopox F 400 resin, cured to a fixed degree of cure α = 0.05, both cured with DDS.

The activation energies calculated for the control resin and Nanopox F 400 resin are tabulated in Table.3.2 and plotted in Figure 3.20.

Table 3.2. Activation energies obtained for the control resin and Nanopox F 400 resin.

Degree of cure (α)	Control resin E_a(KJ/mol)	Nanopox F 400 E_a(KJ/mol)
0.05	77.0	62.8
0.1	72.8	63.9
0.15	69.3	68.2
0.2	69.7	71.3
0.25	68.3	70.3
0.3	69.3	69.0
0.35	74.4	68.0
0.4	72.3	69.1
0.45	73.3	66.7
0.5	74.1	67.1
0.55	77.0	70.8
0.6	79.8	76.0
0.65	82.1	81.2
0.7	86.8	87.5
0.75	93.2	98.5
0.8	99.6	107.6
0.85	110.1	110.4
0.9	119.0	105.8
0.95	128.5	92.9

It is clear that there is some difference in behavior between the cure of control resin and Nanopox F 400 resin at high α. For the control resin, the apparent E_a for cure increases more or less steadily as a function of degree of cure, rising from 69 KJ/mol at $\alpha = 0.3$ to 128 KJ/mol at $\alpha = 0.95$. For the Nanopox F 400 resin, at a low degree of cure ($\alpha = 0.15$), the apparent E_a was

nearly the same as for the control system, but as the degree of cure increased, E_a increases to 110 KJ/mol and then dropped back to 92.83 KJ/mol at $\alpha = 0.95$. For the control system, a sharp ascending Ea in the final stages of cure is observed near the completion of the reaction, because of the diffusion controlled reaction. The low activation energy observed for the cure of Nanopox F 400 resin at higher degrees of cure is unusual and indicated that the silica nanoparticles may have some effect on the cure kinetics and perhaps resin structure in the nanocomposite at high conversions.

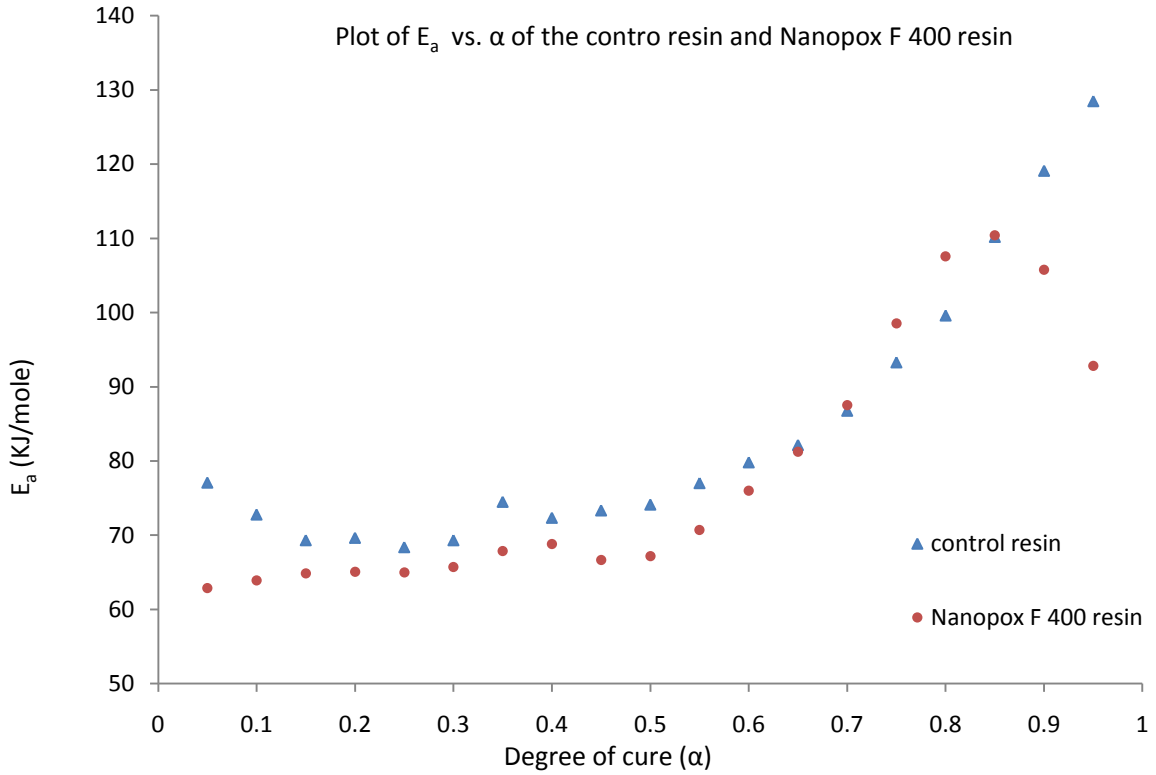

Figure 3.20. Comparison of activation energy (E_a) for cure of the control resin and Nanopox F 400 resin with DDS as a function of degree of cure.

3.2.2 Isothermal Temperature Cure

Isothermal DSC experiments were performed between 140-200 °C with a 10 °C increment to analyze the cure kinetics of the control resin and Nanopox F 400 resin under isothermal conditions.

In isothermal scanning, the sample was ramped quickly to the isothermal temperature at a fast heating rate of 30 °C /min, and then held at that temperature for an hour. After cooling, a second ramped segment was performed to verify any residual curing. The total cure exotherm (total heat of reaction, H_t) was obtained by adding the heat produced during both the isothermal (H_i) and the following ramped exotherm (H_r). The degree of cure (α) at time 't' under isothermal conditions was calculated as the partial area of the isothermal exotherm up to time 't' divided by the area of the total cure exotherm.

Data generated from the isothermal scanning method was used to construct plots for the degree of cure (α) as a function of time over a range of isothermal temperatures (140 ^{o}C to 200 ^{o}C). Figure 3.21 shows that the ultimate degree of cure varies with the cure temperature and time. For the same time, the higher the cure temperature, the higher is the ultimate degree of cure. In addition, at a given temperature, the degree of cure increases rapidly during the initial reaction stage, then increases slowly and finally tends to an intermediate value. This is attributable to the sequence reactions of chain extension, branching and self-cross-linking of DGEBA epoxy resin during the cure process, because these reactions reduce the mobility of the reacting molecules and slow down the reaction rate.

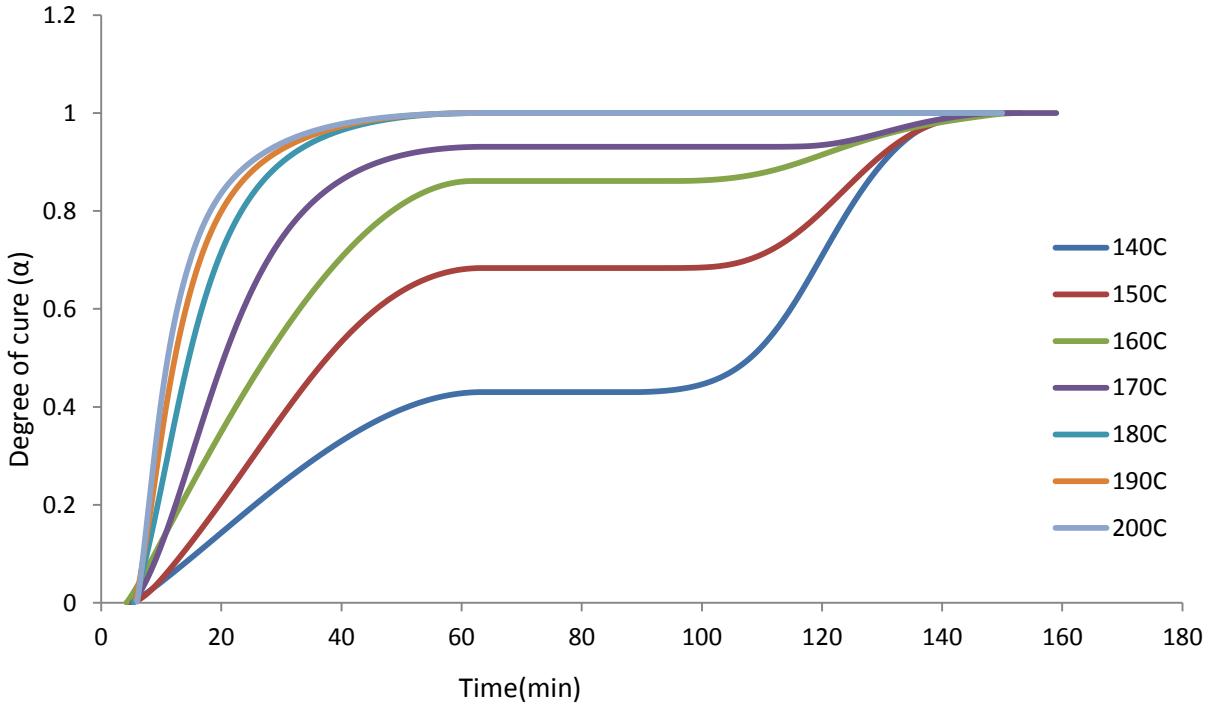

Figure 3.21. Degree of cure (α) as a function of time for the control resin cured with DDS throughout isothermal cure cycles over a range of temperatures.

The rate of cure (dα/dt) is subsequently calculated by differentiating a graph of degree of cure (α) vs. time using origin software. Figure 3.22 summarizes rate of cure vs. time plots obtained for the control resin at isothermal temperatures of 140^{o}C to 200 ^{o}C. The reaction rate, which is proportional to the rate of heat generation, passes through a maximum and then decreases as a function of time. As expected, it is also seen that the higher the isothermal temperature, the higher the cure rate at short times.

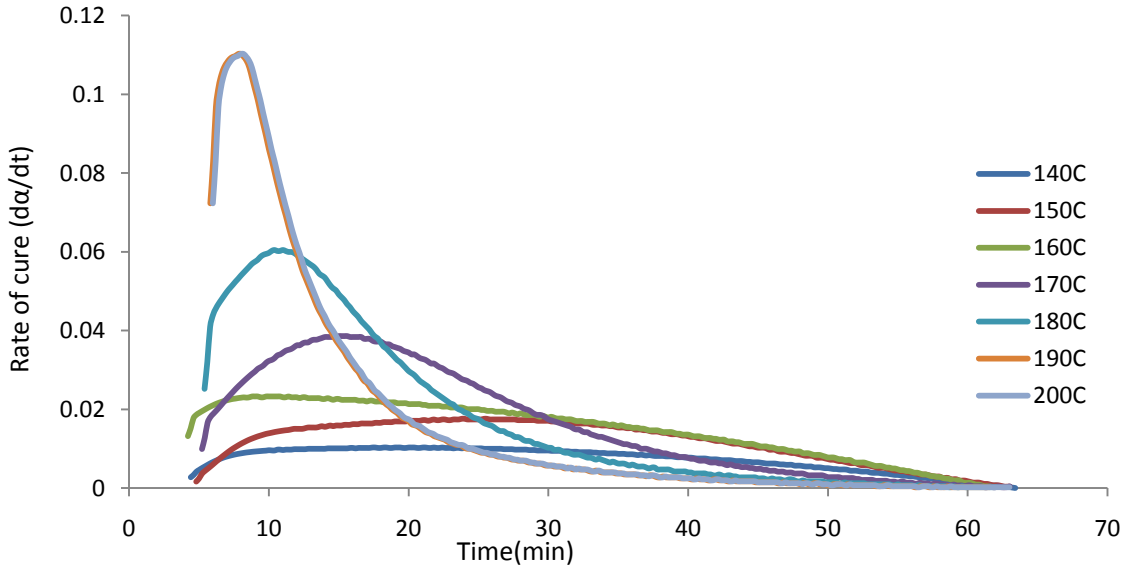

Figure 3.22. Plot of cure rate (dα/dt) as a function of time (min) of the control resin cured with DDS throughout isothermal cure cycles over a range of temperatures.

The degree of cure is plotted as a function of time for Nanopox F 400 resin in Figure 3.23. The cure reaction proceeded rapidly at 200 °C but dropped off at lower temperatures. The plots of rate of conversion versus time for Nanopox F 400 resin cured over a range of isothermal temperatures are shown in Figure 3.24. A measurable difference in a curing exotherm is noticed for the control resin and Nanopox F 400 resin. For example, the maximum degree of cure at the given temperature, α_{max}, is less than 1 ($\alpha_{max} < 1$) for the control resin when cured at lower isothermal temperatures (see Figure 3.25 for isothermal temperature 140 °C). However, Nanopox F 400 resin shows $\alpha_{max} = 1$ at all isothermal temperatures, which shows strong proof of acceleration of cure exotherm by silica nanoparticle and change in resin architecture (see Figure 3.25 and 3.26). From the Figure 3.26, it is also noticed that at higher isothermal temperature, a less effect of silica filler is seen on reaction rate, possibly to a relatively higher influence of temperature on the reaction rate.

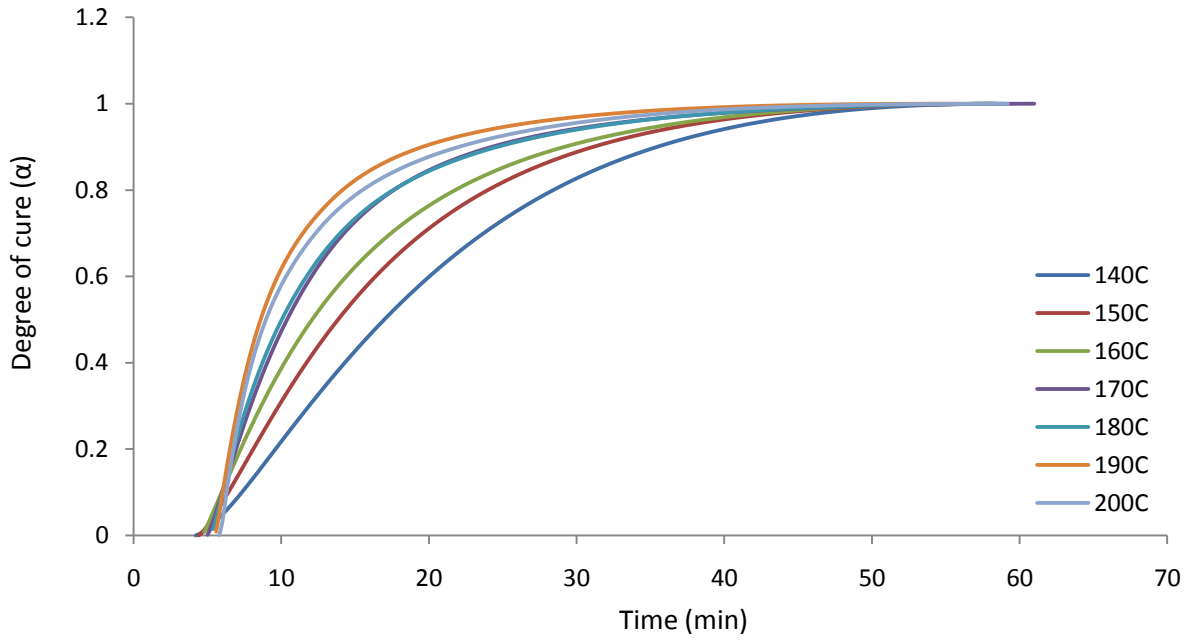

Figure 3.23. Degree of cure as a function of time for Nanopox F 400 resin cured with DDS curative throughout isothermal cure cycles over a range of temperatures (140-200 °C).

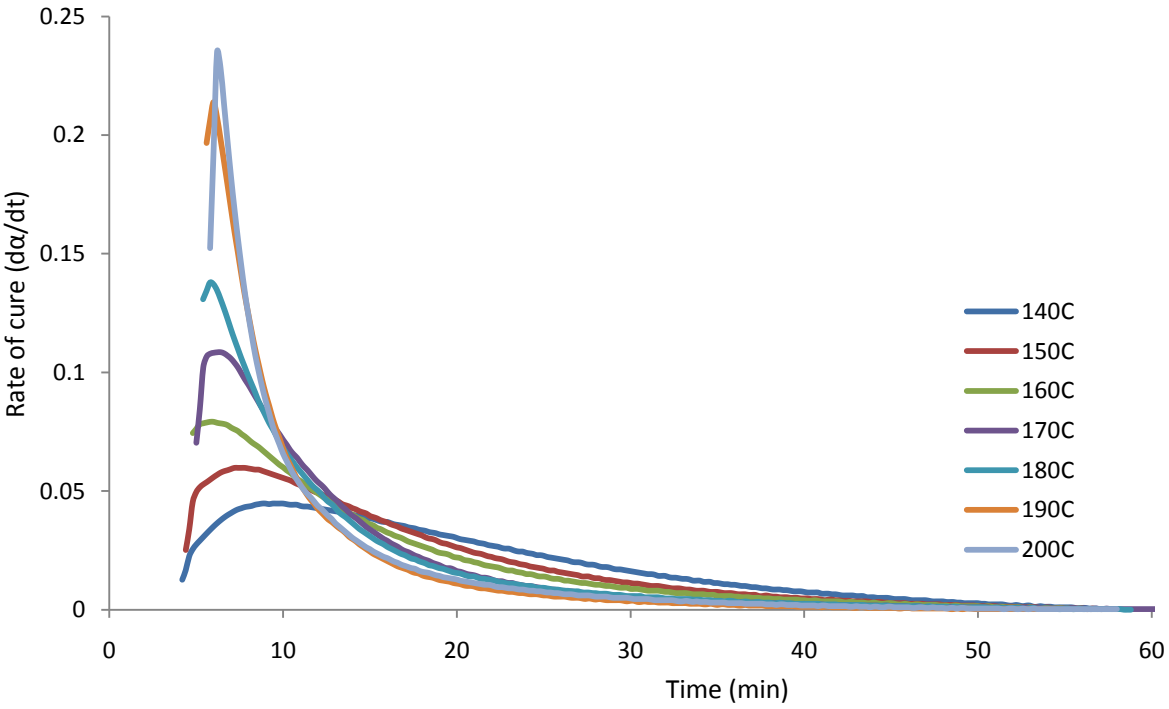

Figure 3.24. Rate of cure as a function of time for Nanopox F 400 resin cured with DDS curative throughout isothermal cure cycles over a range of temperatures (140-200 °C)

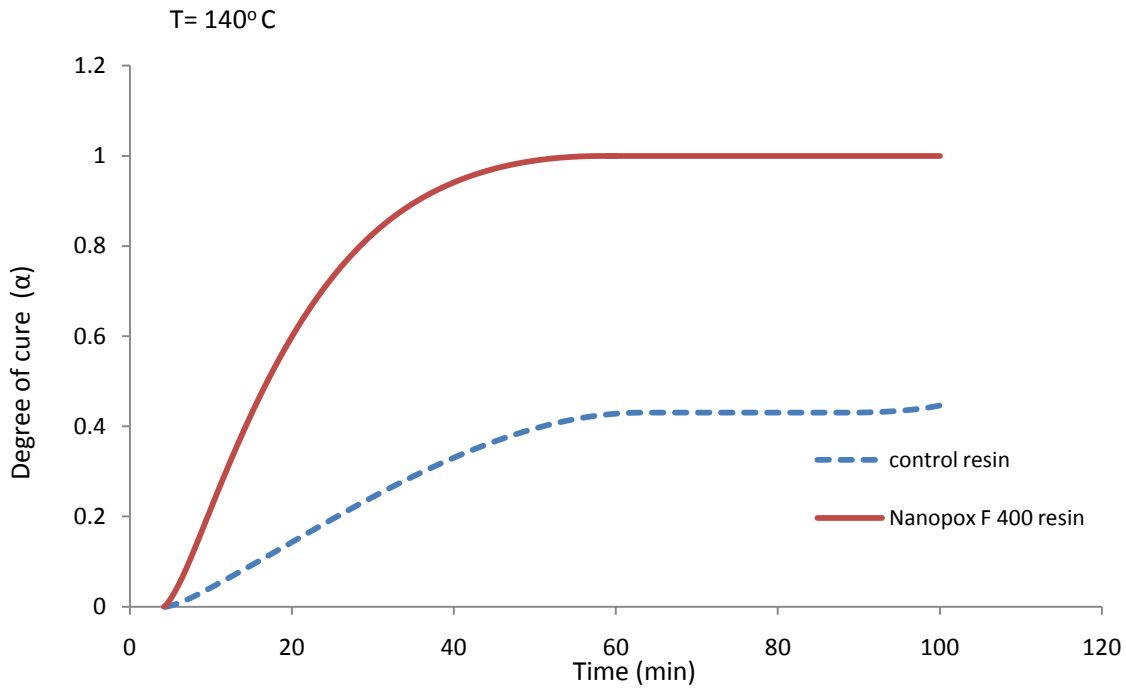

Figure 3.25. Plot of degree of cure versus time to compare conversion between the control resin and Nanopox F 400 resin under isothermal condition at 140 °C.

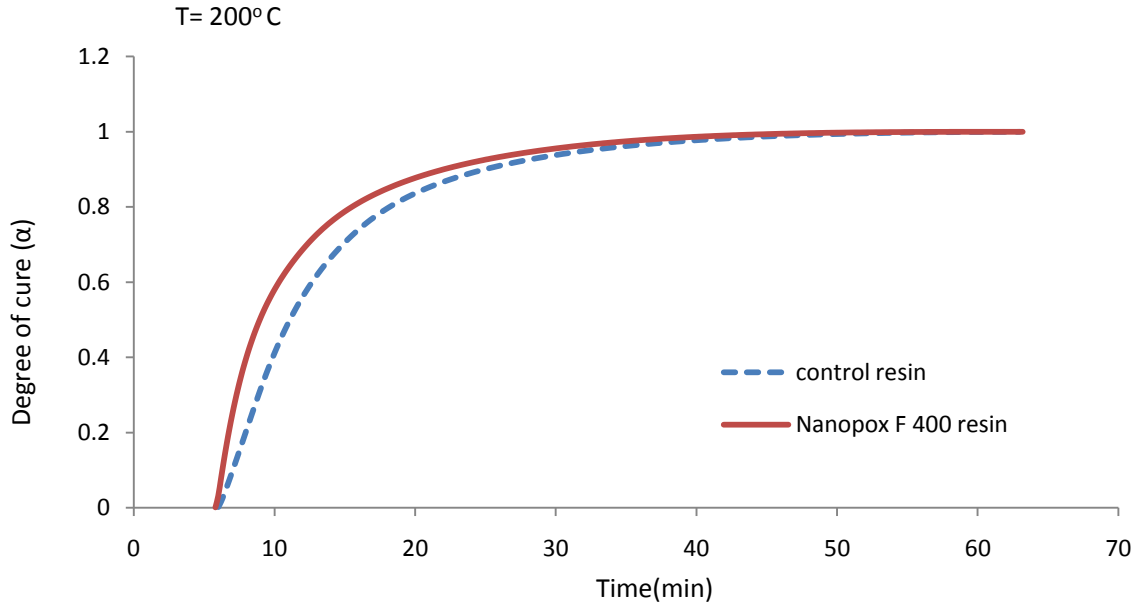

Figure 3.26. Plot of degree of cure versus time to compare conversion between the control resin and Nanopox F 400 resin under isothermal condition at 200 °C.

Apparent Activation Energy for cure under Isothermal Conditions

Activation energies for isothermal cure of the control resin and Nanopox F 400 were determined according to the Kamal kinetic scheme. Rates of cure were correlated with degree of cure, for example at 140°C for the control resin in Figure 3.27.a and Nanopox F 400 resin in Figure 3.27.b. Figure 3.27 shows $\alpha_{max} < 1$ for the control resin whereas in Figure 3.27.b, $\alpha_{max} = 1$ for the Nanopox F 400 resin. As explained earlier, $\alpha_{max} = 1$ was possible for Nanopox F 400 resin due to the accelerating effect of silica nanoparticle in a cure reaction of epoxy resin and amine curative even at low temperatures and, possibly, due to changes in resin architecture and crosslink density. It should also be noted in both instances that a plot of cure rate versus conversion is clearly an autocatalysed reaction i.e., increasing to a rate maximum then decreasing thereafter to zero as the resin vitrifies (see Figure 3.27.a and Figure 3.27.b).

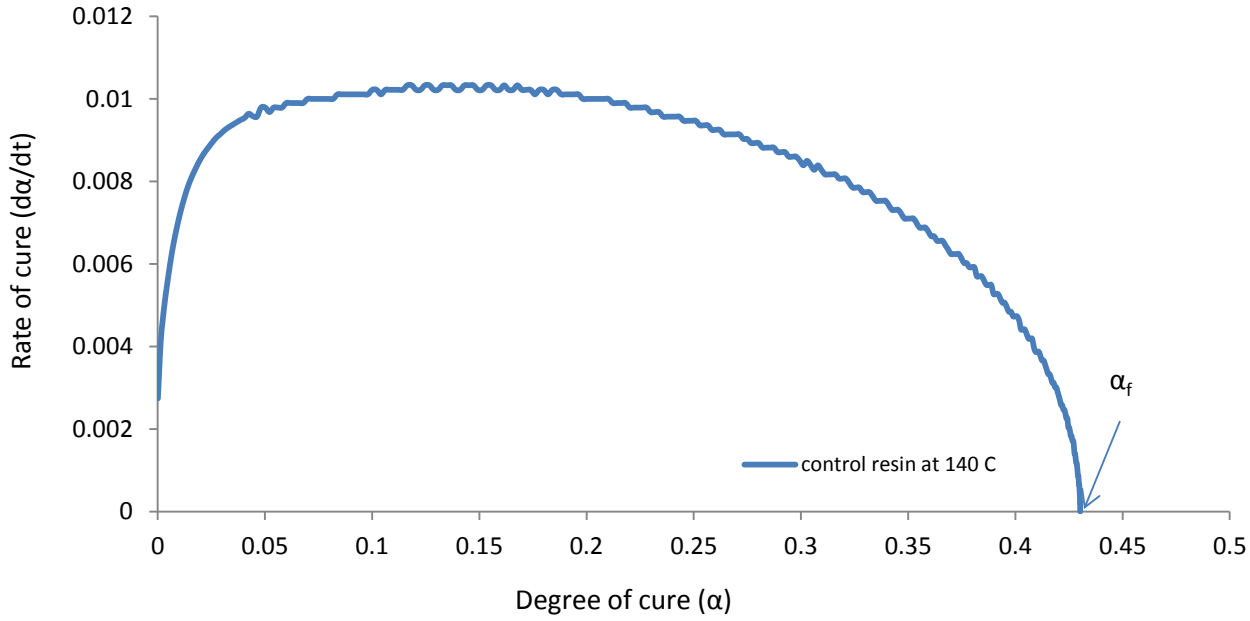

Figure 3.27.a. Plot of rate of cure (dα/dt) vs. degree of cure (α) of the control resin under isothermal condition at 140 °C.

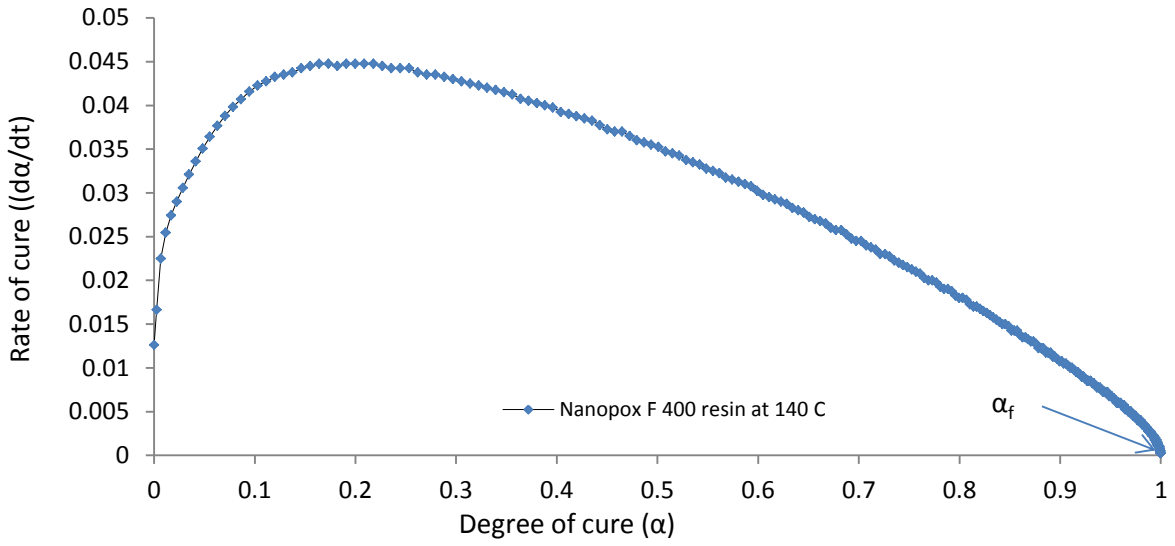

Figure 3.27.b. Plot of rate of cure (dα/dt) vs. degree of cure (α) for Nanopox F 400 resin under isothermal condition at 140 °C.

The isothermal data for the control resin was well fitted to the general Kamal model (equation 3.1). Fitting was done in Origin 8.0 software which uses the Levenberg-Marquardt minimization algorithm. A good correlation was observed over the entire temperature range. Table 3.3 shows the tabulated kinetic parameters for all the temperatures. All four parameters were found to vary with temperatures and degree of cure. The maximum degree of cure achieved at the cure temperature was used in the model.

$$\frac{d\alpha}{dt} = \left(K_1 + K_2\alpha^m\right)\left(\alpha_f - \alpha\right)^n \qquad 3.1$$

K_1 is the rate constant for the reaction catalyzed by groups initially present in the resin, while K_2 is the rate constant for the reaction catalyzed by newly formed groups and represents the influence of the reaction products on the rate of reaction, α is the degree of cure, α_f is the maximum degree of cure at that isothermal temperature, m and n are variables which determine the reaction order and can have different values, with m + n being the overall reaction order.

Assuming K_1 and K_2 follow Arrhenius rate constant dependence, activation energies and pre-exponential factors can be calculated.

$$\ln(K_1) = \frac{-E_{a1}}{RT} + \ln(A_1) \qquad 3.2$$

$$\ln(K_2) = \frac{-E_{a2}}{RT} + \ln(A_2) \qquad 3.3$$

Values of ln{k1} and ln{k2} so obtained were plotted versus inverse temperature and corresponding values of E_{a1} and E_{a2} were obtained from the slope of the plot, which was equal to –{Ea / R}, which is shown in Figure 3.28.a &b.

From the isothermal data of the control resin, E_{a1} and E_{a2} were found to be 78 KJ/mole and 55 KJ/mole respectively. Plots of rate of cure vs. degree of cure for temperature from 150 to 200 °C for the control resin are shown in Appendix C. (The plot of degree of cure vs. rate of cure for 140 °C is shown in Figure 3.27.a).

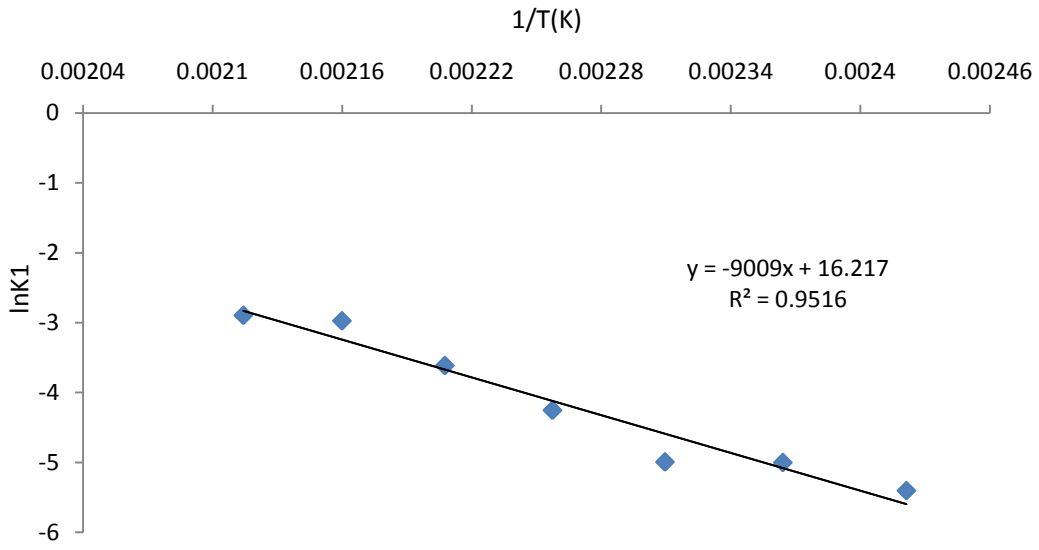

Figure 3.28. a. Plot of $\ln K_1$ versus reciprocal temperature of the control resin. The gradient of the best fit straight line is set to $-E_a/R$.

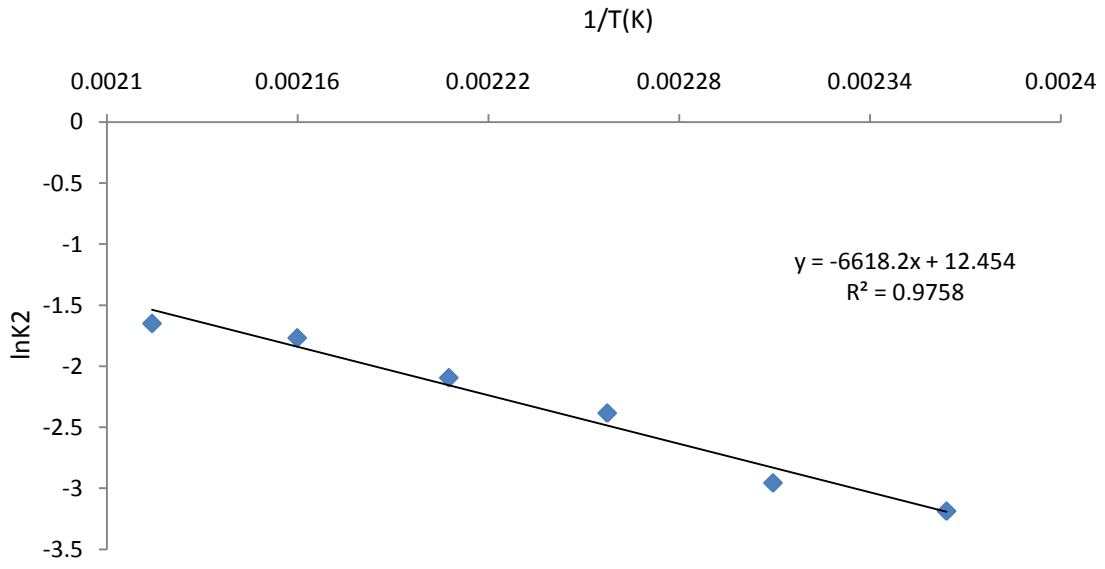

Figure 3.28.b. Plot of $\ln K_2$ versus reciprocal temperature of the control resin. The gradient of the best fit straight line is set to $-E_a/R$.

Table 3.3. Values of K_1, K_2, m & n for the control resin obtained at various temperatures.

Temperature(°C)	α_{max}	K_1	K_2	m	n
140	0.43	0.00451	0.23146	1.25553	5.68747
150	0.68	0.00674	0.0413	0.30728	0.51398
160	0.86	0.0068	0.05203	0.05865	0.45929
170	0.93	0.01424	0.09219	0.53711	0.94917
180	1	0.02697	0.12315	0.55919	1.14401
190	1	0.05114	0.17064	0.63531	1.40554
200	1	0.05534	0.19207	0.42941	1.42411

From the results of dynamic temperature cure analysis, it is clear that the silica nanoparticles have some effect on the cure kinetics of epoxy resin and amine cure reaction. When the general Kamal model was fitted into the experimental data of Nanopox F 400 resin, the model curves of cure rate ($d\alpha/dt$) vs. α do not match well with the experimental data and result in negative values of either K_1 or K_2 (see Table 3.4).

Table 3.4. Values of K_1, K_2, m & n of Nanopox F 400 resin obtained using the General Kamal model.

Temperature(°C)	α_{max}	K_1	K_2	m	n
140	1	-0.00229	0.0764	0.21157	0.83365
150	1	0.01372	0.08447	0.22311	0.98478
160	1	-3.14435	3.24963	0.00211	1.04754
170	1	0.03869	0.14795	0.2388	1.26643
180	1	0.14455	-0.12848	1.67642	0.59021
190	1	0.22469	-0.20652	1.85487	0.69544
200	1	0.21467	-0.20714	1.8239	0.84859

The plot of 1/T (K) as X and K_1 as Y is shown in Figure 3.29. The plot of 1/T (K) as X and K_2 as Y is shown in Figure 3.30. Figure 3.29 and 3.30 shows that R^2 indicates poor linearity in both the cases which supports the fact that the general Kamal model does not fit the experimental isothermal data for Nanopox F 400 resin.

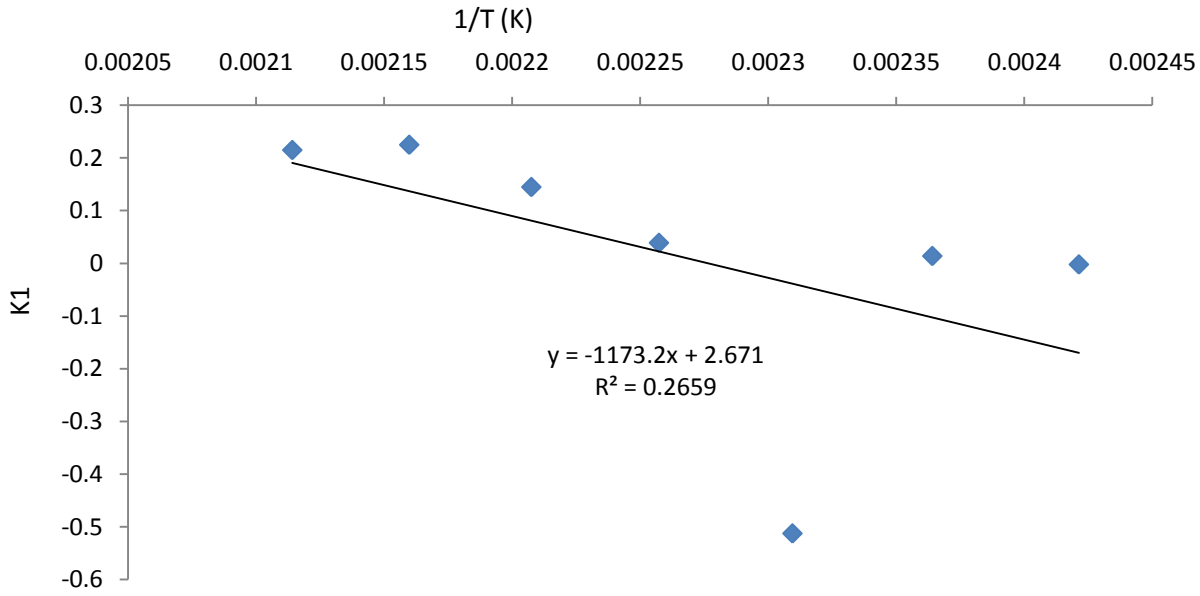

Figure 3.29. Plot of 1/T (K) as X and K_1 as Y showing the quantized R^2 value.

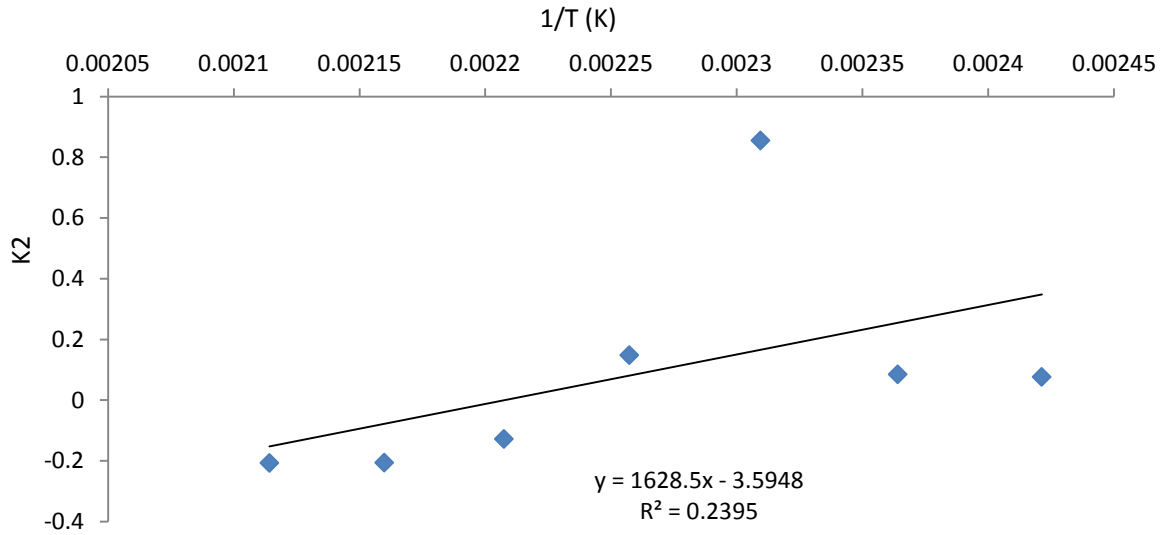

Figure 3.30. Plot of 1/T (K) as X and K_2 as Y showing the quantized R^2 value.

Since, it is not possible to obtain first activation energy (E_{a1}) and second activation energy (E_{a2}) with negative values of K_1 and K_2, Nanopox F 400 resin is better fitted to the modified Kamal model below (equation 3.4) assuming $K_1 = 0$ at t=0, when there is a total ultimate conversion.

$$\frac{d\alpha}{dt} = K_2 \alpha^{m} (1-\alpha)^{n} \qquad 3.4$$

Where K_2 is the rate constant for the reaction catalyzed by newly formed hydroxyl groups, α is the degree of cure and m and n are variables which determines the reaction order, and can have different values, with m + n being the overall reaction order.

K_2 is the rate constant for cure as defined by the Arrhenius relationship:

$$K_2(T) = A_2 \exp(E_{a2}/RT) \qquad 3.5$$

Where A_2 is the frequency factor or pre-exponential constant, E_{a2} is the activation energy, R is the universal gas constant, T is the processing temperature expressed in degrees kelvin (K).

Three parameters *m, n* and *k* were computed from the experimental data using the modified Kamal model (equation 3.4) for the Nanopox F 400 resin. The results are furnished in Table 3.5. A good correlation was obtained for the entire range of temperatures. By plotting the values of $\ln\{K_2\}$ as Y and 1/T as X (Figure 3.31), corresponding value of E_{a2} is obtained from the slope of the plot, which is equal to $-\{E_a/R\}$. The activation energy (E_{a2}) calculated for Nanopox F 400 resin is 42 KJ/mole.

Plots of rate of cure vs. degree of cure for temperature from 150 to 200 °C are shown in Appendix D for the Nanopox F 400 resin (The plot of rate of cure vs. degree of cure for temperature 140 °C is shown in Figure 3.27).

Table 3.5. Values of *m*, *n*, and K_2 estimated at various temperatures for Nanopox F 400 resin fitted to the modified Kamal model.

Temperature(°C)	α_{max}	K_2	m	n
140	1	0.07469	0.22411	0.8378
150	1	0.09435	0.1643	0.9615
160	1	0.10704	0.07851	1.05677
170	1	0.17661	0.15055	1.23293
180	1	0.17875	0.06447	1.29816
190	1	0.30564	0.09248	1.46801
200	1	0.33832	0.1118	1.70821

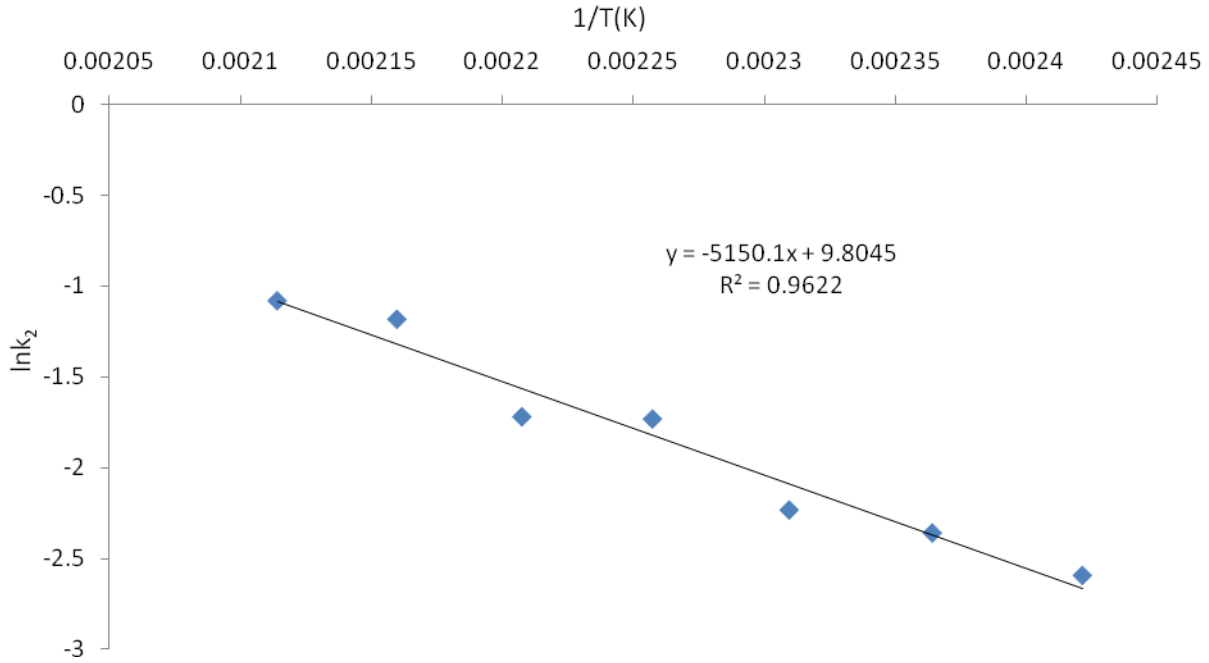

Figure 3.31. Plot of $\ln K_2$ versus reciprocal temperature for Nanopox F 400 resin. The gradient of the best fit straight line is set to –Ea/R.

3.2.3 Dynamic Mechanical Analysis (DMA)

DMA measures shear stiffness and damping, these are reported as shear modulus (G) and the phase lag angle, Tanδ. Figure 3.32 shows the dynamic-mechanical spectra expressed in terms of shear storage modulus (Figure 3.32.a) and loss factor (Figure 3.32.b), Tanδ, as a function of temperature for the control resin and Nanopox F 400 resin.

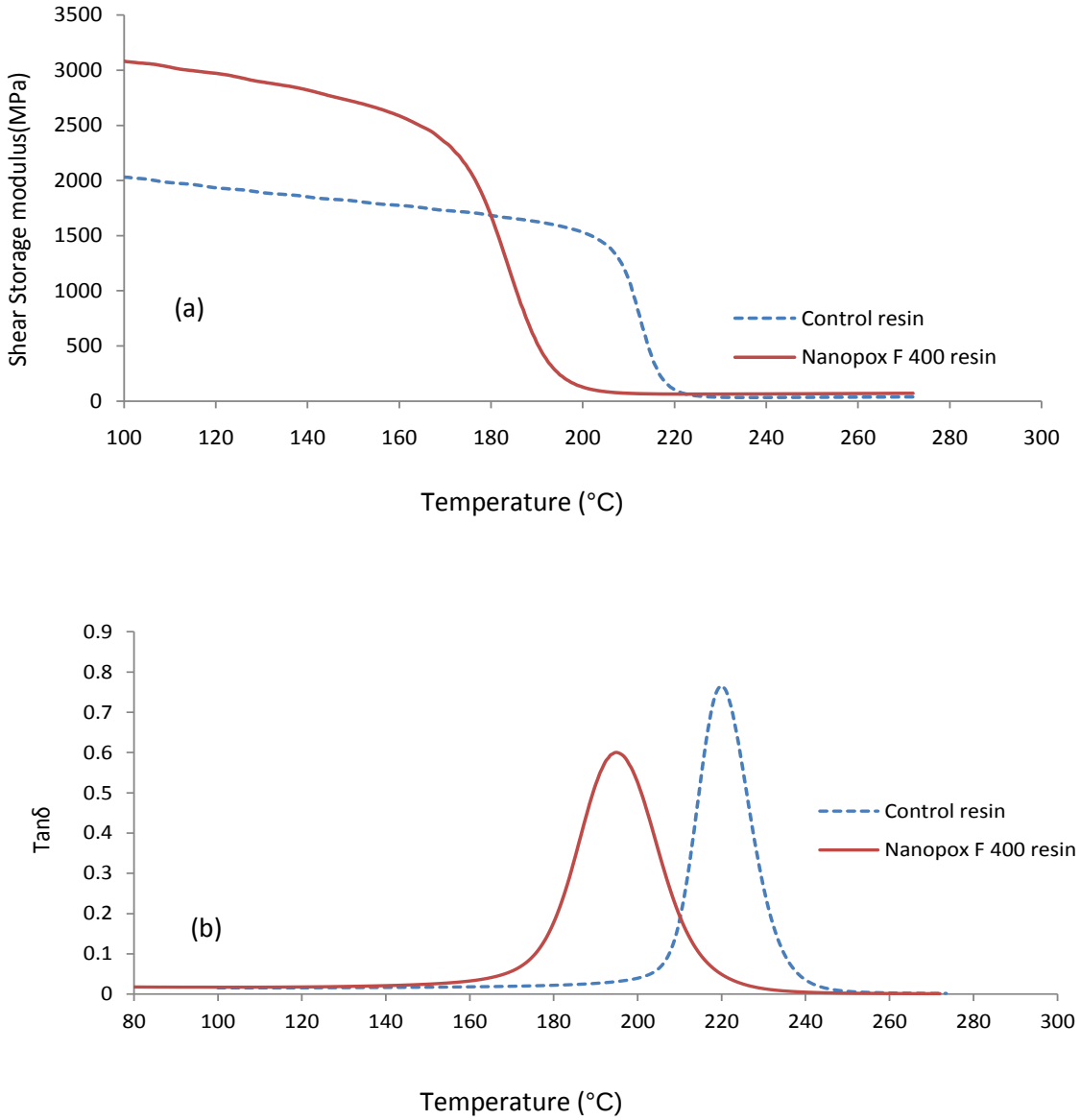

Figure 3.32. Variation of storage modulus (a) and Tanδ (b) as a function of temperature for the control resin and Nanopox F 400 resin.

As the temperature increased, both the control resin and Nanopox F 400 resin show a gradual drop in storage modulus (Figure 3.32.a). The subsequent sharp drop in modulus in both the resins is related to the materials transition from a glassy to a rubbery state and is usually referred to as T_α or T_g. The results of Figure 3.32.a and Figure 3.32.b are summarized in Table 3.6. Both the onset of the loss of storage modulus and $Tan(\delta)_{max}$ values indicate that there is a reduction in the glass transition temperature of Nanopox F 400 resin in comparison with the control resin. As mentioned, surface modification of the silica filler increases the interfacial interaction between silica filler and epoxy matrix. The increased resin-filler interface possibly creates extra free volume which assists the large-scale segmental motion in the Nanopox F 400 resin, thus, resulting in a lower T_g. The reduction of the height of relaxation processes for the Nanopox F 400 resin is observed than the control resin, which is possibly due to the less amount of resin in Nanopox F 400 resin i.e. 60 wt.% resin and 40 wt.% silica filler than the control resin (100 wt.% resin).

Table 3.6. Summary of glass transitions temperatures observed for the control resin and for Nanopox F 400 resin from Dynamic Mechanical Analysis (DMA).

	N-H/epoxy ratio	**Onset of loss of the Storage Modulus**	**$Tan(\delta)_{max}$**
Sample #		Tg[°C]	Tg[°C]
Control resin	1.1/1	210.4	219.9
Nanopox F 400 resin	1.1/1	179.9	195.2

.

3.2.4 Thermal Mechanical Analysis

A TMA analysis of the control resin and Nanopox F 400 resin, is shown in Figure 3.33.a and 3.33.b. The TMA penetration results shows that the control resin expresses a softening temperature (T_s) at 206 °C (Figure 3.33.a) and Nanopox F 400 resin at 150 °C (Figure 3.33.b).

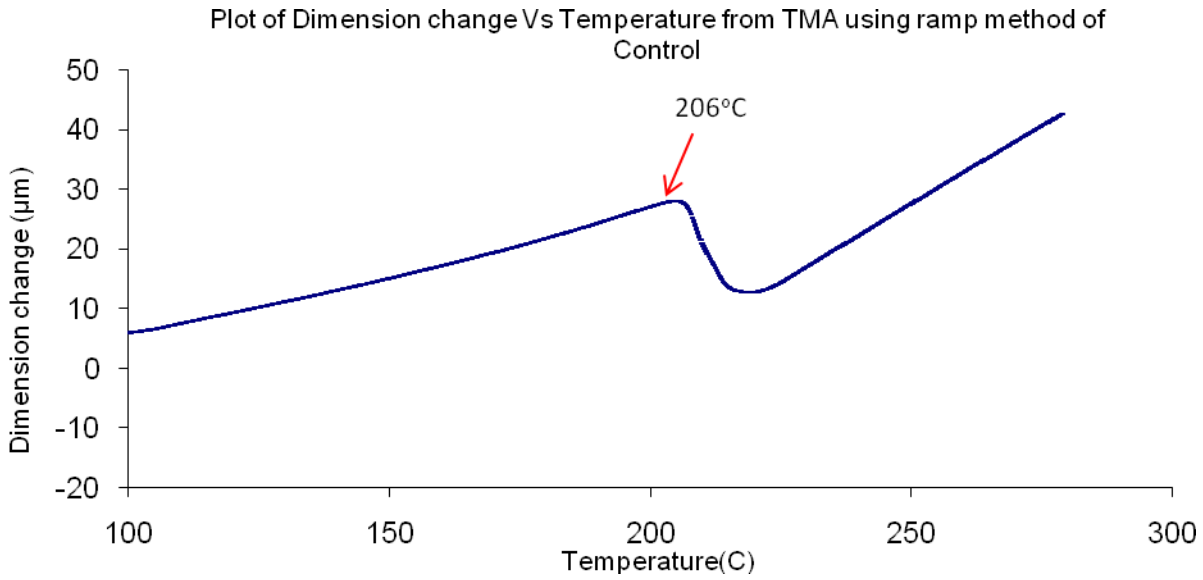

Figure 3.33.a. Plot of dimension change vs. temperature obtained by TMA for the control resin cured with DDS curative.

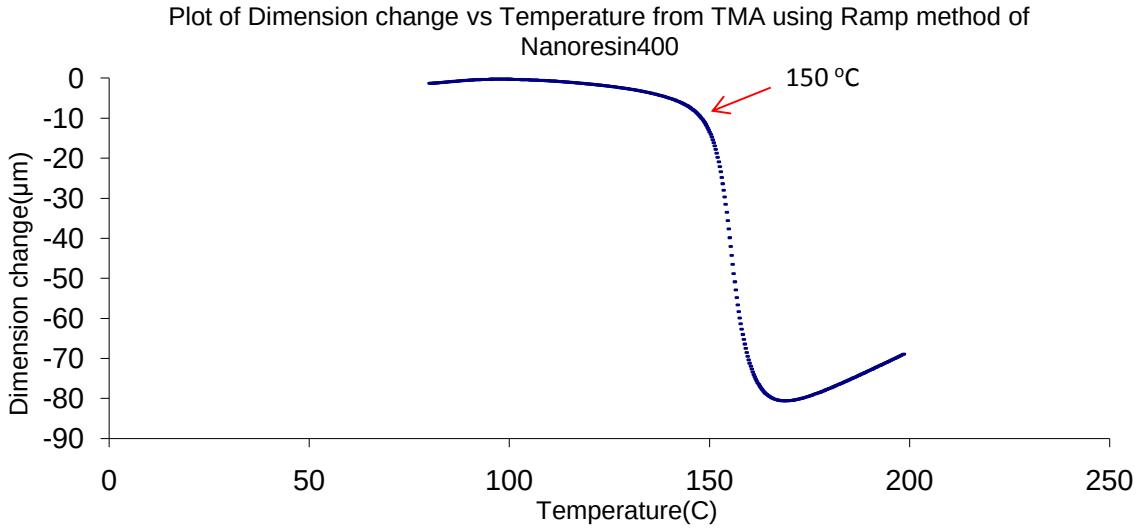

Figure 3.33.b. Plot of dimension change vs. temperature obtained by TMA for Nanopox F 400 resin cured with DDS curative.

Table 3.7. Softening point for the control resin and Nanopox F 400 resin.

Sample name	% wt. of silica filler	T_s(^{o}C)
Control resin	0	206.4
Nanopox F 400 resin	40	150.3

Results shown in Table 3.7 indicate a drop in the onset of the softening temperatures (T_s) with the addition of silica filler in an epoxy resin. It is possible that the reduced softening temperature of Nanopox F 400 resin is due to changes in the resin network structure brought about by cure in the presence of the silica nanoparticle.

As expected, the glass transition temperature and changes in the T_g found in TMA analysis are in line with DSC analysis and DMA analysis. In all three analyses, T_g of the control resin is higher than that of the Nanopox F 400 resin.

3.3 Mechanical Properties

3.3.1 Tensile Properties

3.3.1.1 Effect of Curing agent/Resin Ratio on the tensile properties of silica reinforced epoxy resin

Stoichiometric relationships between curing agent and epoxy resin have significant effects on the tensile properties, such as Young's modulus (E), ultimate tensile strength (σ_u), and ultimate elongation (ϵ_u) of the epoxy resin. The changes observed on the mechanical properties of completely cured epoxy resin, when the epoxy resin to curing agent ratio is varied are considered a direct consequence of the formation of different macromolecular structures. The cure reactions first take place by the primary amino addition reaction, occurring between the primary amines (~NH_2) and the epoxide group according to the following reaction:

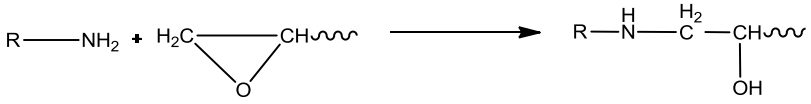

(a)

Such reactions lead to the formation of secondary amines and hydroxyl groups (-OH). Further reaction of secondary amines with another epoxide group forms second hydroxyl and tertiary amine group.

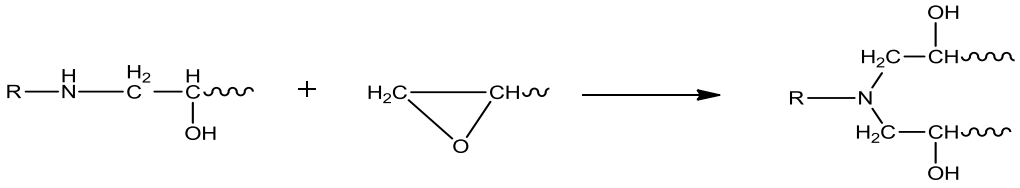

(b)

Etherification reactions may take place between the hydroxyl groups formed in the above reactions (a) and (b) and any excess epoxy group not consumed by reaction with amines.

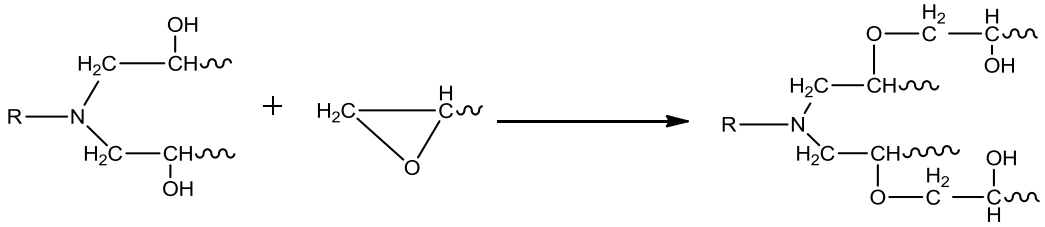

Homopolymerization reactions may occur in presence of excess epoxy monomer, leading to the formation of the dioxane ring structures as follows:

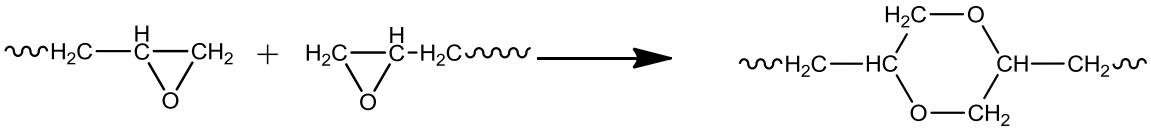

To study the effects of curing agent/resin molar ratio on the tensile properties of a silica reinforced epoxy system, the tensile properties of the control resin (pure DGEBA epoxy resin + DDS curative) and the commercially available silica reinforced epoxy resin (Nanopox F 400 resin + DDS curative) were compared. Nanopox F 400 resin contains 40 wt. % of surface modified silica nanoparticles in DGEBA epoxy resin prepared by the sol gel technique. The preparation of Nanopox F 400 resin constituted a "trade secret" that the supplier would not divulge. The control resin and Nanopox F 400 resin were cured with curing agent, DDS, and prepared in three molar N-H/epoxy ratios: 0.9:1 (N-H below stoichiometry), 1:1(N-H/epoxy stoichiometry), 1.1:1(N-H above stoichiometry) respectively.

The stress (σ)-strain (ϵ) curve at low strain is used to calculate Young's modulus (E), which is the slope of the stress-strain plot. For example-the initial portion of the stress strain curve for the first control resin (DGEBA+DDS) specimen cured with DDS with an N-H/epoxy

ratio of 1.1:1 is reproduced in Figure 3.34. Summary data from all the control resin specimens cured with DDS at an N-H/epoxy molar ratio 1.1:1 are reproduced in Figure 3.35 and the tensile results are furnished in Table 3.8. The summary of stress-strain curves of the control specimens cured with DDS at an N-H/epoxy molar ratio of 0.9:1 and 1:1 are reproduced in Appendix E. The averages of five resin specimens were tested for each sample type. Tensile test results of the control resin specimens cured with the three different molar ratios of DDS are summarized in Table 3.9.

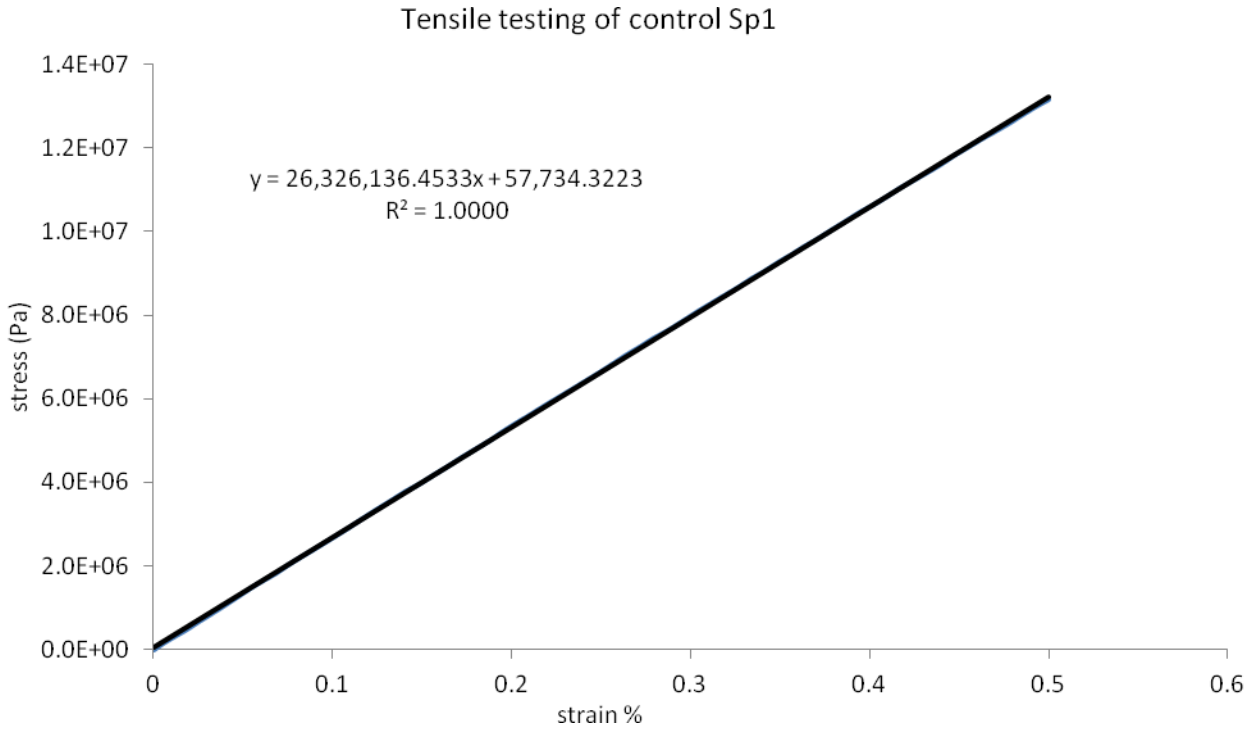

Figure 3.34 . Stress-strain curve at low strain (ϵ) for the first specimen of the control resin cured with DDS curative at an N-H/epoxy ratio 1.1:1. (Sample specimen was stretched at a speed of 5 mm/min)

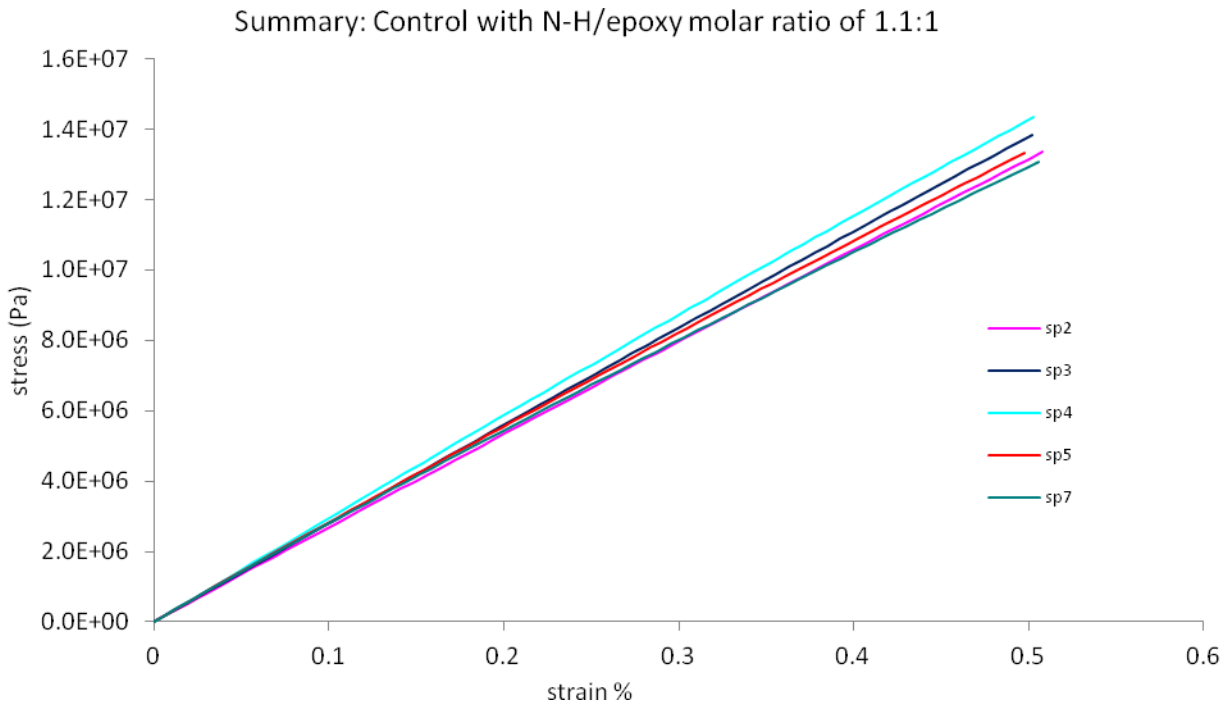

Figure 3.35. Summary of stress-strain plot at low strain (ε) for the control specimens cured with DDS curative at an N-H/epoxy molar ratio of 1.1:1. (Sample specimen were stretched at a speed of 5 mm/min)

Table 3.8. Tensile test results of the control resin cured with DDS at an N-H/epoxy molar ratio of 1.1:1. (Percentage relative standard deviation, %RSD)

Sample	Modulus (E) GPa	Strain to failure (ε_u)	Stress at break (σ_u) MPa)
2	2.63	5.3	74.0
3	2.76	6.1	77.3
5	2.67	6.2	75.9
6	2.87	5.5	59.8
7	2.54	4.1	73.9
Ave	2.69	5.4	72.2
Std.dev	1.3	0.8	7.1
%RSD	4.7	15.5	9.8

Table 3.9. Summary of tensile test results of the control resin cured with the three different molar ratios of DDS curative. (Standard deviation is shown as ±)

Material	molar ratio of DGEBA	molar ratio of DDS	Modulus (E) GPa	Stress at break (σ_u) MPa	Strain to failure (ϵ_u) %
Control resin	1	0.9	2.0±1.2	62±9.2	2.94±0.6
Control resin	1	1	2.4±0.3	70±6.9	5.57±0.4
Control resin	1	1.1	2.7±1.2	72±7.1	5.47±0.8

Stress-strain curve at low strain (ε) is also plotted for Nanopox F 400 resin cured with DDS curative at an N-H/epoxy molar ratio 1.1:1 as shown in Figure 3.36 for the first specimen. The summary plot and tensile results are given in Figure 3.37 and Table 3.10. The summary of stress-strain curves of Nanopox F 400 resin specimens cured with DDS at an N-H/epoxy molar ratio of 0.9:1 and 1:1 are reproduced in Appendix E. Tensile test results of Nanopox F 400 resin specimens cured with the three different molar ratios of DDS curative are summarized in Table 3.11.

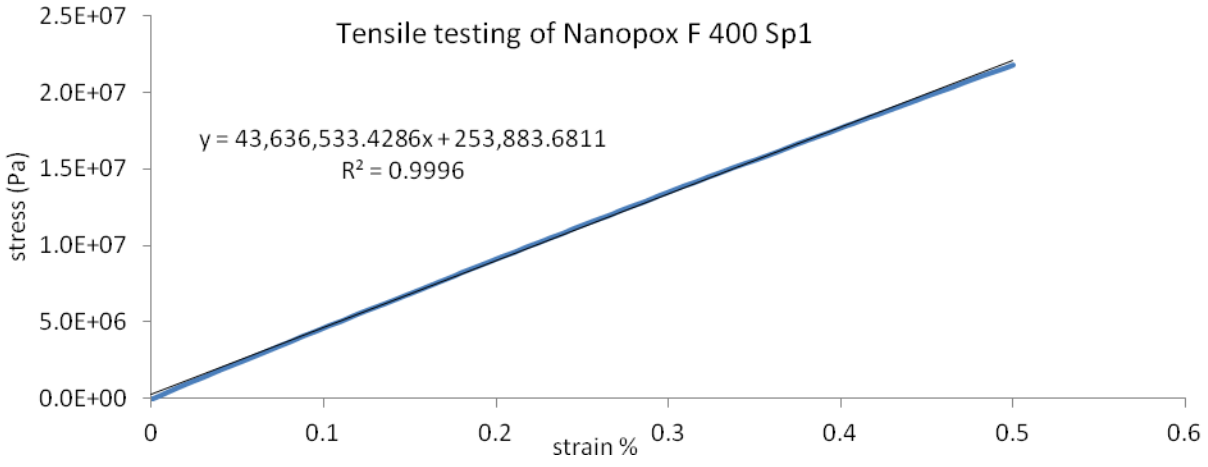

Figure 3.36. Stress-strain curve at low strain (ε) for the first specimen of Nanopox F 400 resin cured with DDS curative at an N-H/epoxy molar ratio 1.1:1. (Sample specimen was stretched at a speed of 5 mm/min)

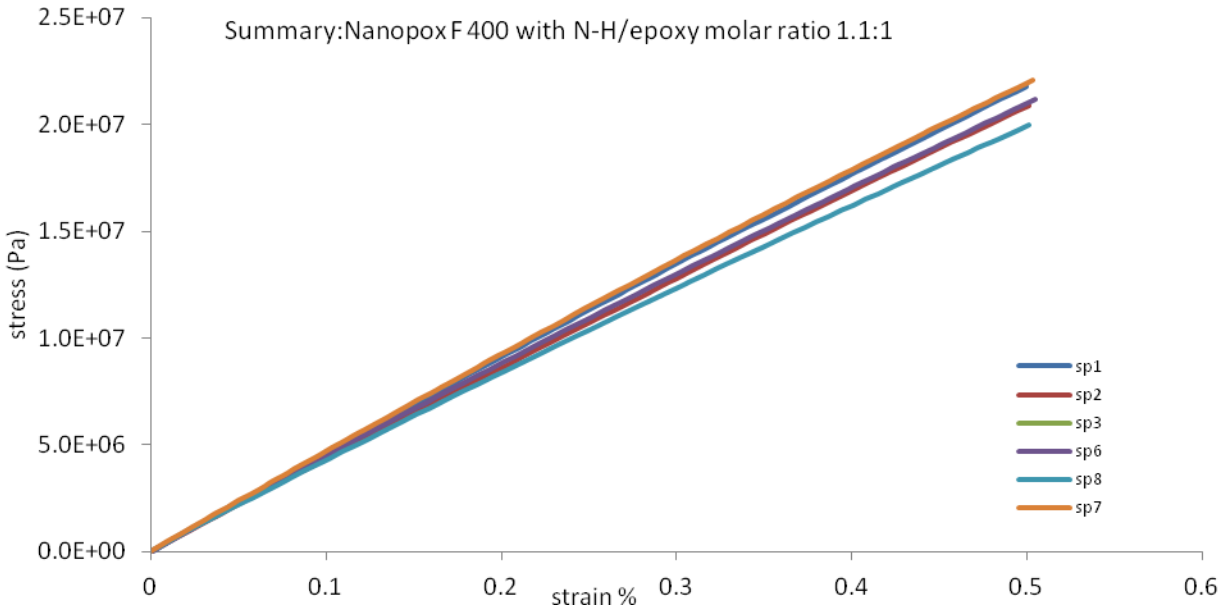

Figure 3.37. Summary of stress-strain plot at low strain (ε) for Nanopox F 400 resin specimens cured with DDS curative in N-H/epoxy ratio of 1.1:1. (Sample specimen were stretched at a speed of 5 mm/min)

Table 3.10. Tensile test results of Nanopox F 400 resin cured with DDS at an N-H/epoxy molar ratio of 1.1:1. (Percentage relative standard deviation, %RSD)

Sample	Modulus (E) GPa	Strain to failure (ε_u) %	stress at break (σ_u) MPa
1	4.36	3.3	62.7
2	4.59	1.6	52.8
3	4.18	3.7	72.3
6	4.18	2.1	59.0
8	3.98	2.3	57.2
7	4.41	3.3	74.1
Ave	4.28	2.7	63.0
Std dev.	2.2	0.8	8.5
%RSD	5.0	30.9	13.5

Table 3.11. Summary of tensile test results of Nanopox F 400 resin cured with the three different molar ratios of DDS curative.

Material	molar ratio of DGEBA	molar ratio of DDS	Modulus (E) GPa	Stress at break(σ_u) MPa	Strain to failure (ε_u) %
Nanopox F 400 resin	1	0.9	3.5±1.3	47±7.6	2.05±0.4
Nanopox F 400 resin	1	1	3.8±2.3	57±6.1	2.04±0.2
Nanopox F 400 resin	1	1.1	4.3±2.1	63±8.5	2.72±0.9

The effect of curing agent/resin molar ratio on the tensile properties of the control resin and Nanopox F 400 resin both cured with DDS curative is discussed in terms of Young's modulus (E), stress at break (σ_u) and strain at break (ε_u) below.

3.3.1.1. a. Effect of the curing agent/resin molar ratio in the elastic modulus (E)

Figure 3.38 summarizes the Young's modulus (E) obtained for the control resin and Nanopox F 400 resin systems both cured with DDS curative as a function of active amine/epoxy mole ratio.

The control resin cured with DDS at an N-H/epoxy molar ratio 0.9:1 shows a brittle behavior with lower Young's modulus (E) compared to N-H/epoxy molar ratio 1.1:1. This could be related to the relatively excess of resin monomer in a cured epoxy resin. The excess resin monomer could not find enough curing agent to form crosslinks and acts like soft spots or voids in the polymer structure from where cracks may nucleate, thus, showing brittle behavior. It can be seen from the Figure 3.38, the higher the concentration of amine group in the epoxy resin, the higher is the Young's modulus (E) of the epoxy system. This higher Young's modulus (E) of amine rich epoxy system (N-H/epoxy molar ratio 1.1:1) is due to the formation of a highly crosslinked network with some secondary amine content and the high crosslinked material shows higher resistance to the pulling load.

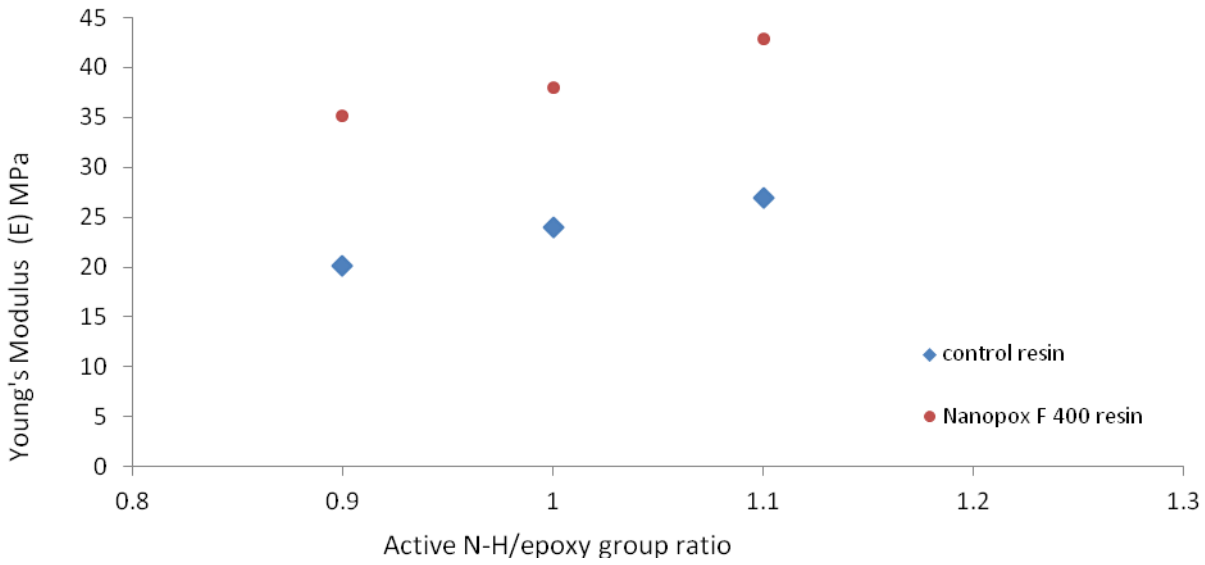

Figure 3.38. Plot of Young's modulus (E) obtained from the stress-strain curve at low strain (ε) (Refer Figure 3.34 & 3.36) with respect to active N-H/epoxy group ratio of the control resin and Nanopox F 400, both cured with DDS curative.

For the Nanopox F 400 resin, the Young's modulus values varied from the epoxy rich system i.e. N-H/epoxy ratio 0.9:1 to the amine rich epoxy system i.e. N-H/epoxy ratio 1.1:1 as shown in Figure 3.38. The trend of increase in stiffness is seen with increasing the amine concentration in Nanopox F 400 system. Nanopox F 400 cured with DDS at an N-H/epoxy molar ratio 1.1:1 shows higher modulus which could be possible, due to formation of cross-linked network provided by the higher concentration of amine curing agent. However, Nanopox F 400 resin cured with DDS at an N-H/epoxy molar ratio 0.9:1 shows lower Young's modulus (E) than the Nanopox F 400 cured with DDS at an N-H/epoxy molar ratio 1:1 which could be due to less crosslinked network than the stoichiometric formulation.

The Young's modulus (E) for the Nanopox F 400 resin system is found to be higher than that for the control resin system. This is due to the addition of high modulus silica nanoparticles

in Nanopox F 400 resin, which imparts a better rigidity to the epoxy resin system making the material more stable and showing higher resistance to the pulling load.

3.3.2.1. b. Effect of curing agent/resin molar ratio on the Ultimate Tensile Strength (σ_u)

The tensile strength, or ultimate tensile strength (UTS), is the maximum load divided by the original cross-sectional area of the specimen. Figure 3.39 shows the relation between the ultimate tensile strength (σ_u) and the active N-H/epoxy group ratio of the control resin and Nanopox F 400 resin systems both cured with DDS curative.

The control resin cured with DDS at an N-H/epoxy molar ratio 1.1:1, exhibits higher stress at break at all times which is due to the higher degree of cross-linking between epoxy monomer and curing agent. A higher degree of cross-linking makes the material strong and shows higher resistance to the pulling load. However, the control resin cured with DDS at an N-H/epoxy molar ratio 0.9:1 needs a lower strength to break due to fewer secondary N-H groups to form bonds with the epoxy resin which results in a less crosslinked network. The control resin cured with DDS at an N-H/epoxy molar ratio of 1:1 (stoichiometric formulation) shows higher tensile strength than the control resin cured with DDS at an N-H/epoxy molar ratio 0.9:1 but still the control resin cured with DDS at an N-H/epoxy molar ratio 1.1:1 is the best.

For the Nanopox F 400 resin system, the material also shows an increase in tensile strength with an increasing amine concentration in the cure mixture. As the amine concentration increases in the mixture, the tensile strength increases and a maximum forms at N-H/epoxy molar ratio 1.1:1. Nanopox F 400 cured with DDS at an N-H/epoxy molar ratio 1.1:1 shows high ultimate tensile strength due to increase in intermolecular packing and some hydrogen bonding provided by a little excess of amine concentration in the mixture.

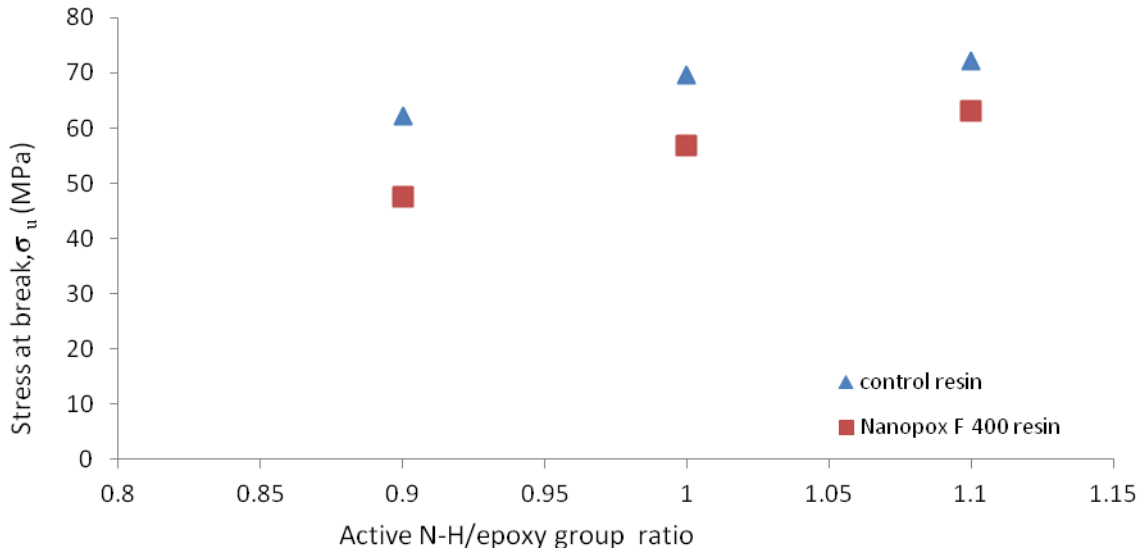

Figure 3.39. Ultimate tensile strength (σ_u) vs. active N-H/epoxy group ratio of the control resin and Nanopox F 400 resin cured with DDS curative.

The tensile strength of Nanopox F 400 resin system is lower than that of the control resin system. This is attributed to the increased tendency of silica nanoparticles to form agglomerates at higher concentrations (40 wt. % surface modified silica filler in Nanopox F 400 resin) which acts as defects initiating the fracture at high strain, despite the increased adhesion of surface modified silica nanoparticles in an epoxy matrix.

3.3.2.1. c. Effect of the curing agent/resin molar ratio on the Elongation at break

The elongation at break is obtained by dividing the elongation of the gage length of the specimen, **d**, by its original length.

$$e = \frac{d}{L_0} = \frac{\Delta L}{L} = \frac{L - L_0}{L_0}$$

Figure 3.40 shows elongation at break (ε_u) of the control resin and Nanopox F 400 resin systems cured with DDS at an N-H/epoxy molar ratio of 0.9:1, 1:1, and 1.1:1 respectively.

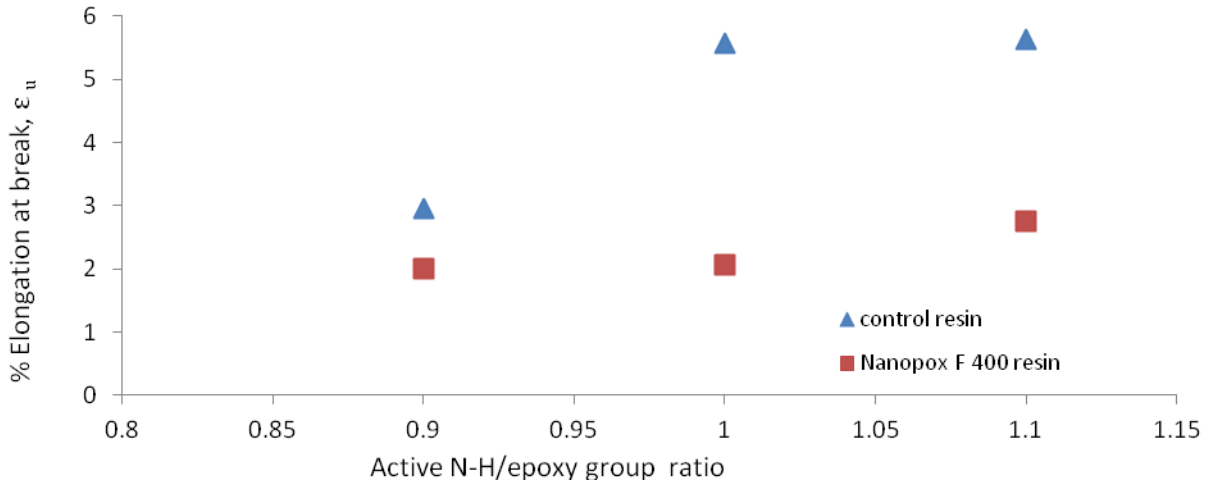

Figure 3.40. Elongation at break (ε_u) vs. active N-H/epoxy group ratio for the control resin and Nanopox F 400 resin cured with DDS curative.

The control resin cured with DDS in an N-H/epoxy molar ratio 1.1:1 shows the highest strain at break (ε_u). This is due to the higher degree of crosslinking in an amine rich epoxy mixture with the presence of some secondary N-H and hydrogen bonds. The control resin cured with DDS in N-H/epoxy molar ratio 0.9:1 shows a lower strain at break (ε_u) due to the possible etherification reaction and homopolymerization reaction, as a result, the material becomes more brittle than the other formulations.

For the Nanopox F 400 resin system, the strain at break (ε_u) is maximum, at the N-H/epoxy molar ratio 1.1:1. However, Nanopox F 400 resin cured with DDS at an N-H/epoxy molar ratio 0.9:1 shows more brittle behavior due to presence of unreacted epoxy monomer and possible etherification reaction. Nanopox F 400 resin cured with DDS in N-H/epoxy molar ratio 1:1 shows a higher strain at break (ε_u) than the Nanopox F 400 resin cured with DDS at an N-H/epoxy molar ratio 0.9:1 but still Nanopox F 400 resin cured with DDS at an N-H/epoxy molar ratio 1.1:1 is the best and avoids any etherification reaction which might be possible if

insufficient concentration of amine curative is added during the cure reaction of epoxy resin with amine curative.

The Nanopox F 400 resin, in general, exhibits lower elongation at break than the control resin (see Figure 3.43) in all curing agent/epoxy molar ratio formulation. Thus, the overall result shows that material became stiff with brittle behavior.

3.3.2.2. Tailoring the Tensile Properties of Epoxy Resin by Various Nanoparticles

The dispersion of nanoparticles in an epoxy resin has a significant impact on the mechanical properties of the polymer. In our study, we used tensile testing as a measure of mechanical properties in terms of Young's modulus (E), ultimate tensile strength (σ_u), and ultimate elongation (ϵ_u). In the present work, two kinds of nanosilica particles were chosen to tailor the tensile properties of the bisphenol-A epoxy resin. These nanoparticles were introduced into the epoxy resin by different processing methods, such as blending method and a sol gel method. In blending method, silica nanoparticles (size 10-20nm) were directly mixed with DGEBA epoxy resin and DDS curing agent with the help of high shear mixer. The curing agent/epoxy resin molar ratio was 1.1:1. Silica reinforced epoxy systems were prepared by the blending method and compared with commercially available surface modified silica reinforced epoxy system prepared by the sol gel technique (Nanopox F 400 resin). Hereafter, the commercial surface modified silica reinforced epoxy system prepared by the sol gel technique is referred as Nanopox F 400.

By employing the blending method without modifying the surface of the silica filler, we were able to incorporate a maximum of 10% by weight of silica nanoparticle in an epoxy resin (DGEBA). Incorporating more than 10% by weight of unmodified silica nanoparticles in

DGEBA resin resulted in putty like substance. Hereafter, silica reinforced epoxy systems prepared by the blending method is referred as "homemade silica reinforced nanocomposite".

To directly compare with the homemade epoxy nanocomposite, the 40 wt. % surface modified silica of Nanopox F 400 resin was diluted to 10 % and cured with DDS at an N-H/epoxy molar ratio of 1.1:1. The initial portion of the stress-strain curve for the first specimen and summary plot of the homemade 10 wt. % of non-modified SiO_2 reinforced nanocomposites are given in Figure 3.41 and 3.42. The tensile result is shown in Table 3.12.

The initial portion of the stress-strain curve for the first specimen and summary plot for 10 wt. % surface modified SiO_2 Nanopox F 400 resin are given in Figure 3.43 and 3.44. The tensile result is shown in Table 3.13.

To compare the tensile properties of the homemade material and 10 wt. % surface modified SiO_2 Nanopox F 400 resin, the tensile results are summarized in Table 3.14.

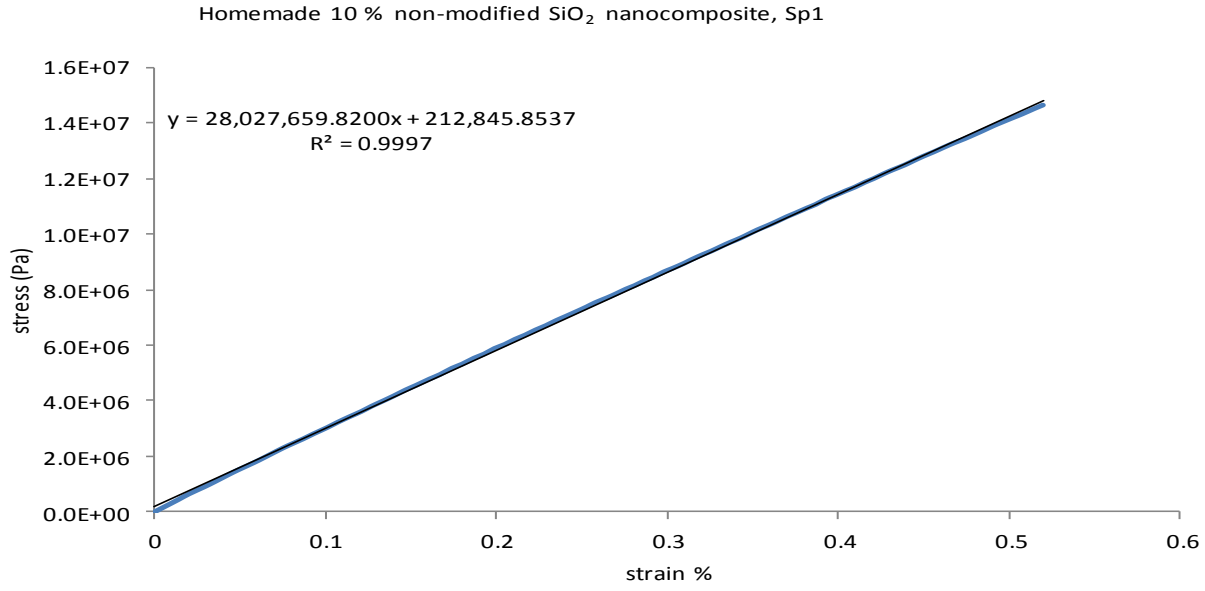

Figure 3.41. The stress-strain curve at low strain (ε) for the first specimen of the homemade 10 wt. % non-modified SiO_2 nanocomposite cured with DDS curative. (Sample specimen was stretched at a speed of 5 mm/min).

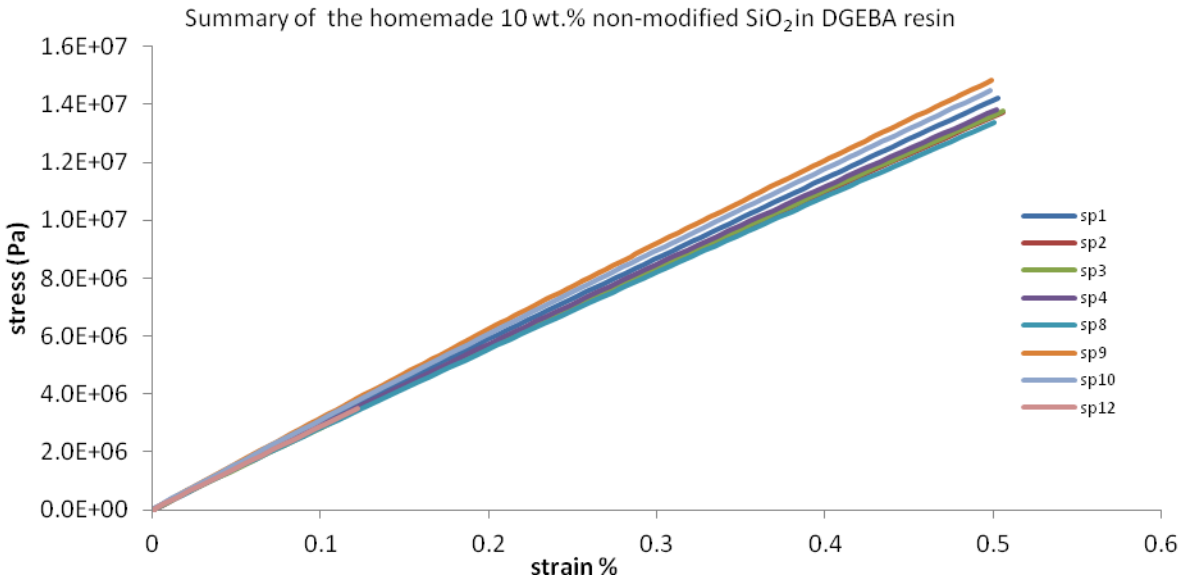

Figure 3.42. Summary of the stress-strain curve at low strain (ε) for the homemade 10 wt. % non-modified SiO_2 nanocomposite specimens cured with DDS curative. (Sample specimens were stretched at a speed of 5 mm/min)

Table 3.12. Summary table of tensile test results of the homemade 10 wt. % non-modified SiO_2 nanocomposite.

Sample	Modulus (E) GPa	strain to failure (ε_u) %	stress at break (σ_u) MPa
Control	2.69	5.48	72.29
Homemade composite			
1	2.80	4.19	58.12
2	2.68	4.19	75.92
3	2.68	3.05	60.46
4	2.74	4.32	75.99
8	2.83	3.08	69.57
9	2.96	4.33	60.57
10	2.75	4.17	76.52
12	2.75	4.18	64.57
Ave	2.77	3.94	67.71
Std dev.	0.92	0.54	7.77
%RSD	3.32	13.79	11.47

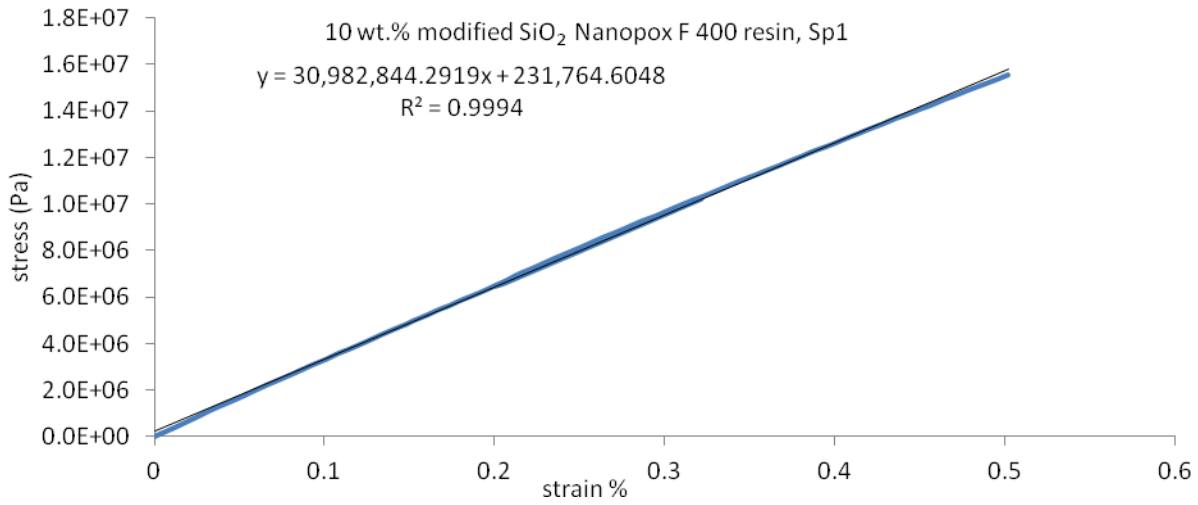

Figure 3.43. The stress-strain curve at low strain (ε) for the first specimen of 10 wt. % surface modified SiO_2 Nanopox F 400 resin cured with DDS curative. (Sample specimen was stretched at a speed of 5 mm/min)

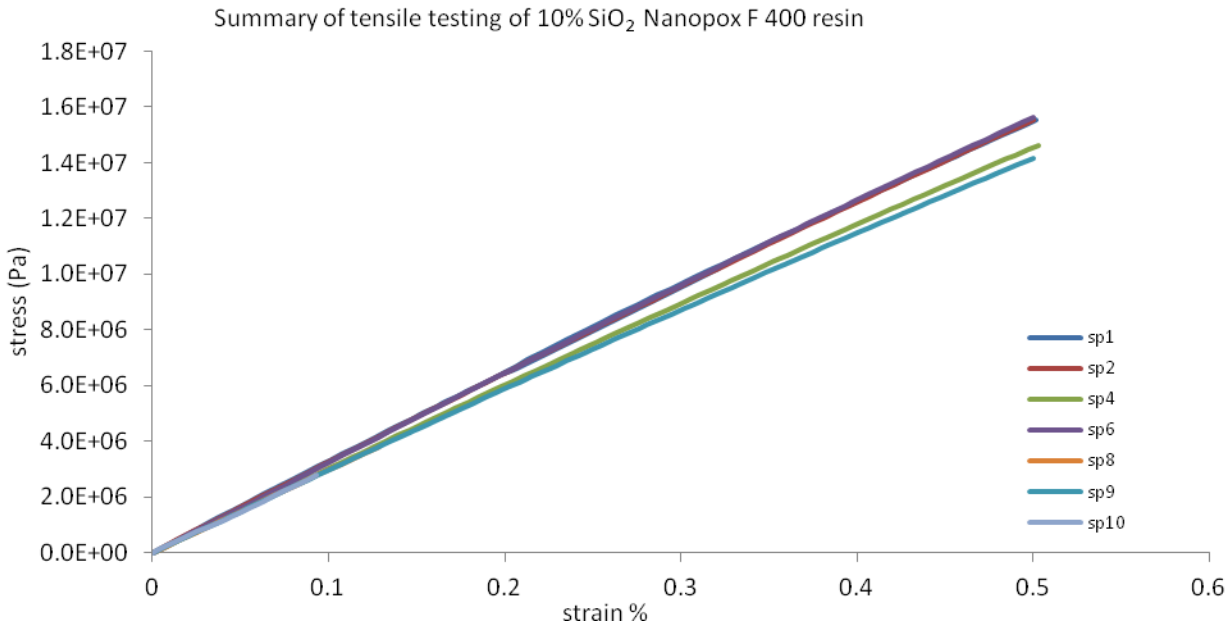

Figure 3.44. Summary of the stress-strain curve at low strain (ε) for the 10 wt. % surface modified SiO_2 Nanopox F 400 resin specimens cured with DDS curative. (Sample specimens were stretched at a speed of 5 mm/min)

Table 3.13. Summary table of tensile test results of 10 wt. % surface modified SiO_2 Nanopox F 400 resin.

Sample	Modulus (E) GPa	strain to failure (ϵ_u) %	stress at break (σ_u) MPa
Control resin	2.6.9	5.48	72.29
10 wt.% SiO_2 Nanopox F 400			
1	3.09	3.39	69.48
2	3.10	3.70	74.94
4	3.26	4.18	83.38
6	3.14	4.20	80.98
9	3.36	3.82	69.34
8	3.05	3.57	71.26
10	3.09	6.50	92.29
Ave	3.16	4.19	77.38
Std dev.	1.14	1.06	8.58
%RSD	3.60	25.29	11.09

Table 3.14. Comparison of the results of tensile testing of the control resin, homemade 10 wt. % non-modified SiO_2 nanocomposite prepared by blending method and 10 wt. % surface modified SiO_2 Nanopox F 400 resin prepared by a sol gel method.

Material	**Modulus (E) GPa**	**Stiffness % change**	**stress at break (σ_u) MPa**	**stress at break % change**	**strain at break (ε_u) MPa**	**extension at break % change**
Control resin	2.7 ± 1.2		72 ± 7.1		5.4 ± 0.8	
10 wt.% surface modified SiO_2 Nanopox F 400	3.2 ± 1.1	18.5	77 ± 8.5	6.9	4.1 ± 1.0	-24.0
Homemade 10wt.% non-modified SiO_2 Nanocomposite	2.8 ±0.9	3.8	68 ± 11.5	-5.9	3.9 ± 0.5	-27.8

The stiffness of both silica reinforced nanocomposites was increased in comparison with the control resin irrespective of the silica filler type. The increase in Young's modulus (E) in both silica reinforced nanocomposites is due to the presence of high modulus silica nanoparticles, which imparts better rigidity to the epoxy resin system making the material more physically stable. However, 10 wt. % surface modified SiO_2 Nanopox F 400 resin shows a higher Young's modulus (E) than the homemade 10 wt. % non-modified SiO_2 reinforced nanocomposite. This effect could be attributed to an improved dispersion of SiO_2 throughout the epoxy matrix and interaction between epoxy matrix and surface modified silica nanoparticle. Improved interaction between the silica filler and the resin results in better stress transfer from the polymer matrix to the silica filler.

The ultimate tensile strength of the homemade 10 wt. % non-modified SiO_2 reinforced nanocomposite tended to be less than the control resin leading to easier crack propagation. A major problem of such materials was the poor dispersion of the filler in the epoxy matrix. Well-dispersed 10 wt. % surface modified SiO_2 Nanopox F 400 resin system has higher tensile strength than the control resin and the homemade 10 wt. % non-modified SiO_2 reinforced nanocomposite. As explained earlier, higher tensile strength results due to the improved dispersion and interaction between the epoxy matrix and surface modified silica nanoparticle. In contrast, the elongation at break of the silica reinforced nanocomposites decreased dramatically with the addition of silica nanoparticle in an epoxy matrix irrespective of filler type.

The results discussed above indicate that the increased adhesion between polymer matrix and silica filler in nanocomposites enhance the tensile properties of the silica reinforced nanocomposites. Coupling agents are used to modify the surface of silica filler to increase the interaction between epoxy resin and silica filler. The coupling agent was introduced as the

surface modifier for silica filler. The surface modified silica filler was used in preparing the silica reinforced nanocomposite by the blending method and their tensile properties were studied.

3.3.2.3 Tensile properties of the homemade 10 wt. % surface modified silica reinforced nanocomposite

To prepare the homemade surface modified silica reinforced nanocomposite, we used surface modifying agent to modify the surface of the silica nanoparticles namely using 3-aminopropyltriethoxysilane (3-APTES). Silane coupling agents are the most used type of modifying agent. They are generally represented by $RSiX_3$. The functional group 'X' reacts with hydroxyl groups on the SiO_2 surface and the 'R' group reacts with the epoxy group of the epoxy resin forming the covalent bond as shown in Figure 3.45.

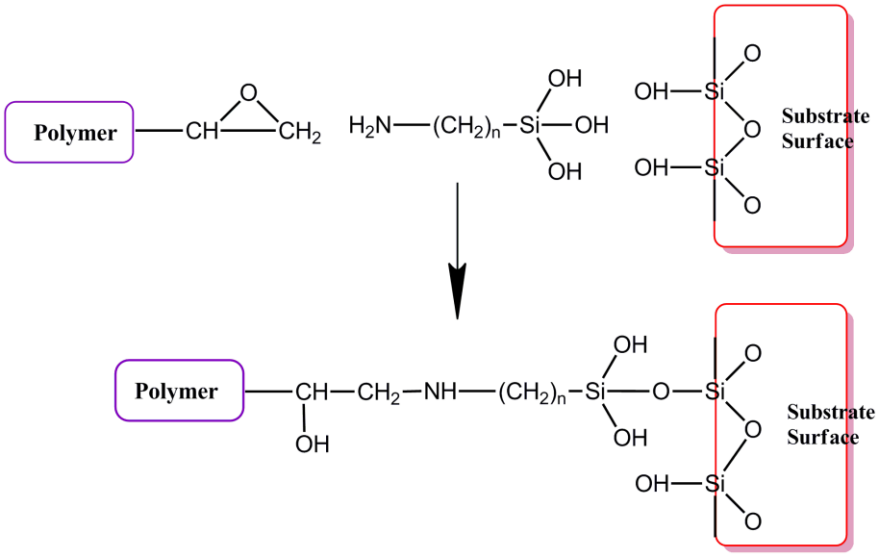

Figure 3.45. Linkers for surface attachment to silica filler and epoxy polymer.

The mechanism and procedure of surface modification of silica nanoparticles by the coupling agent has been discussed in Chapter 1 and Chapter 2. The 10 wt. % of surface modified SiO_2 was added to the DGEBA resin and DDS curative using a high shear mixer. The curing

agent/epoxy molar ratio was 1.1:1. The stress-strain curves for the first specimen of the homemade 10 wt. % of surface modified SiO_2 reinforced nanocomposites are shown in Figure 3.46. A summary plot is shown in Figure 3.47 and tensile results are shown in Table 3.15.

The tensile properties of this homemade 10 wt. % surface modified SiO_2 nanocomposite is compared with the homemade 10 wt. % non-surface modified SiO_2 nanocomposite and the control resin in Table 3.16.

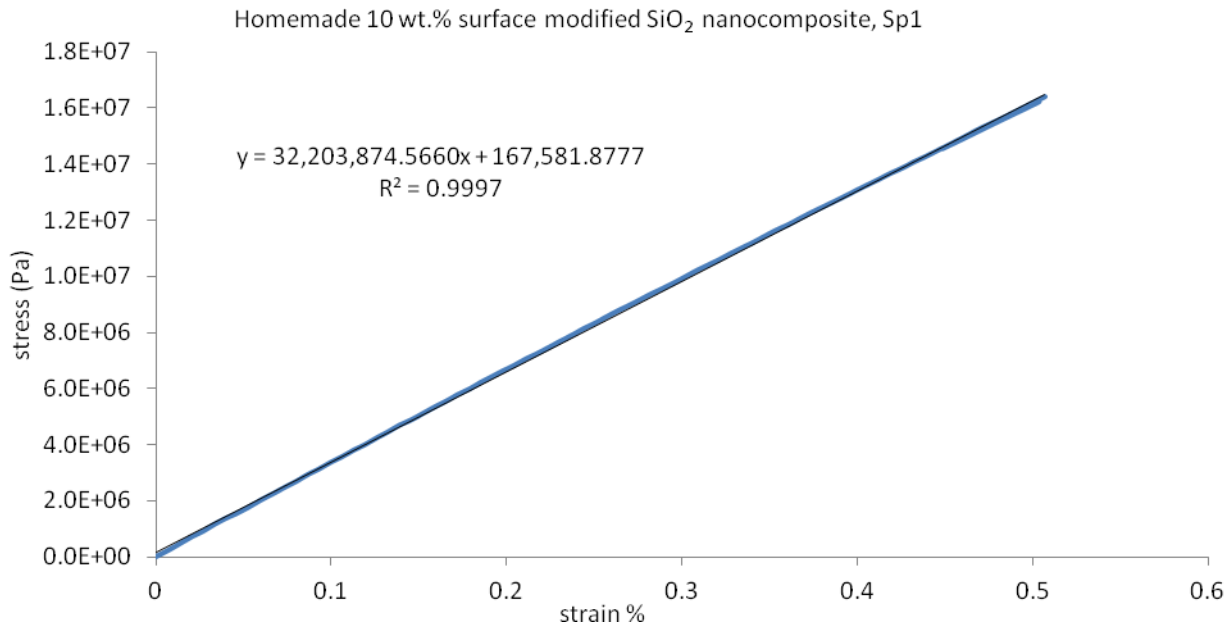

Figure 3.46. The stress-strain curve at low strain (ε) for the first specimen of the homemade 10 wt. % surface modified SiO_2 nanocomposite cured with DDS curative. (Sample specimen was stretched at a speed of 5 mm/min)

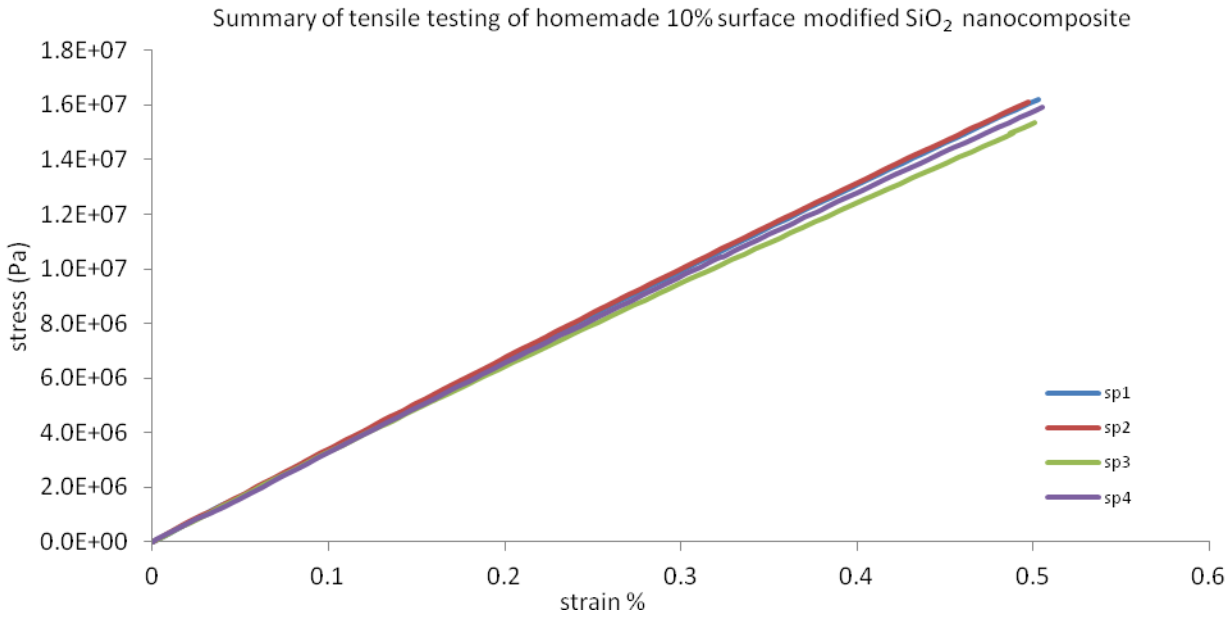

Figure 3.47. Summary of the stress-strain curve at low strain (ε) for the homemade 10 wt. % surface modified SiO_2 nanocomposite cured with DDS curative. (Sample specimens were stretched at a speed of 5 mm/min)

Table 3.15. Summary table of tensile test results of the homemade 10 wt. % surface modified SiO_2 nanocomposite.

Sample	Modulus (E) GPa	strain to failure (ε_u)	stress at break (σ_u) MPa
Control	26.97	5.48	72.29
Homemade composite			
1	3.22	4.18	82.19
2	3.24	3.93	80.28
3	3.05	3.57	71.26
4	3.14	4.97	82.35
Ave	3.16	4.16	79.02
Std dev.	0.87	0.60	5.26
%RSD	2.75	14.34	6.65

Table 3.16. Results of tensile testing of the homemade 10 wt. % non-modified and surface modified SiO_2 reinforced nanocomposites and control resin.

Material	Modulus E (GPa)	Stiffness % change	stress at break σ_u (MPa)	stress at break % change	strain at break ε_u (%)	extension at break % change
Control resin	2.7 ± 1.2		72 ± 7.1		5.4 ± 0.8	
Homemade 10 wt.% non-modified SiO_2 nanocomposite	2.8 ± 0.9	3.7	68 ± 11.5	-5.6	3.9 ± 0.5	-27.8
Homemade 10 wt.% surface modified SiO_2 nanocomposite	3.2 ± 0.8	18.0	79 ± 5.2	9.8	4.1 ± 0.6	-24.1

As shown in Table 3.16, the homemade 10 wt. % surface modified SiO_2 reinforced nanocomposite possessed improved stiffness over that of the homemade 10 wt. % non-modified SiO_2 reinforced nanocomposite. The higher modulus of the homemade 10 wt. % surface modified SiO_2 reinforced nanocomposite could be due to increased interfacial interaction between polymer matrix and silica filler. The increased interfacial interaction also improves the homogenous dispersion of silica filler which in turn increases the stiffness of the nanocomposite. However, the stiffness is improved by the addition of silica filler irrespective of the kind of filler. This indicates that the silica nanoparticles can significantly stiffen a mid-performance epoxy resin.

The tensile strength of the homemade 10 wt. % surface modified SiO_2 reinforced nanocomposite is higher than the homemade 10 wt. % non-modified SiO_2 reinforced nanocomposite. Such effect is due to the addition of coupling agent which increases dispersion of silica filler and compatibility between silica filler and epoxy matrix. Under tensile stress, force was transferred to silica particles through the interphase and the silica particles became the

receptor of the tensile force. The tensile strength of the homemade 10 wt. % non-modified SiO_2 reinforced nanocomposite is lower than the control resin due to poor interaction between silica filler and an epoxy matrix.

The strain at break (ε_u) is lower for the silica reinforced nanocomposites than the control resin irrespective of filler type.

The results show that the brittleness of the epoxy polymer can be reduced significantly by the addition of 10 wt. % of surface modified silica nanoparticles in an epoxy matrix.

3.3.2.4. The effect of preparation technique and silica content on the tensile properties of surface modified SiO_2 reinforced nanocomposite.

Surface modified silica reinforced epoxy nanocomposites can be prepared by two ways-blending and the sol-gel method. The tensile properties of the homemade 10 wt. % and 40 wt. % surface modified SiO_2 reinforced composite prepared by the blending method were compared with commercially available diluted 10 wt.% and 40 wt.% SiO_2 Nanopox F 400 resin prepared by a sol-gel technique.

The tensile results of diluted 10 wt. % and 40 wt. % surface modified SiO_2 Nanopox F 400 resin are shown in Table 3.11 and Table 3.14. The tensile results of the homemade 10 wt. % surface modified SiO_2 reinforced composite is shown in Table 3.15.The stress-strain curve at low strain (ε) for the first specimen of the homemade 40 wt. % surface modified SiO_2 reinforced nanocomposite is given in Figure 3.48 and a summary plot is shown in Figure 3.49. The tensile results are shown in Table 3.17. The homemade 40 wt. % surface modified SiO_2 reinforced nanocomposite was cured with DDS at an N-H/epoxy molar ratio of 1.1:1. The summarized tensile results of the homemade 10 wt. % and 40 wt. % surface modified SiO_2 reinforced

nanocomposite and diluted 10 wt. % and 40 wt. % surface modified SiO_2 Nanopox F 400 resin are shown in Table 3.18.

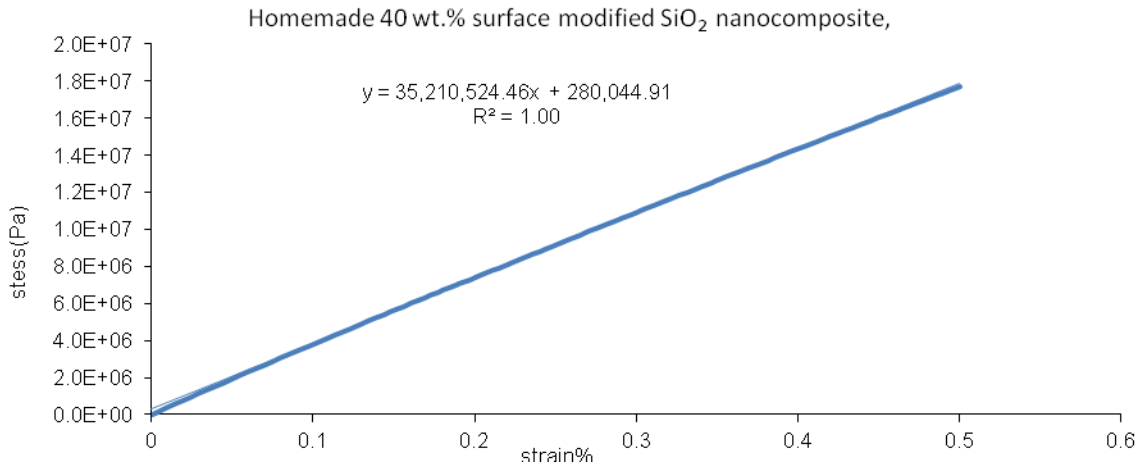

Figure 3.48. The stress-strain curve at low strain (ε) for the first specimen of the homemade 40 wt. % surface modified SiO_2 nanocomposite cured with DDS curative. (Sample specimen was stretched at a speed of 5 mm/min)

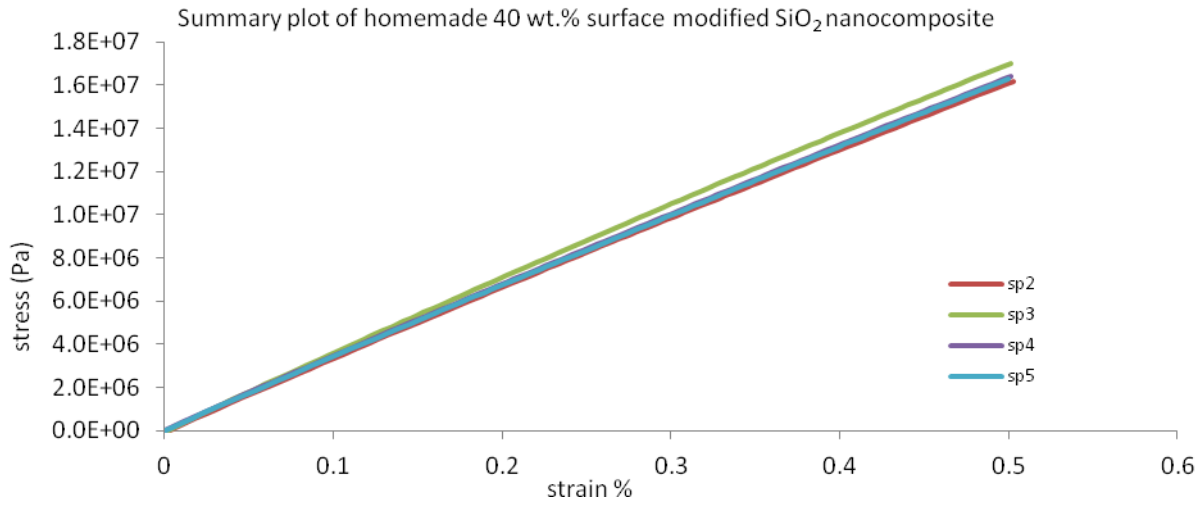

Figure 3.49. Summary of the stress-strain curve at low strain (ε) for the homemade 40 wt. % surface modified SiO_2 nanocomposite cured with DDS curative. (Sample specimens were stretched at a speed of 5 mm/min)

Table 3.17. Summary table of tensile test results of the homemade 40 wt. % surface modified SiO_2 nanocomposite cured with DDS curative.

Sample	Modulus (E) GPa	Strain to failure (ε_u)	Stress at break (σ_u) MPa
Control	2.69	5.48	72.29
Homemade nanocomposite			
2	3.53	2.56	62.24
3	3.59	3.21	55.24
4	3.53	2.68	60.24
5	3.51	3.32	65.96
Ave	3.54	2.94	60.92
Std dev.	0.36	0.38	4.47
%RSD	1.02	12.78	7.34

Table 3.18. Tensile testing results of 10 wt. % and 40 wt. % silica content nanocomposites prepared by blending method (homemade method) and sol gel method.

Material	**Modulus (E) GPa**	**Stiffness % change**	**stress at break (σ_u) MPa**	**stress at break % change**	**strain at break (ε_u) (%)**	**extension at break % change**
Control resin	2.7 ± 1.2		72 ± 7.1		5.4 ± 0.8	
Homemade 10 wt.% surface modified SiO_2 nanocomposite	3.2 ± 0.8	18.5	79 ± 5.2	9.8	4.1 ± 0.6	-24.0
10 wt.% surface modified SiO_2 Nanopox F 400	3.2 ± 1.1	18.5	77 ± 8.4	6.9	4.1 ± 1.0	-24.0
Homemade 40 wt.% surface modified SiO_2 nanocomposite	3.5 ± 0.3	29.7	60 ± 4.4	-16.7	2.9 ± 0.3	-46.2
40 wt.% surface modified SiO_2 Nanopox F 400	4.3 ± 2.1	59.2	63 ± 8.5	-12.5	2.7 ± 0.8	-50.0

The homemade 10 wt. % surface modified SiO_2 reinforced epoxy nanocomposites prepared by the blending method and 10 wt. % surface modified SiO_2 Nanopox F 400 resin prepared by the sol-gel technique shows improved stiffness than the control resin. The tensile strength is also higher for both the 10 wt. % surface modified SiO_2 reinforced epoxy nanocomposites. The increase in tensile properties is due to the increased adhesion of the surface modified silica filler in an epoxy matrix. The strain at break of the control resin is always higher than surface modified silica reinforced epoxy nanocomposites.

The homemade 10 wt. % surface modified SiO_2 reinforced nanocomposite prepared by the blending method can simultaneously improve the stiffness and the tensile strength of the epoxy resin, which could reach to a similar effect of 10 wt. % surface modified SiO_2 Nanopox F 400 resin prepared by the sol gel technique

Moreover, the influences of the silica content on the mechanical properties of the nanosilica epoxy composites were analyzed. It is found that, when the silica content is 40%, the stress and strain to break properties of the nanosilica reinforced epoxy composites are markedly reduced over the 10% silica content nanocomposites independent of preparation techniques (see Table 3.18). This effect is attributed to increase in the tendency of silica nanoparticles to form agglomerates at higher concentrations, despite the increased adhesion between surface modified silica filler and epoxy matrix. However, 40 wt. % SiO_2 Nanopox F 400 resin prepared by the sol gel technique shows better performance than the homemade 40 wt. % SiO_2 reinforced nanocomposite (see Table 3.18) .The reason could be the homogenous dispersion of silica filler in the epoxy matrix of Nanopox F 400 nanocomposite due to better surface modification of the silica nanoparticle. In addition, homogenous dispersion might not be optimal in the homemade 40 wt. % SiO_2 reinforced nanocomposite due to the limited shear force during mixing procedure.

CHAPTER 4

CONCLUSIONS

The cure kinetics of Nanopox F 400 resin (40 wt. % surface modified SiO_2 + 60 wt. % DGEBA resin) and the control resin (100 wt. % DGEBA resin) both cured with DDS at an N-H/epoxy molar ratio of 1.1:1 was investigated using DSC. Two sets of DSC experiments were performed: dynamic temperature scanning and isothermal scanning. In the dynamic temperature scanning measurements, the cure reaction of the Nanopox F 400 system was shifted to lower temperatures than the control system. This revealed that surface modified silica fillers have an acceleration effect on the reaction kinetics of the Nanopox F 400 system. The IR and ^1H NMR spectra shows the hydroxyl group (-OH) on the surface of the silica filler. This suggests that a catalytic effect for epoxide ring opening in the initial stage of the cure reaction is related to the –OH groups on the surface of the silica filler. The low activation energy was observed for the cure of Nanopox F 400 system at lower degrees of cure due to catalytic effect of silica nanoparticles. However, substantially lower activation energy at higher degrees of cure is unusual and indicated that the silica nanoparticles may have some effect on the cure kinetics and perhaps resin structure in the nanocomposite at high conversions. The ultimate T_g of the Nanopox F 400 system cured under dynamic temperature scanning was averaged to 132 ± 2 ^oC which is lower than the control system (T_g= 173 ± 6 ^oC). As expected, the glass transition temperature and changes in the T_g found in DSC analysis were in line with TMA analysis and DMA analysis.

Isothermal scanning experiments were performed from 140°C to 200°C for the control system and Nanopox F 400 system. It was found that the conversion of both materials increased with increasing time and temperature. For the control system, the maximum degree of cure at the given temperature, α_{max}, is less than 1 ($\alpha_{max} > 1$) at lower isothermal temperatures. However,

Nanopox F 400 system shows $\alpha_{max} = 1$ at all isothermal temperatures. It is also found that at higher isothermal temperature, less effect of silica filler is seen on reaction rate.

The isothermal data of the control system were found to fit the general kinetic model proposed by Kamal. Kinetics parameters (k_1, k_2, m and n) and activation energies (E_{a1} and E_{a2}) were calculated. From the values of k_1, k_2, activation energies E_{a1} and E_{a2} were calculated. The general Kamal model did not fit the experimental data of the Nanopox F 400 system, thus, the general Kamal model was modified by assuming $k_1=0$ at t=0, when there was a total ultimate conversion. The fitting of the modified Kamal model to the experimental data showed a very good agreement in the whole conversion range for the Nanopox F 400 system. Kinetic parameters (k_2, m and n) and activation energy E_{a2} were calculated.

Data from tensile testing shows that the inclusion of 40 wt. % surface modified SiO_2 in an epoxy resin (Nanopox F 400 resin) cured with DDS at an N-H/epoxy molar ratio of 1.1:1 was not able to improve the tensile properties than the control resin. However, diluted 10 wt. % surface modified SiO_2 Nanopox F 400 system showed improve tensile properties than the control resin. Furthermore, an influence of preparation technique on the mechanical properties of surface modified SiO_2 reinforced nanocomposite was analyzed. It is found that the homemade 10 wt. % surface modified SiO_2 reinforced nanocomposite prepared by blending method has similar tensile properties to those of the 10 wt. % surface modified SiO_2 Nanopox F 400 system prepared by the sol gel technique. However, the tensile results of 40 wt. % surface modified SiO_2 Nanopox F 400 system showed better performance than the homemade 40 wt. % surface modified SiO_2 reinforced nanocomposite.

REFERENCES

LIST OF REFERENCES

1. Lee, H., *Handbook of epoxy resins [by] Henry Lee [and] Kris Neville*. McGraw-Hill handbooks, ed. K.j.a. Neville. 1967, New York: McGraw-Hill.

2. Okazaki, M., et al., *Curing of epoxy resin by ultrafine silica modified by grafting of hyperbranched polyamidoamine using dendrimer synthesis methodology.* Journal of Applied Polymer Science, 2001. **80**(4): p. 573-579.

3. Nakamura, Y., et al., *Effects of particle size on mechanical and impact properties of epoxy resin filled with spherical silica.* Journal of Applied Polymer Science, 1992. **45**(7): p. 1281-1289.

4. Zee, R.H., et al., *Properties and processing characteristics of dielectric-filled epoxy resins.* Polymer Composites, 1989. **10**(4): p. 205-214.

5. *Handbook of fillers and reinforcements for plastics / edited by Harry S. Katz, John V. Milewski*, ed. H.S. Katz and J.V. Milewski. 1978, New York :: Van Nostrand Reinhold Co.

6. McGrath, L.M., et al., *Investigation of the thermal, mechanical, and fracture properties of alumina-epoxy composites.* Polymer, 2008. **49**(4): p. 999-1014.

7. Zheng, Y., Y. Zheng, and R. Ning, *Effects of nanoparticles SiO_2 on the performance of nanocomposites.* Materials Letters, 2003. **57**(19): p. 2940-2944.

8. Rosso, P., et al., *A toughened epoxy resin by silica nanoparticle reinforcement (vol 100, pg 1849, 2006).* Journal of Applied Polymer Science, 2006. **101**(2): p. 1235-1236.

9. Johnsen, B.B., et al., *Toughening mechanisms of nanoparticle-modified epoxy polymers.* Polymer, 2007. **48**(2): p. 530-541.

10. Lin, J.C., et al., *Mechanical behavior of various nanoparticle filled composites at low-velocity impact.* Composite Structures, 2006. **74**(1): p. 30-36.

11. Ragosta, G., et al., *Epoxy-silica particulate nanocomposites: Chemical interactions, reinforcement and fracture toughness.* Polymer, 2005. **46**(23): p. 10506-10516.

12. ADEBAHR, et al., *Reinforcing nanoparticles in reactive resins*. 2001, Hannover, ALLEMAGNE: Vincentz. 5.

13. Chen, C., et al., *Highly dispersed nanosilica–epoxy resins with enhanced mechanical properties.* Polymer, 2008. **49**(17): p. 3805-3815.

14. Weng, W.H., et al., *Thermal property of epoxy/SiO2 hybrid material synthesized by the sol–gel process.* Journal of Applied Polymer Science, 2004. **91**(1): p. 532-537.

LIST OF REFERENCES (continued)

15. Kinloch, A.J., BB Mohammed, RD Taylor, AC Sprenger, S, *Toughening Mechanisms in Novel Nano-silica Epoxy Polymers*, in *Australasian Congress on Applied Mechanics (5th : 2007 : Brisbane, Qld.)*.

16. Baller, J., et al., *Interactions between silica nanoparticles and an epoxy resin before and during network formation.* Polymer, 2009. **50**(14): p. 3211-3219.

17. Lu, S.R., et al., *Preparation and characterization of epoxy-silica hybrid materials by the sol-gel process.* Journal of Materials Science, 2005. **40**(5): p. 1079-1085.

18. Davis, S.R., A.R. Brough, and A. Atkinson, *Formation of silica/epoxy hybrid network polymers.* Journal of Non-Crystalline Solids, 2003. **315**(1-2): p. 197-205.

19. Hajji, P., et al., *Synthesis, structure, and morphology of polymer–silica hybrid nanocomposites based on hydroxyethyl methacrylate.* Journal of Polymer Science Part B: Polymer Physics, 1999. **37**(22): p. 3172-3187.

20. Jana, S.C. and S. Jain, *Dispersion of nanofillers in high performance polymers using reactive solvents as processing aids.* Polymer, 2001. **42**(16): p. 6897-6905.

21. Zou, H., S.S. Wu, and J. Shen, *Polymer/silica nanocomposites: Preparation, characterization, properties, and applications.* Chemical Reviews, 2008. **108**(9): p. 3893-3957.

22. Battistella, M., et al., *Fracture behaviour of fumed silica/epoxy nanocomposites.* Composites Part a-Applied Science and Manufacturing, 2008. **39**(12): p. 1851-1858.

23. Manna, A.K., et al., *Bonding between precipitated silica and epoxidized natural rubber in the presence of silane coupling agent.* Journal of Applied Polymer Science, 1999. **74**(2): p. 389-398.

24. www.gelest.com/pdf/couplingagents.pdf. *silane coupling agent*, Retrived on 06-13-2010.

25. Hussain, M., et al., *Effects of coupling agents on the mechanical properties improvement of the TiO_2 reinforced epoxy system.* Materials Letters, 1996. **26**(6): p. 299-303.

26. Bugnicourt, E., et al., *Effect of sub-micron silica fillers on the mechanical performances of epoxy-based composites.* Polymer, 2007. **48**(6): p. 1596-1605.

27. Rosso, P. and L. Ye, *Epoxy/silica nanocomposites: Nanoparticle-induced cure kinetics and microstructure.* Macromolecular Rapid Communications, 2007. **28**(1): p. 121-126.

LIST OF REFERENCES (continued)

28. Liu, H.P., et al., *Influence of substituents on the kinetics of epoxy/aromatic diamine resin systems.* Journal of Polymer Science Part a-Polymer Chemistry, 2004. **42**(13): p. 3143-3156.

29. Girard-Reydet, E., et al., *Epoxy-Aromatic Diamine Kinetics. Part 1. Modeling and Influence of the Diamine Structure.* Macromolecules, 1995. **28**(23): p. 7599-7607.

30. Mijovic, J., A. Fishbain, and J. Wijaya, *Mechanistic Modeling of Epoxy Amine Kinetics .1. Model-Compound Study.* Macromolecules, 1992. **25**(2): p. 979-985.

31. Sung, C.S.P., E. Pyun, and H.L. Sun, *Characterization of epoxy cure by UV-visible and fluorescence spectroscopy: azo chromophoric labeling approach.* Macromolecules, 1986. **19**(12): p. 2922-2932.

32. Smith, I.T., *The mechanism of the crosslinking of epoxide resins by amines.* Polymer, 1961. **2**: p. 95-108.

33. Enikolopiyan, N.S., *New aspects of nucleophillic opening of the epoxide ring* Pure and Applied Chemistry 1976. **48**: p. 317-328.

34. Levita, G., et al., *Crosslink density and fracture toughness of epoxy resins.* Journal of Materials Science, 1991. **26**(9): p. 2348-2352.

35. Ghaemy, M., M. Barghamadi, and H. Behmadi, *Cure kinetics of epoxy resin and aromatic diamines.* Journal of Applied Polymer Science, 2004. **94**(3): p. 1049-1056.

36. Ghaemy, M., S.M.A. Nasab, and M. Barghamadi, *Nonisothermal cure kinetics of diglycidylether of bisphenol-A/amine system reinforced with nanosilica particles.* Journal of Applied Polymer Science, 2007. **104**(6): p. 3855-3863.

37. Harsch, M., J. Karger-Kocsis, and M. Holst, *Influence of fillers and additives on the cure kinetics of an epoxy/anhydride resin.* European Polymer Journal, 2007. **43**(4): p. 1168-1178.

38. Altmann, N., et al., *The effects of silica fillers on the gelation and vitrification of highly filled epoxy-amine thermosets.* Macromolecular Symposia, 2001. **169**(1): p. 171-177.

39. Ton-That, M.T., et al., *Epoxy nanocomposites: Analysis and kinetics of cure.* Polymer Engineering and Science, 2004. **44**(6): p. 1132-1141.

40. Mijovic, J. and J. Wijaya, *Reaction Kinetics of Epoxy/Amine Model Systems. The Effect of Electrophilicity of Amine Molecule.* Macromolecules, 1994. **27**(26): p. 7589-7600.

LIST OF REFERENCES (continued)

41. Cole, K.C., J.J. Hechler, and D. Noel, *A new approach to modeling the cure kinetics of epoxy/amine thermosetting resins. 2. Application to a typical system based on bis[4-(diglycidylamino)phenyl]methane and bis(4-aminophenyl) sulfone.* Macromolecules, 1991. **24**(11): p. 3098-3110.

42. Cole, K.C., *A new approach to modeling the cure kinetics of epoxy/amine thermosetting resins. 1. Mathematical development.* Macromolecules, 1991. **24**(11): p. 3093-3097.

43. G.Gandikota, R., *CURE KINETICS AND SYNTHESIS OF SOME RESINS AND PREPREG SYSTEMS*, in *Chemistry Department*. 2009, Wichita State University

44. D.FLores, J., *Chemical Characterization and two step cure cure kinetics of a high performance epoxy adhesive system*, in *Chemistry*. 2006, Wichita State University: Wichita.

45. Sourour, S. and M.R. Kamal, *Differential scanning calorimetry of epoxy cure: isothermal cure kinetics.* Thermochimica Acta, 1976. **14**(1-2): p. 41-59.

46. White, S.R. and H.T. Hahn, *Process Modeling of Composite-Materials - Residual-Stress Development during Cure .1. Model Formulation.* Journal of Composite Materials, 1992. **26**(16): p. 2402-2422.

47. White, S.R., P.T. Mather, and M.J. Smith, *Characterization of the cure-state of DGEBA-DDS epoxy using ultrasonic, dynamic mechanical, and thermal probes.* Polymer Engineering and Science, 2002. **42**(1): p. 51-67.

48. Seifi, R. and M. Hojjati, *Heat of reaction, cure kinetics, and viscosity of Araldite LY-556 resin.* Journal of Composite Materials, 2005. **39**(11): p. 1027-1039.

49. Woo Il Lee, A.C. Loos, and G.S. Springer, *Heat of Reaction, Degree of Cure, and Viscosity of Hercules 3501-6 Resin.* Journal of Composite Materials, 1982. **16**(6): p. 510-520.

50. Dusi, M.R., et al., *Cure Kinetics and Viscosity of Fiberite 976 Resin.* Journal of Composite Materials, 1987. **21**(3): p. 243-261.

51. O'Brien, D.J. and S.R. White, *Cure kinetics, gelation, and glass transition of a bisphenol F epoxide.* Polymer Engineering & Science, 2003. **43**(4): p. 863-874.

52. Kenny, J.M., et al., *Thermal analysis of standard and toughened high-performance epoxy matrices.* Thermochimica Acta, 1992. **199**: p. 213-227.

LIST OF REFERENCES (continued)

53. Hill, D.J.T., G.A. George, and D.G. Rogers, *A systematic study of the microwave and thermal cure kinetics of the DGEBA/DDS and DGEBA/DDM epoxy-amine resin systems.* Polymers for Advanced Technologies, 2002. **13**(5): p. 353-362.

54. Yousefi, A., P.G. Lafleur, and R. Gauvin, *Kinetic studies of thermoset cure reactions: A review.* Polymer Composites, 1997. **18**(2): p. 157-168.

55. Kamal, M.R. and S. Sourour, *Kinetics and thermal characterization of thermoset cure.* Polymer Engineering & Science, 1973. **13**(1): p. 59-64.

56. Fournier, J., et al., *Changes in Molecular Dynamics during Bulk Polymerization of an Epoxide−Amine System As Studied by Dielectric Relaxation Spectroscopy.* Macromolecules, 1996. **29**(22): p. 7097-7107.

57. Horie, K., et al., *Calorimetric investigation of polymerization reactions. III. Curing reaction of epoxides with amines.* Journal of Polymer Science Part A-1: Polymer Chemistry, 1970. **8**(6): p. 1357-1372.

58. Du, S.Y., et al., *Cure kinetics of epoxy resin used for advanced composites.* Polymer International, 2004. **53**(9): p. 1343-1347.

59. www. Astm.org / standards/ D638.htm. Used by permission on 8-9-2007 from Dr.William T. K. Stevenson.

60. Nara Altman, Peter J. Halley, The effects of silica fillers on the gelation and vitrification of highly filled epoxy-amine thermosets, *Macromolecular Symposium,* **2001,**169, 171-177.

APPENDICES

APPENDIX A

Calculation of Apparent Activation Energy for the cure of the control resin cured with DDS curative at an N-H/epoxy molar ratio 1.1:1 under dynamic cure conditions in the DSC apparatus.

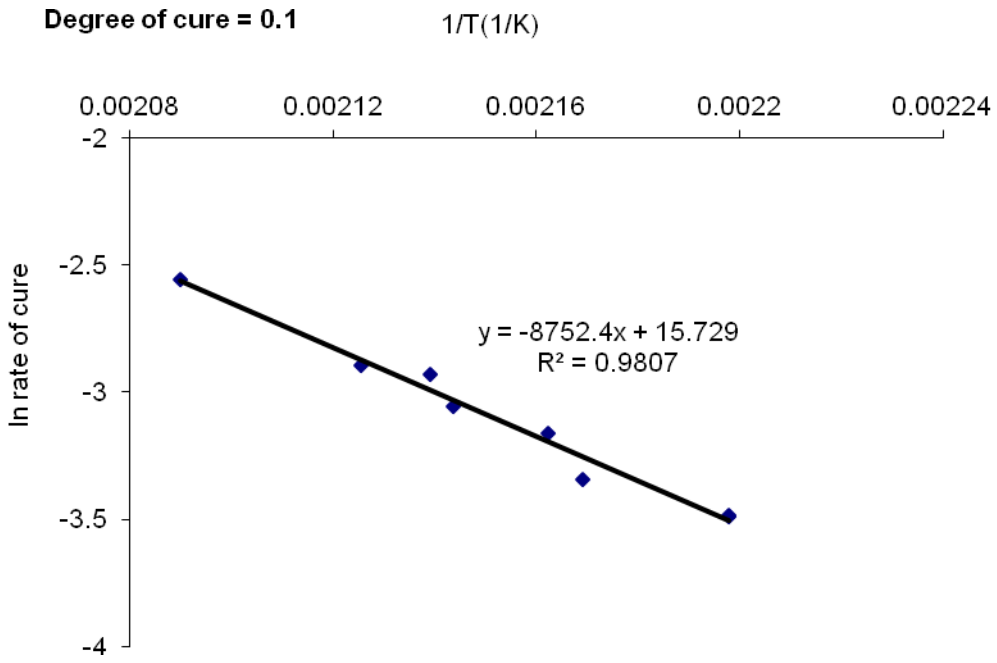

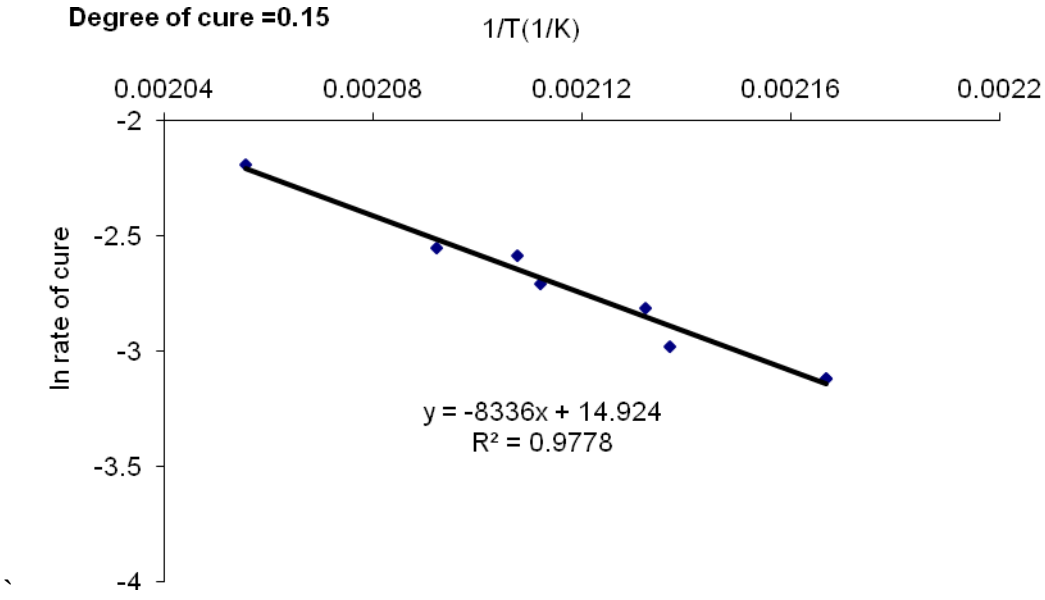

APPENDIX A (continued)

Degree of cure = 0.2

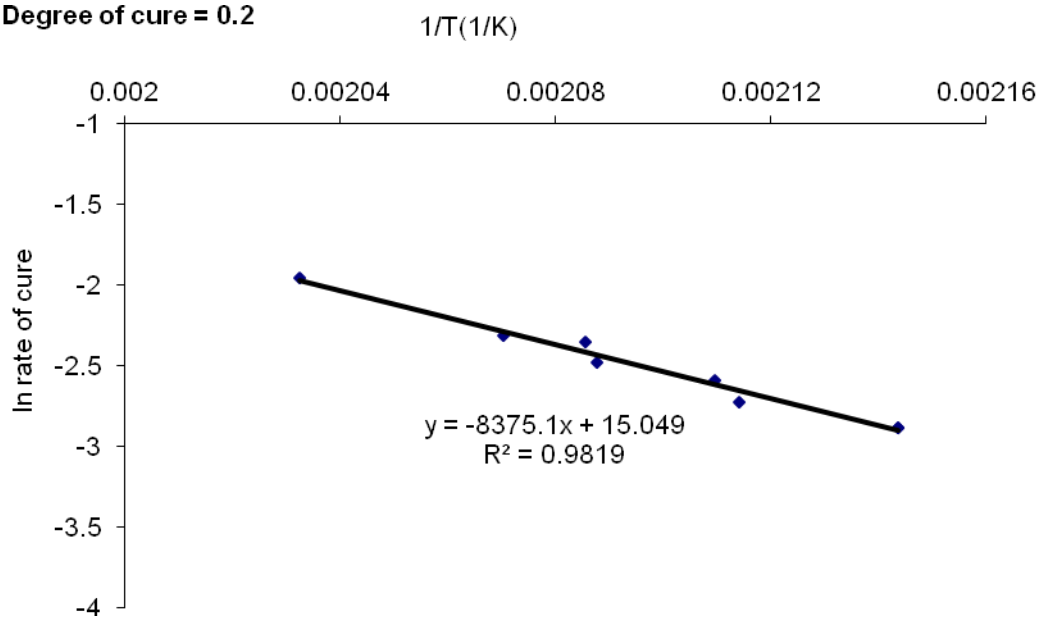

Degree of cure = 0.25

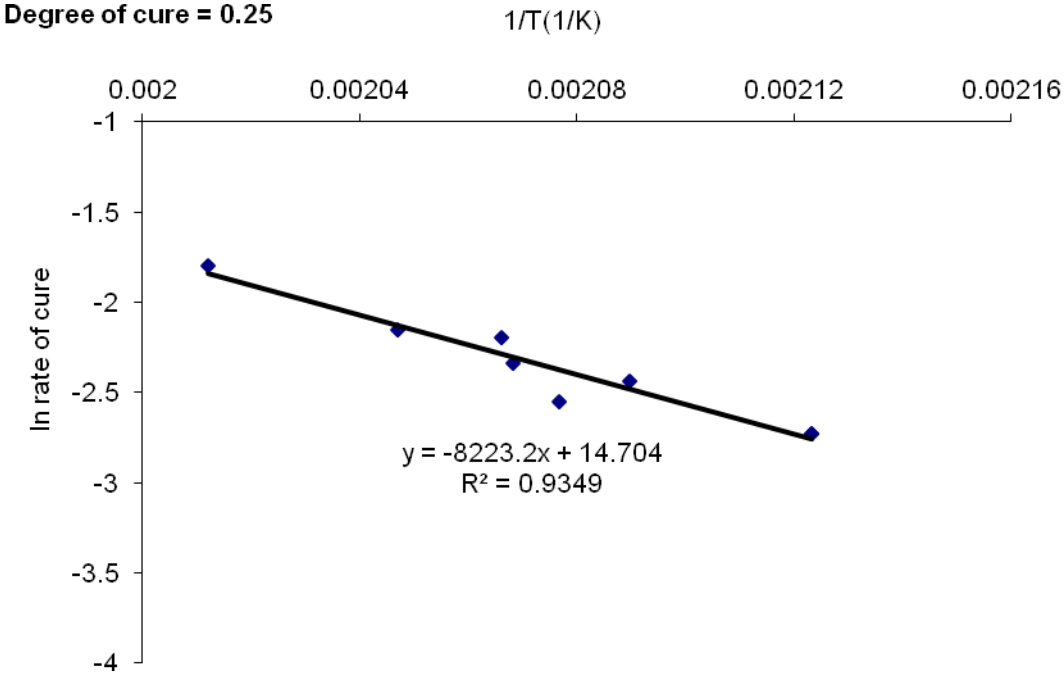

APPENDIX A (continued)

Degree of cure = 0.3

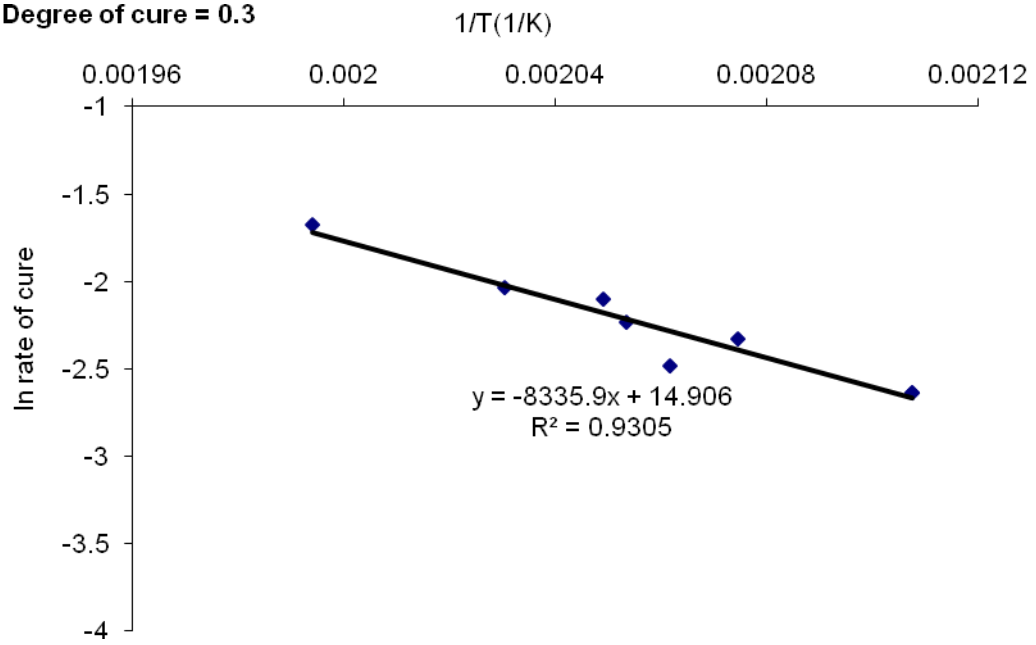

Degree of cure = 0.35

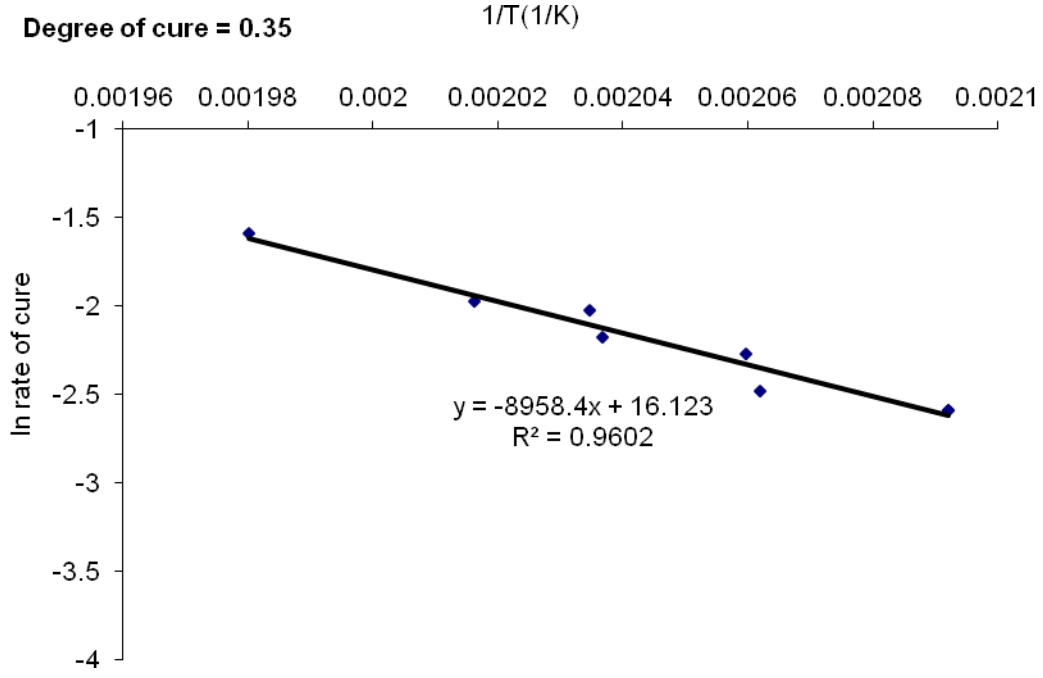

APPENDIX A (continued)

Degree of cure = 0.4

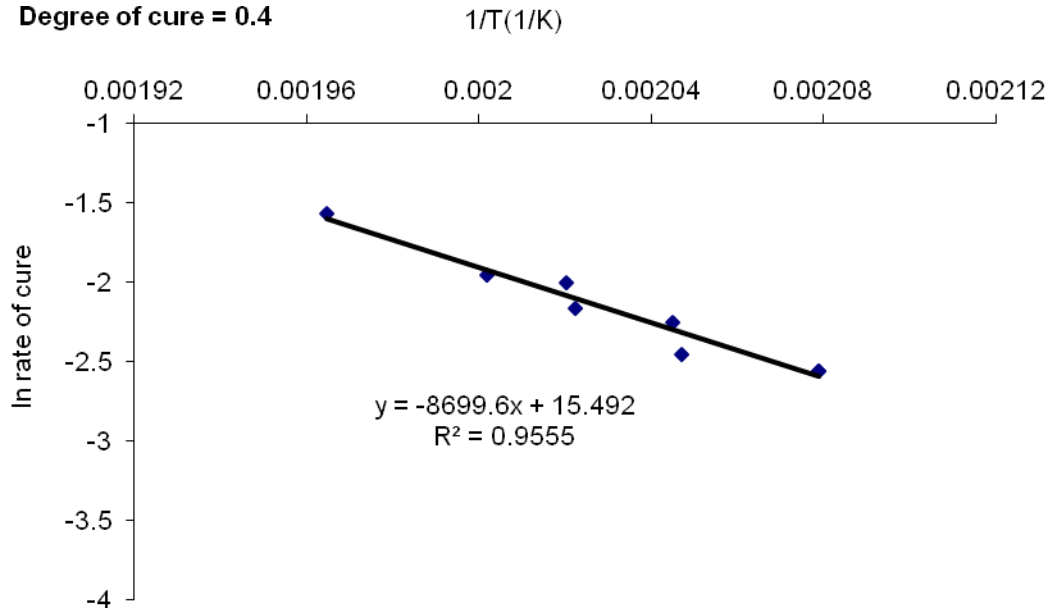

Degree of cure = 0.45

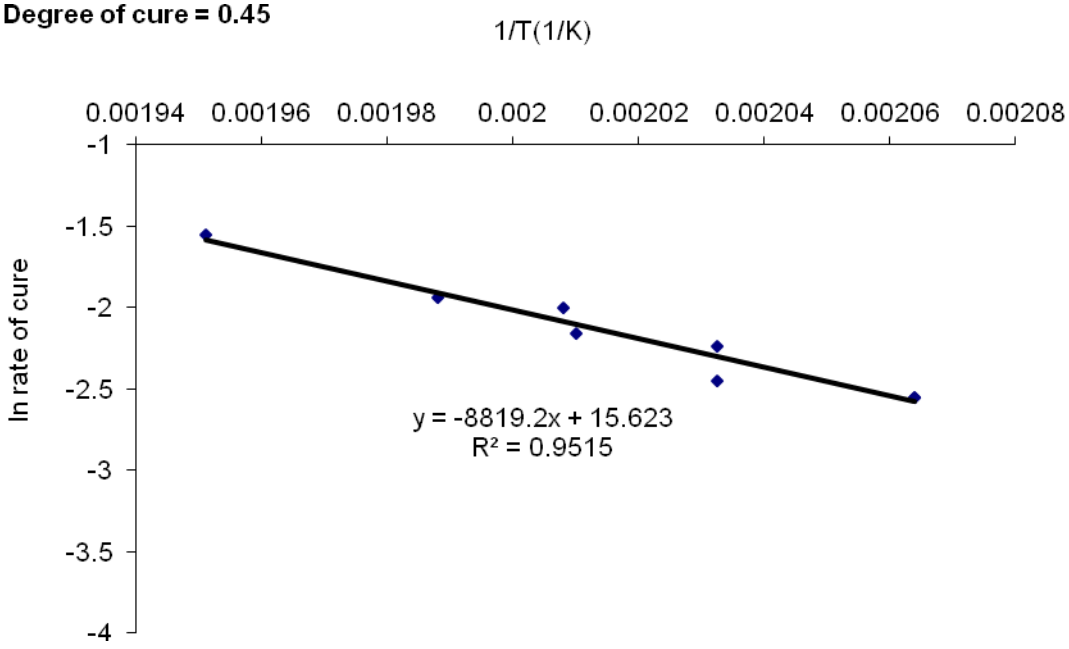

APPENDIX A (continued)

Degree of cure = 0.5

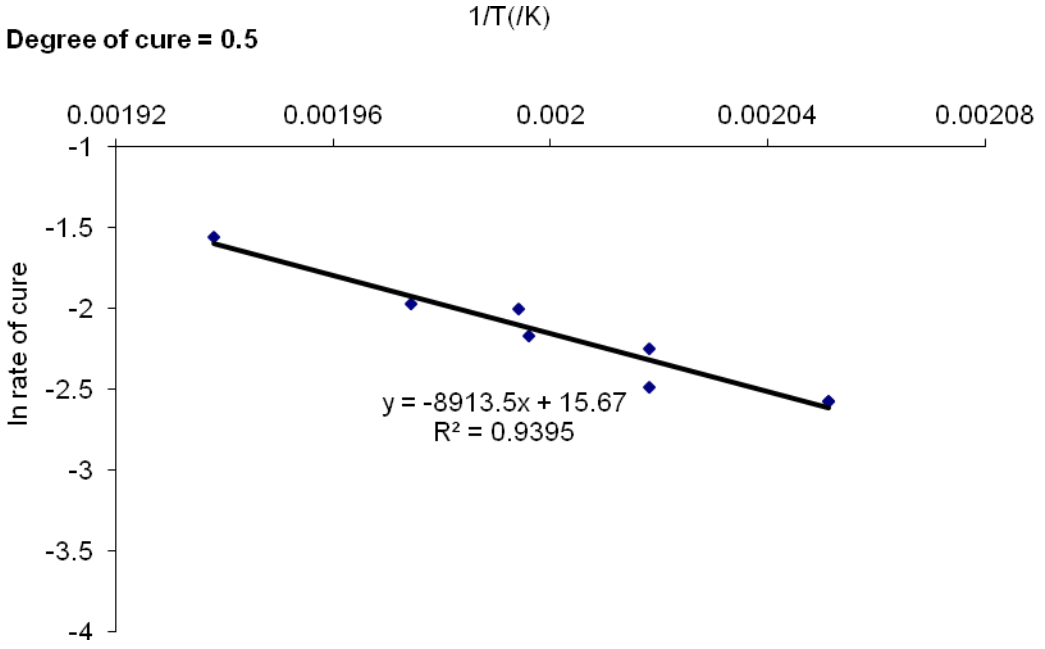

Degree of cure = 0.55

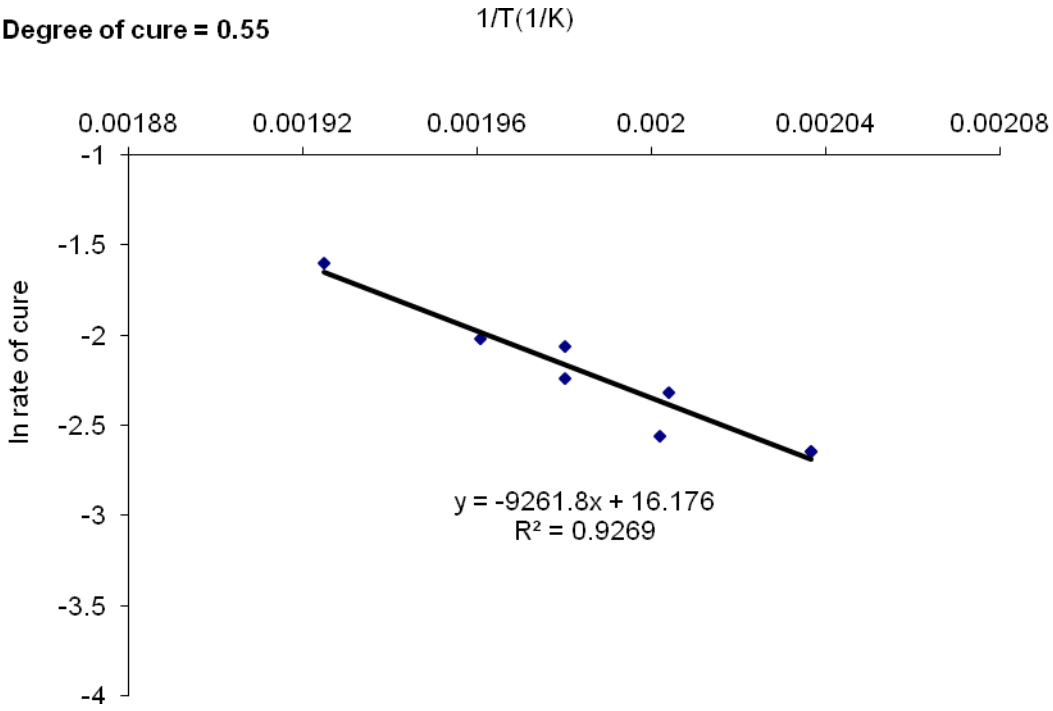

APPENDIX A (continued)

Degree of cure = 0.6

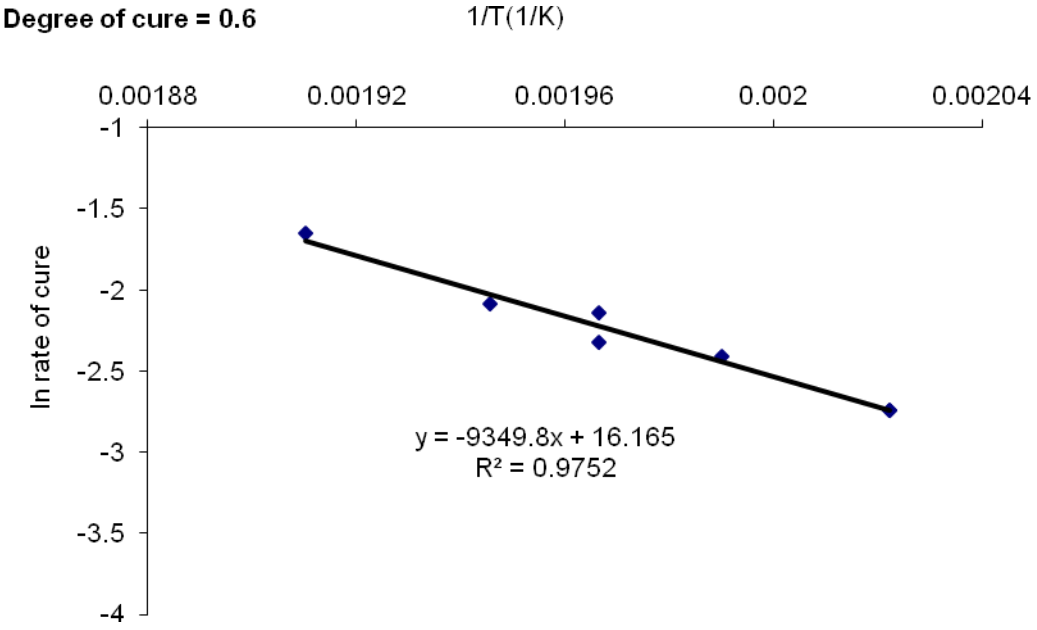

Degree of cure = 0.65

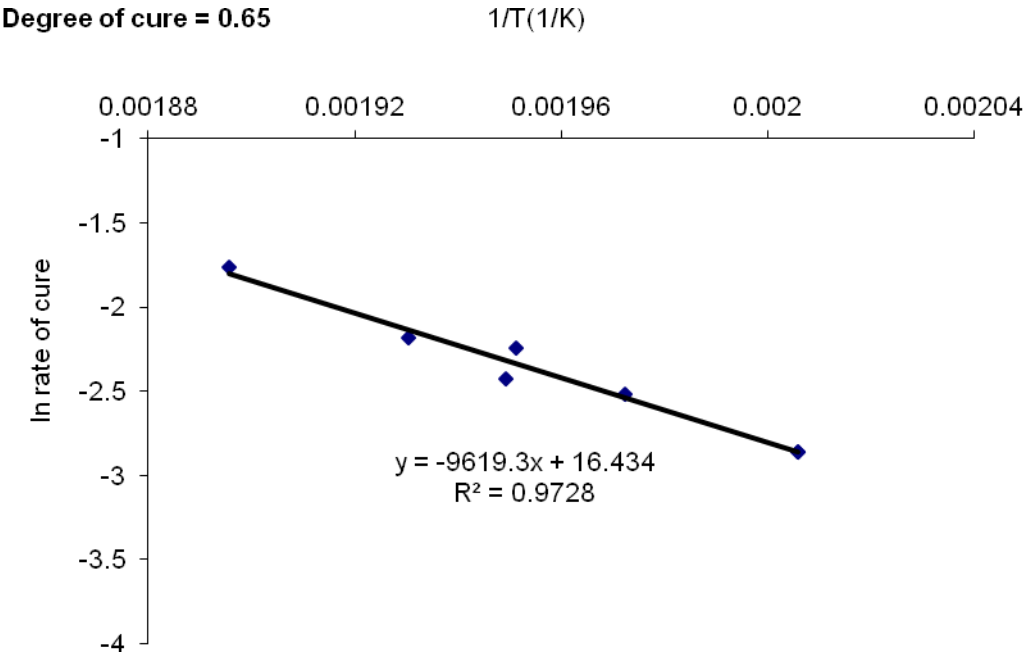

APPENDIX A (continued)

Degree of cure = 0.7

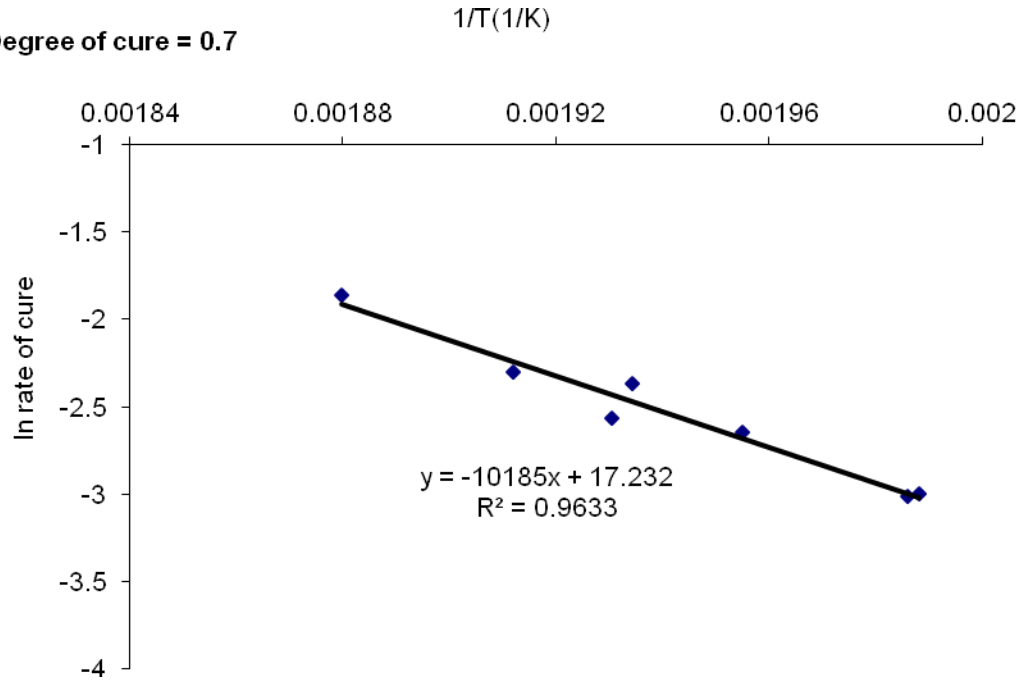

Degree of cure = 0.75

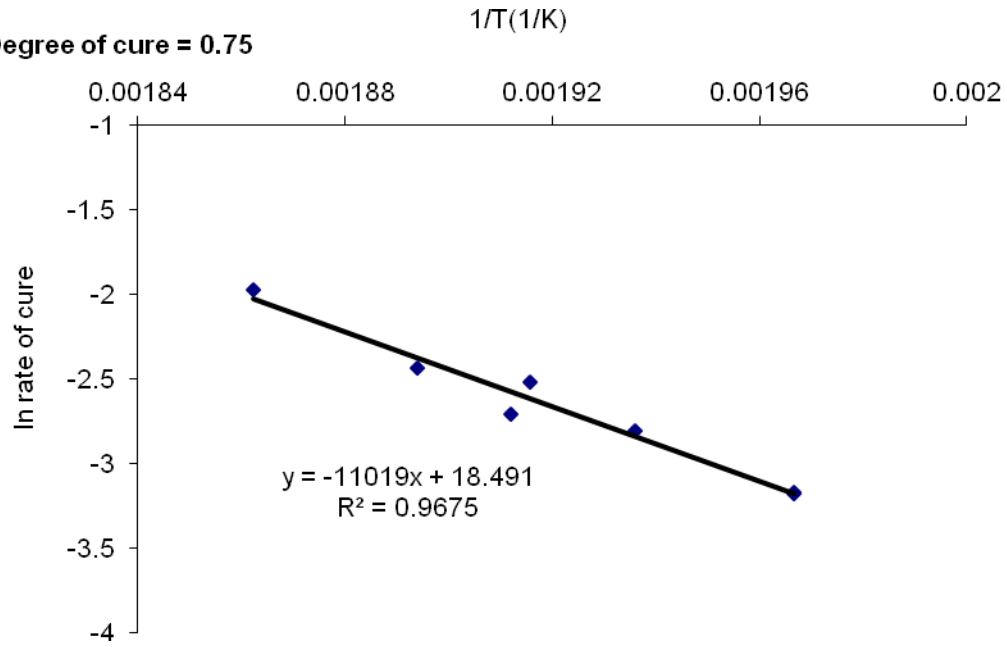

APPENDIX A (continued)

Degree of cure = 0.8

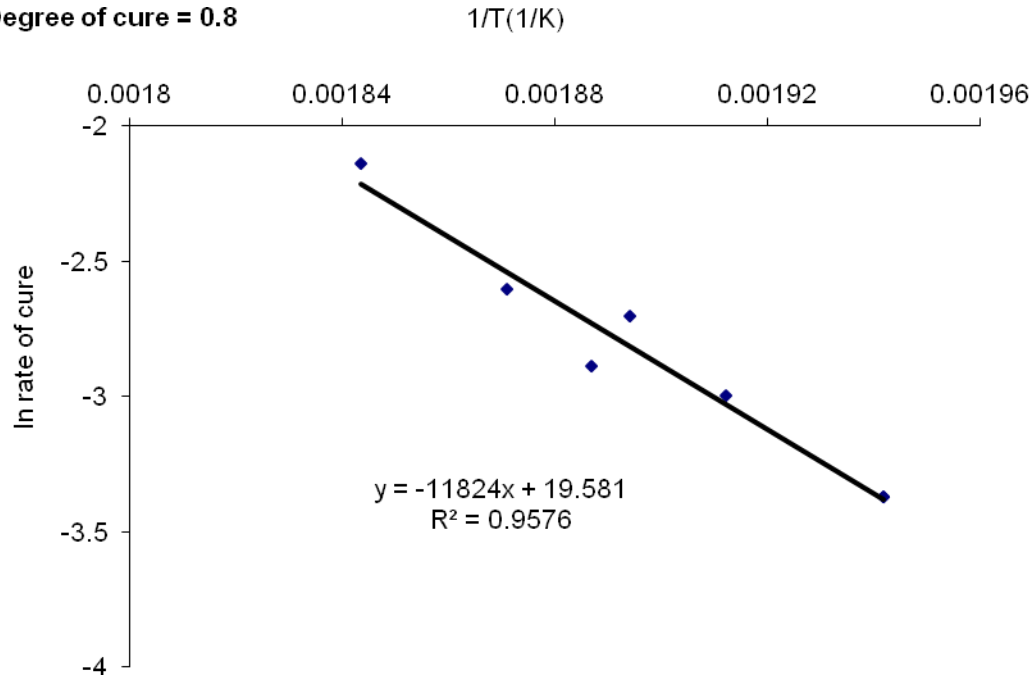

Degree of cure = 0.85

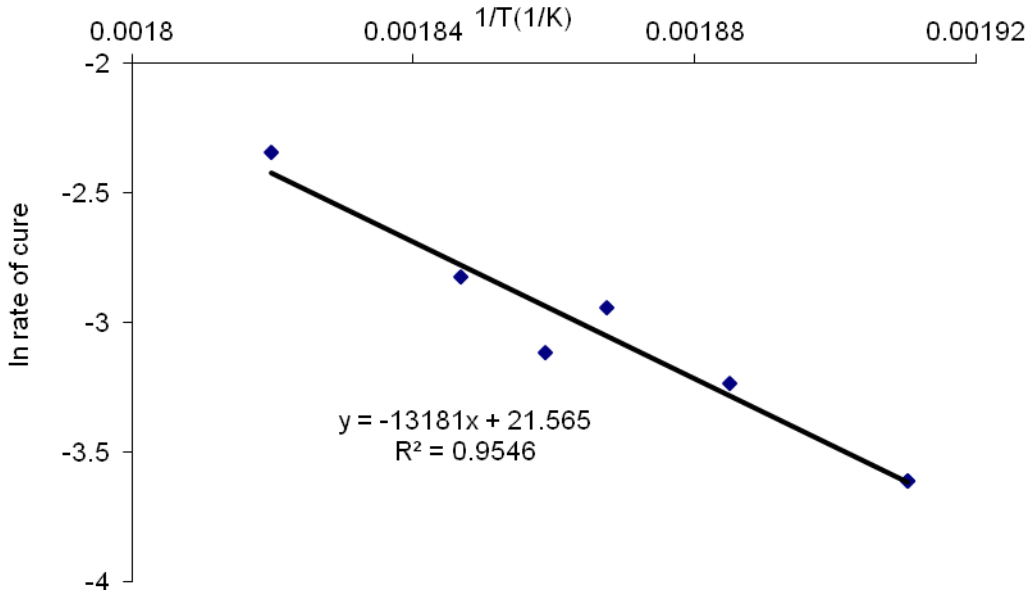

APPENDIX A (continued)

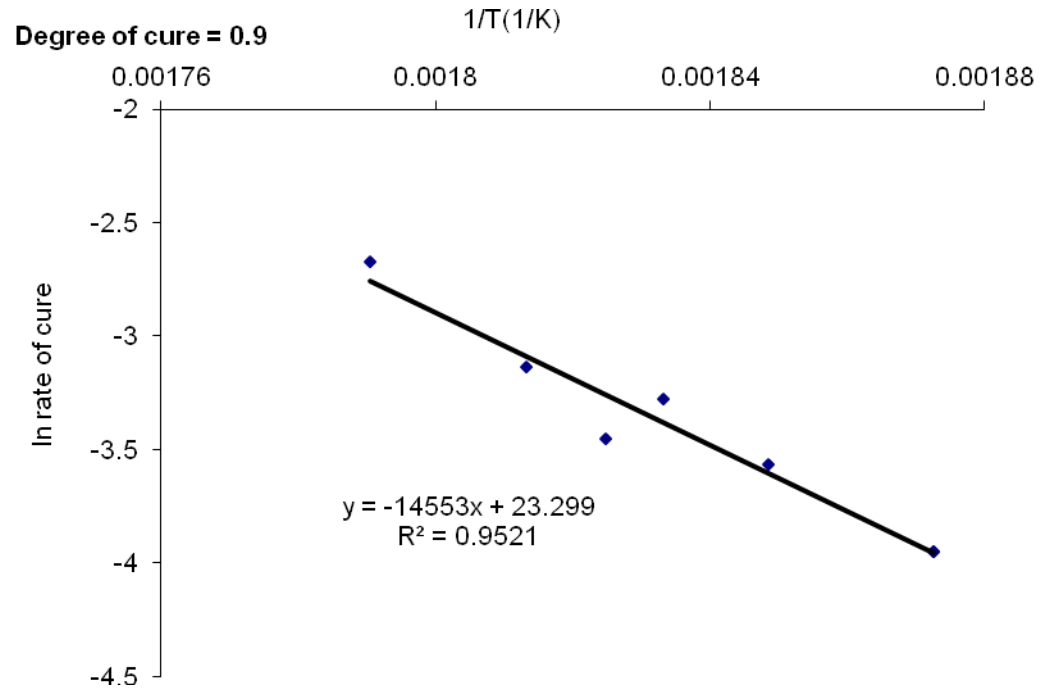

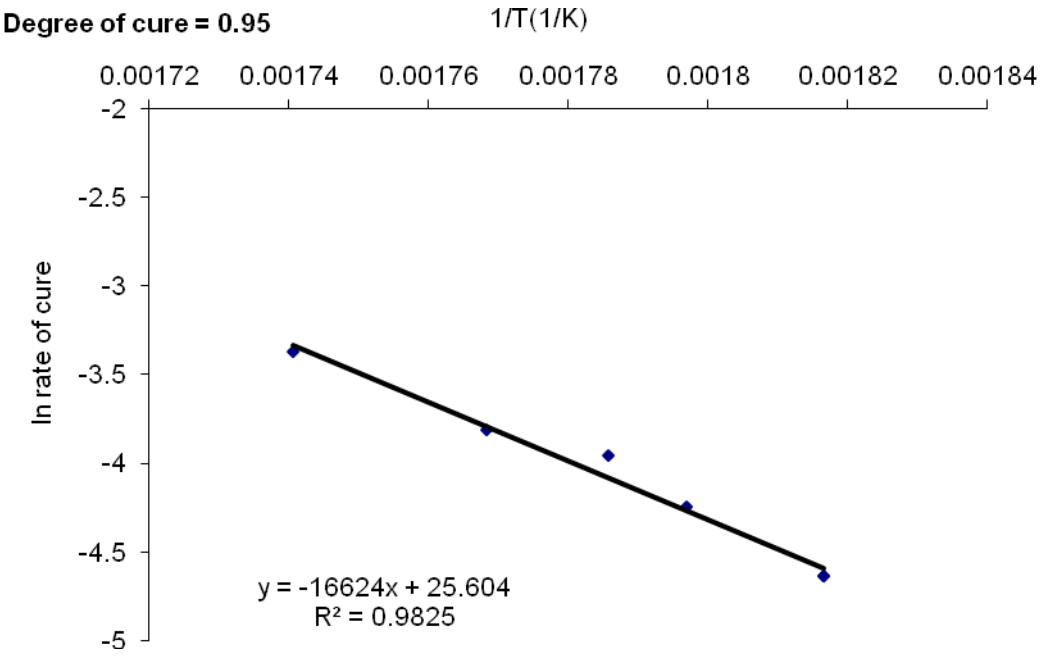

APPENDIX B

Calculation of Apparent Activation Energy for the cure of Nanopox F 400 resin cured with DDS curative at an N-H/epoxy molar ratio 1.1:1 under dynamic cure conditions in the DSC apparatus.

Degree of cure = 0.1

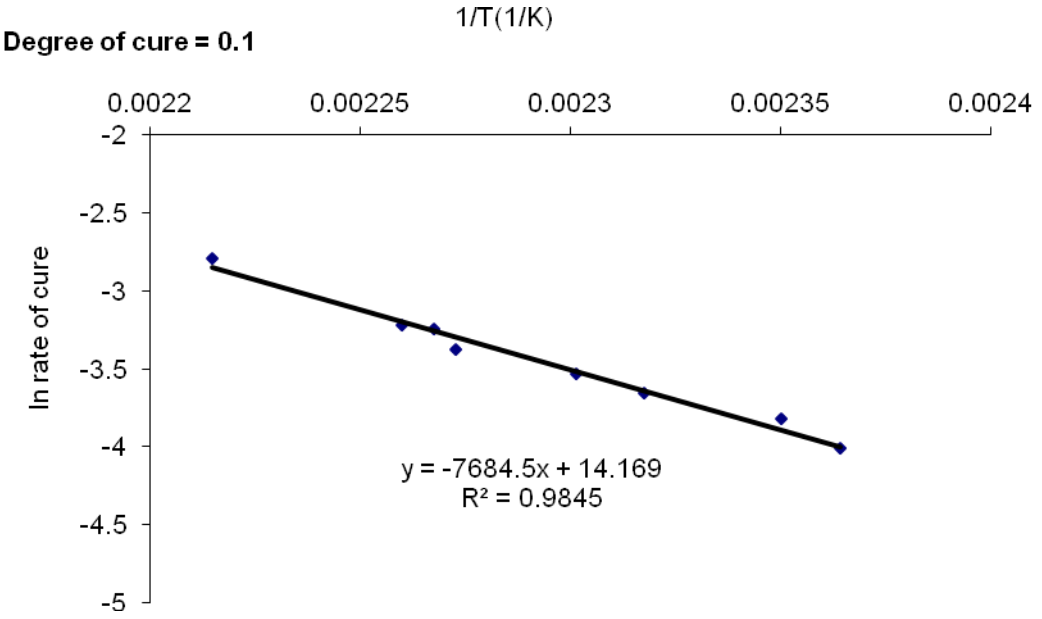

Degree of cure = 0.15

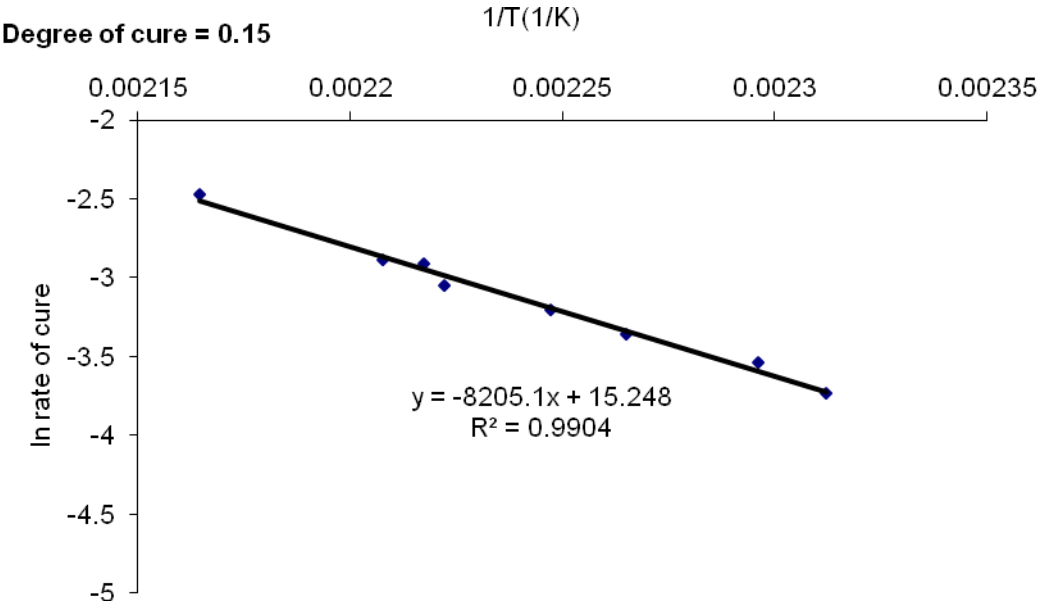

APPENDIX B (continued)

Degree of cure = 0.2

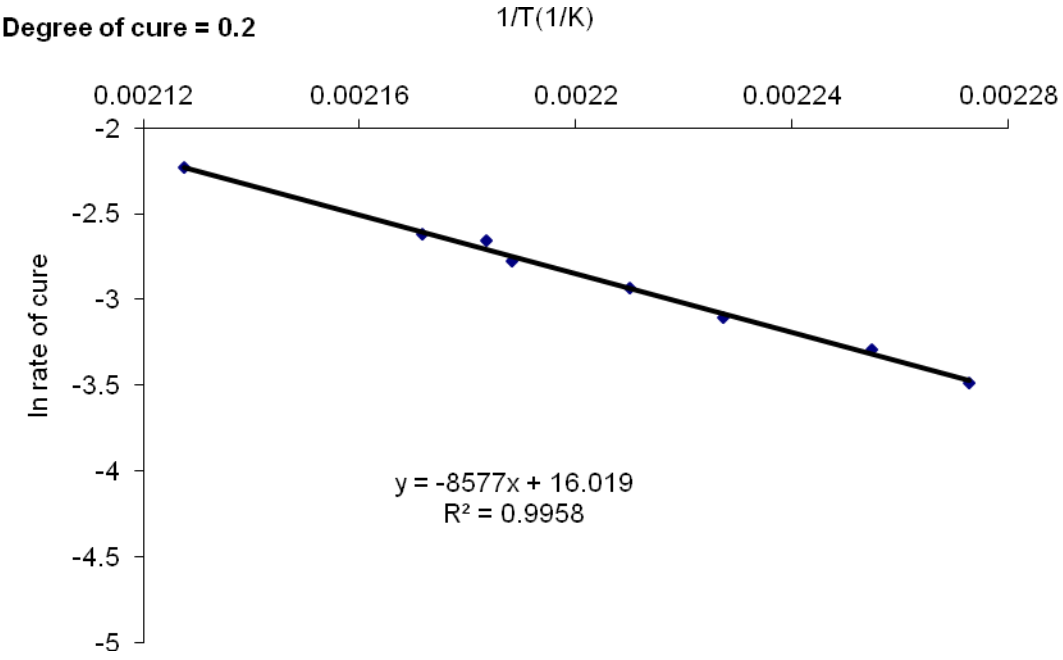

Degree of cure = 0.25

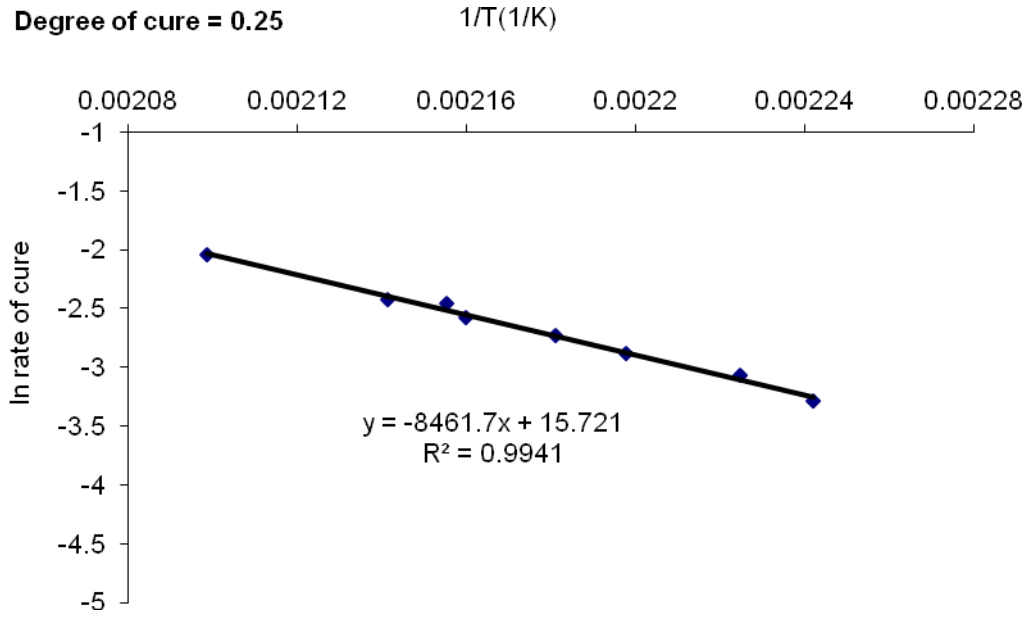

APPENDIX B (continued)

Degree of cure = 0.3

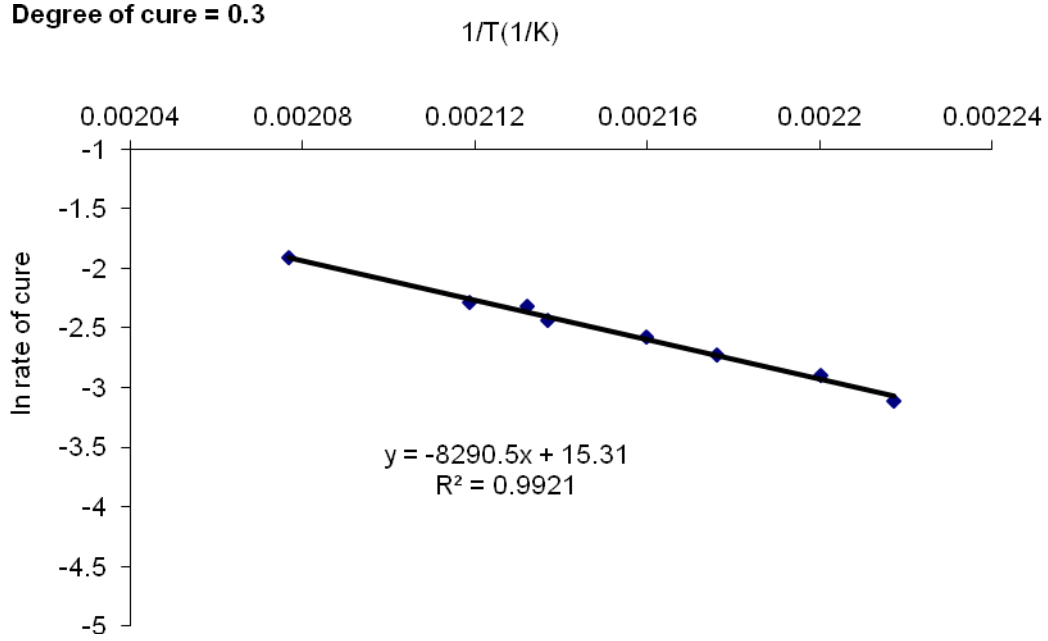

Degree of cure = 0.35

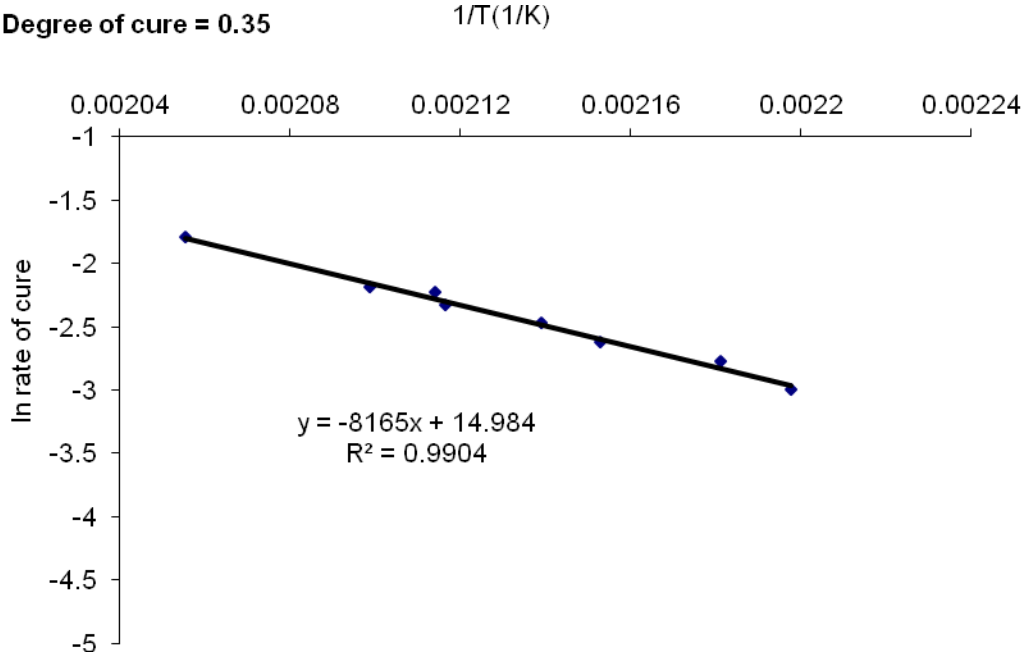

APPENDIX B (continued)

Degree of cure = 0.4

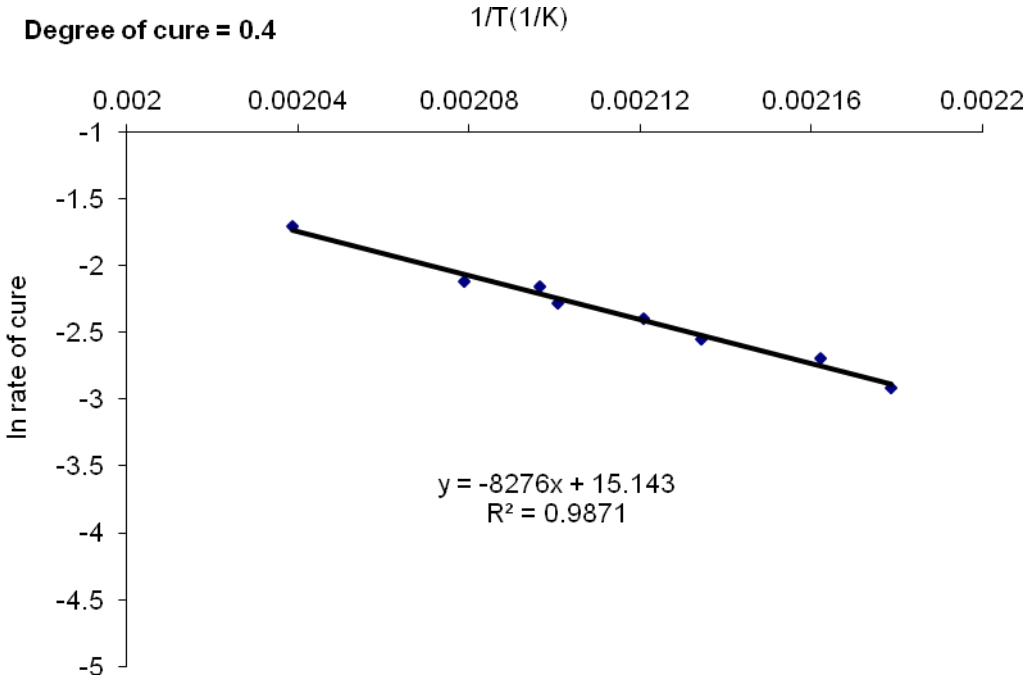

Degree of cure = 0.45

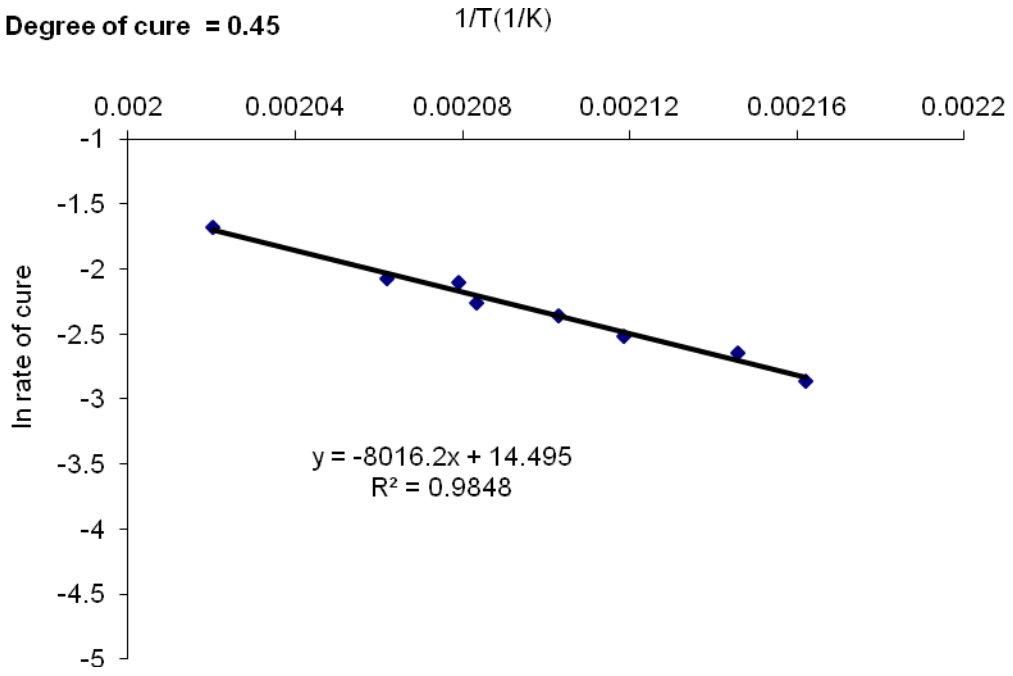

APPENDIX B (continued)

Degree of cure = 0.5

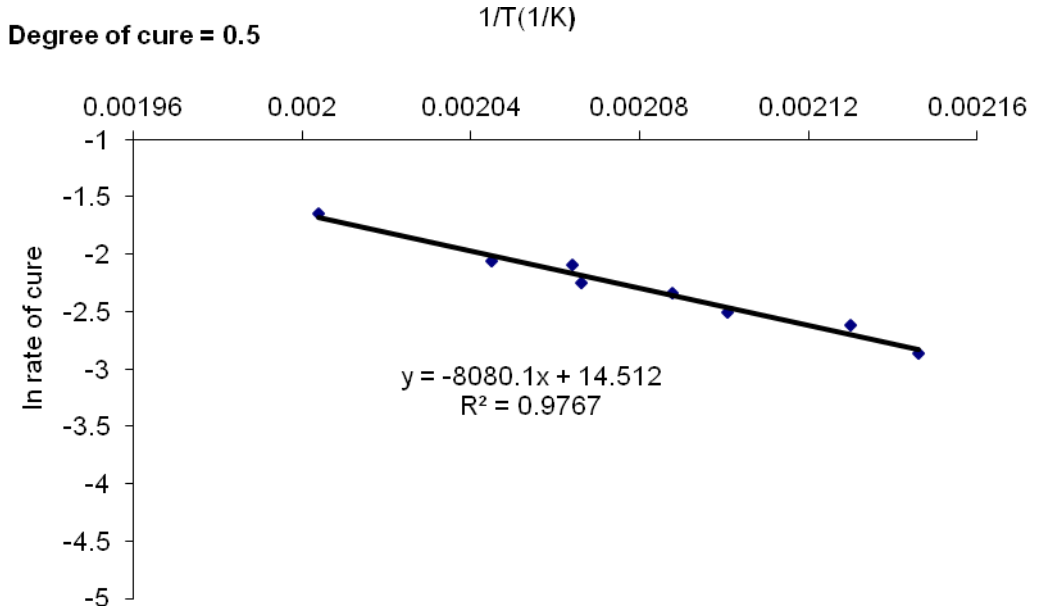

Degree of cure = 0.55

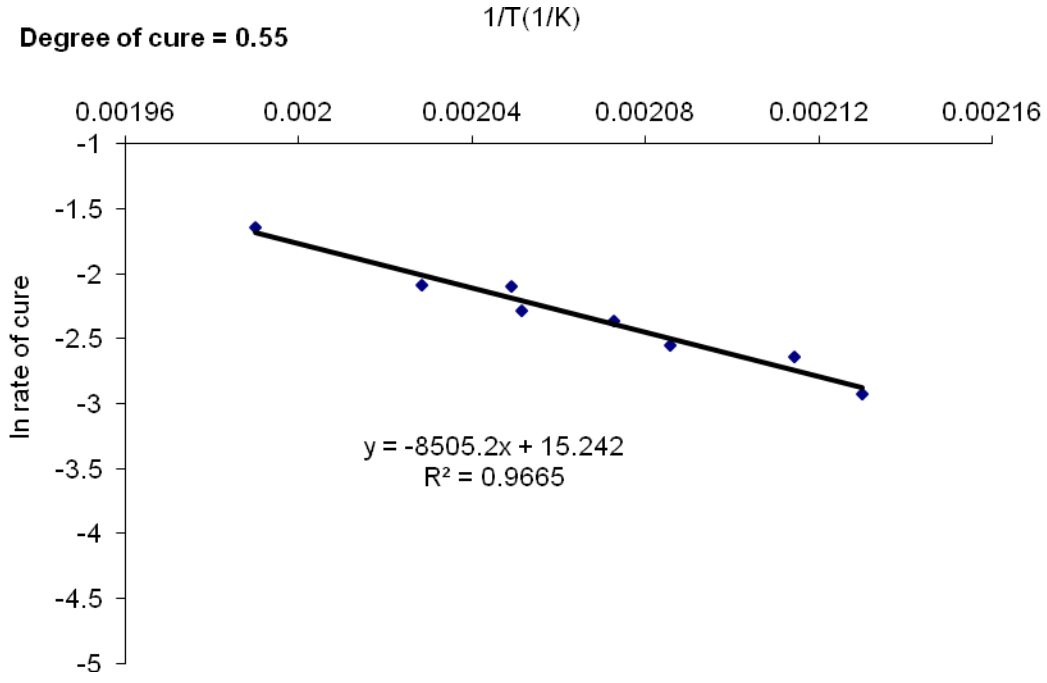

APPENDIX B (continued)

Degree of cure = 0.6

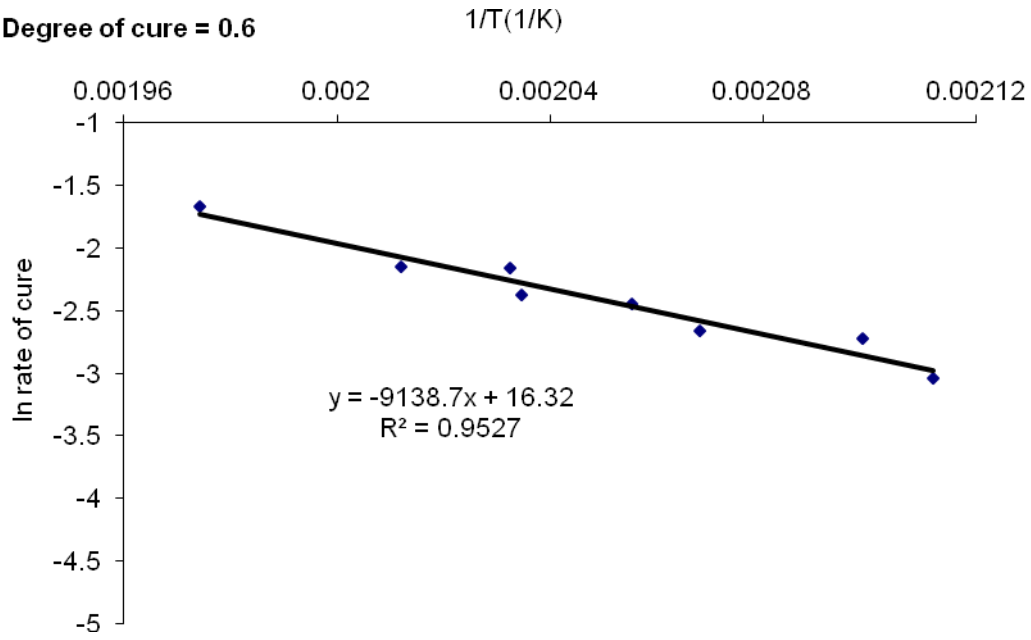

Degree of cure = 0.65

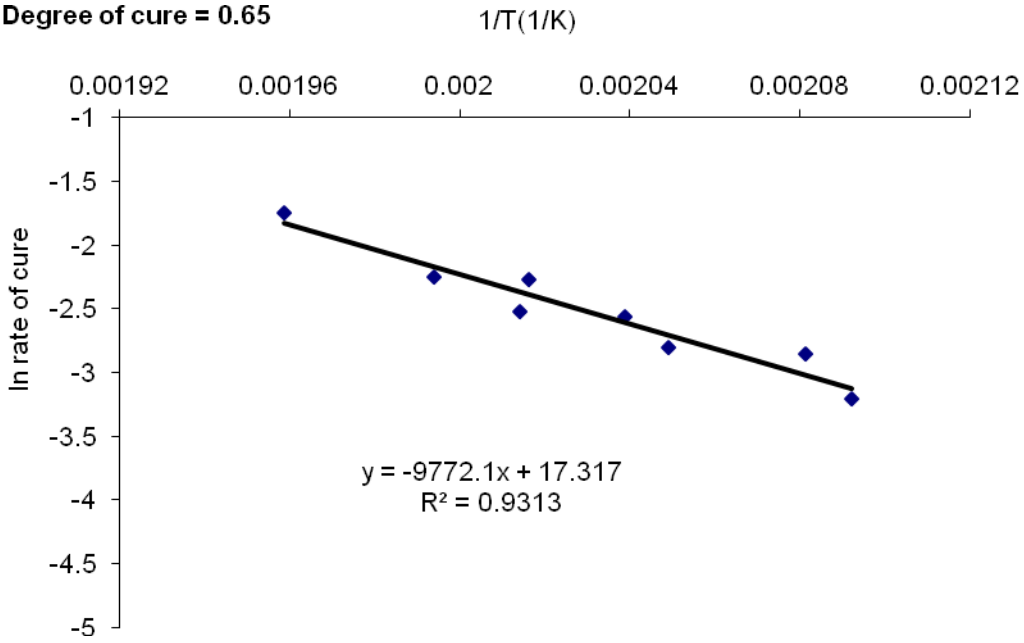

APPENDIX B (continued)

Degree of cure = 0.7

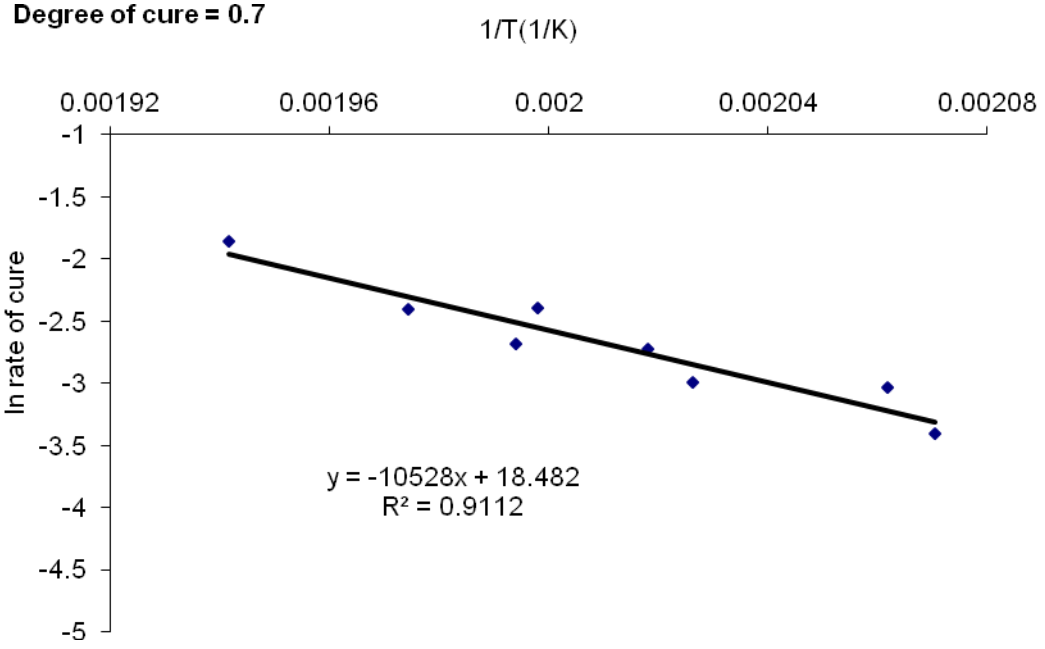

Degree of cure = 0.75

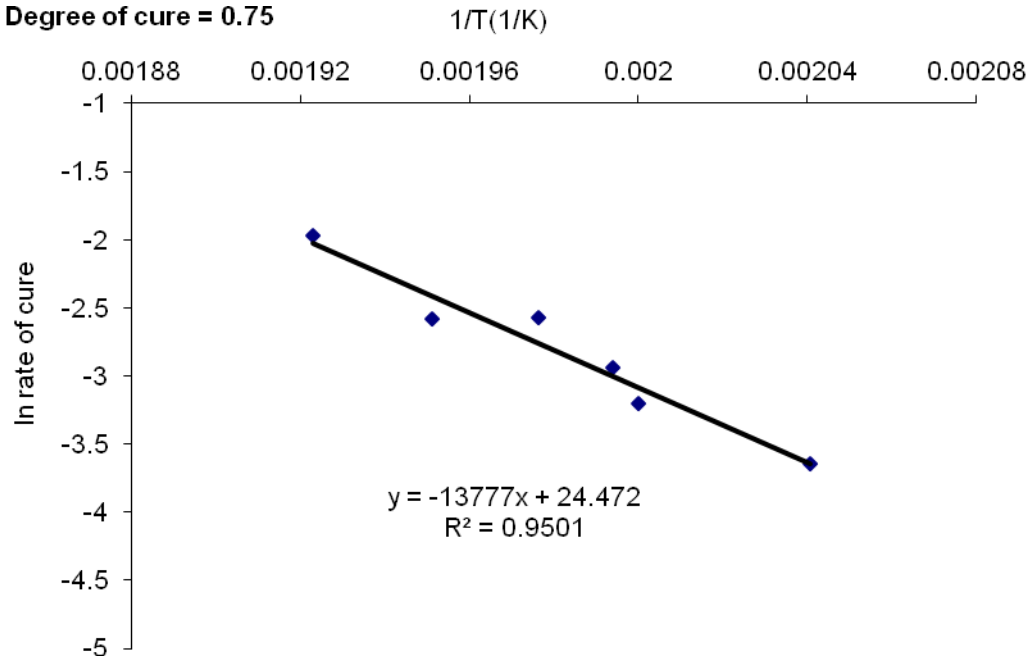

APPENDIX B (continued)

Degree of cure = 0.8

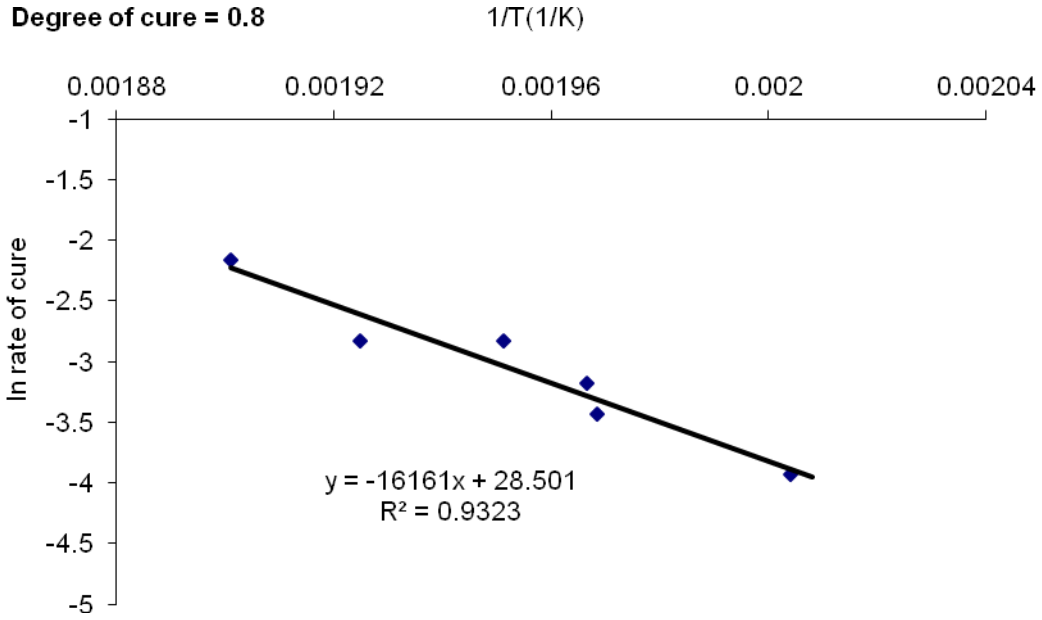

Degree of cure = 0.85

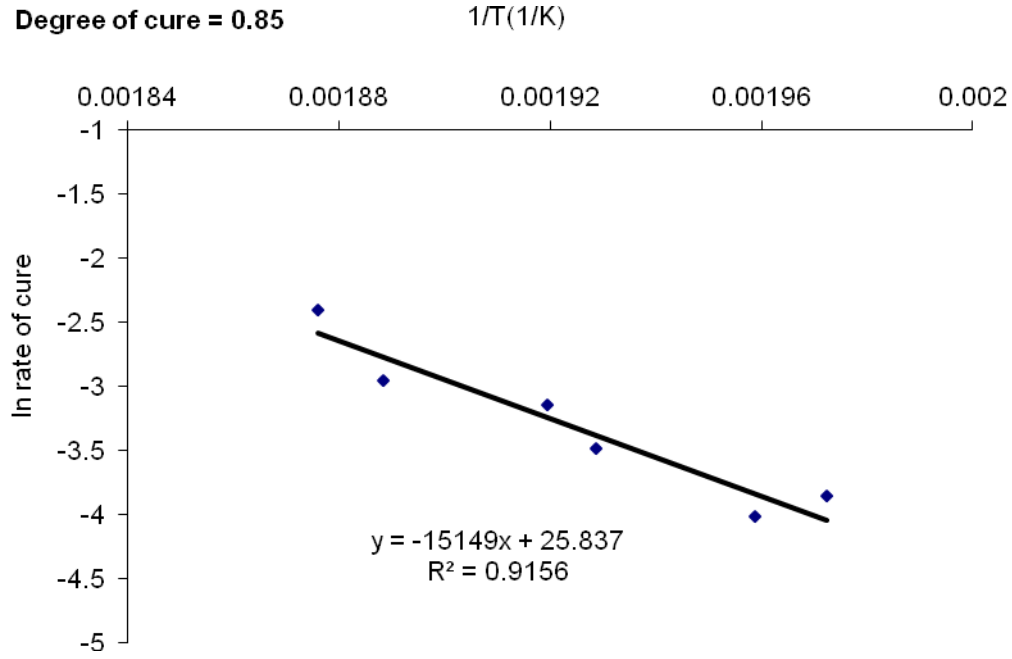

APPENDIX B (continued)

Degree of cure = 0.90

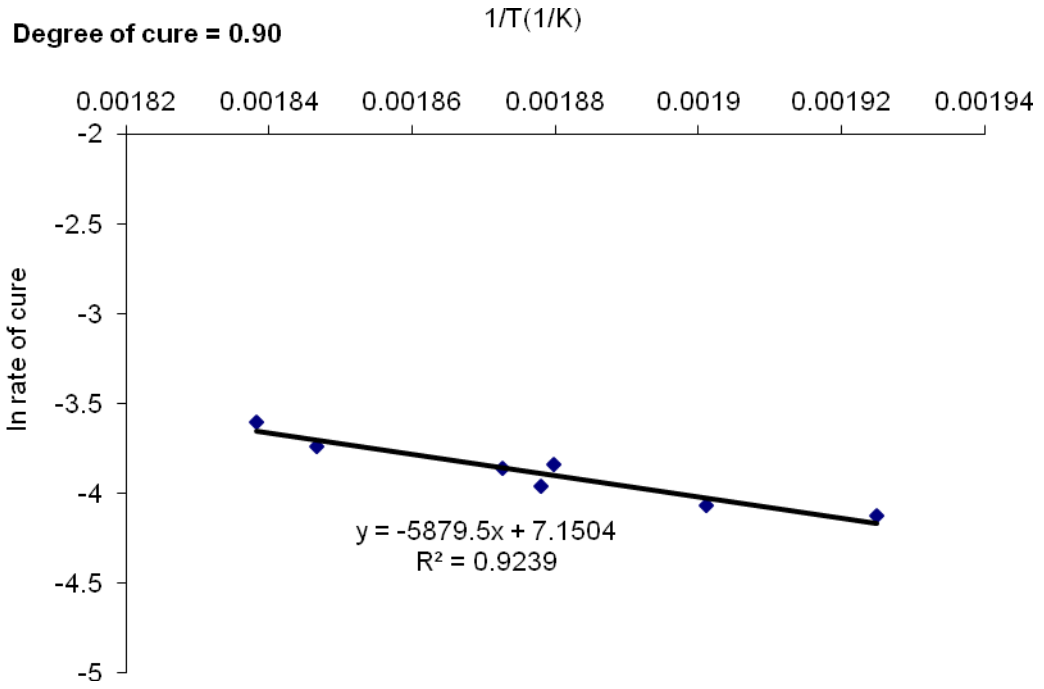

Degree of cure = 0.95

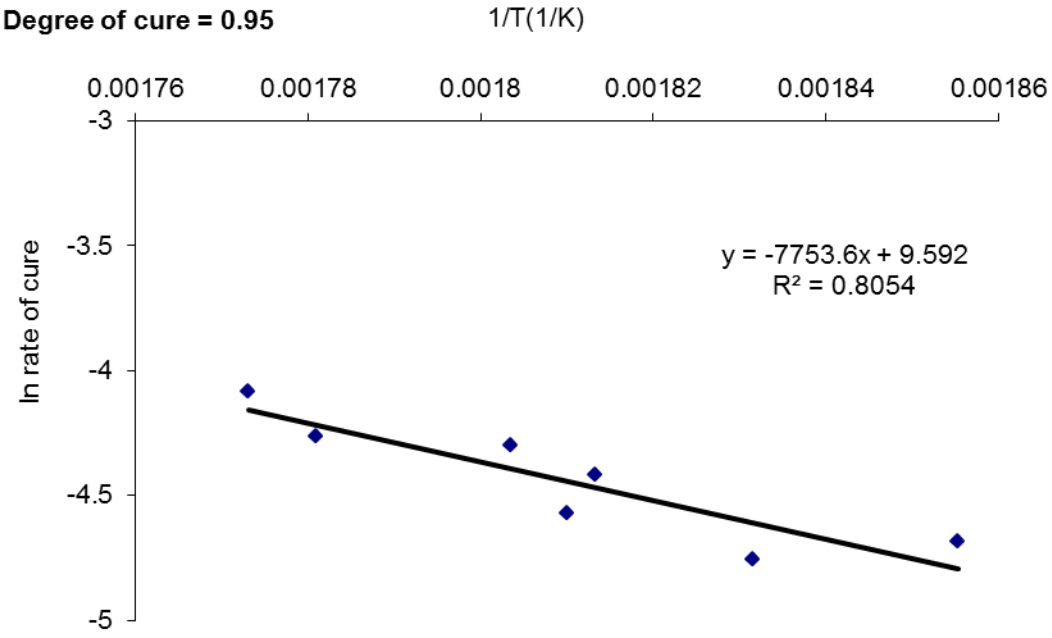

APPENDIX C

Rate of Cure vs. Degree of Cure at various temperatures for the control resin cured with DDS curative under isothermal conditions in the DSC apparatus

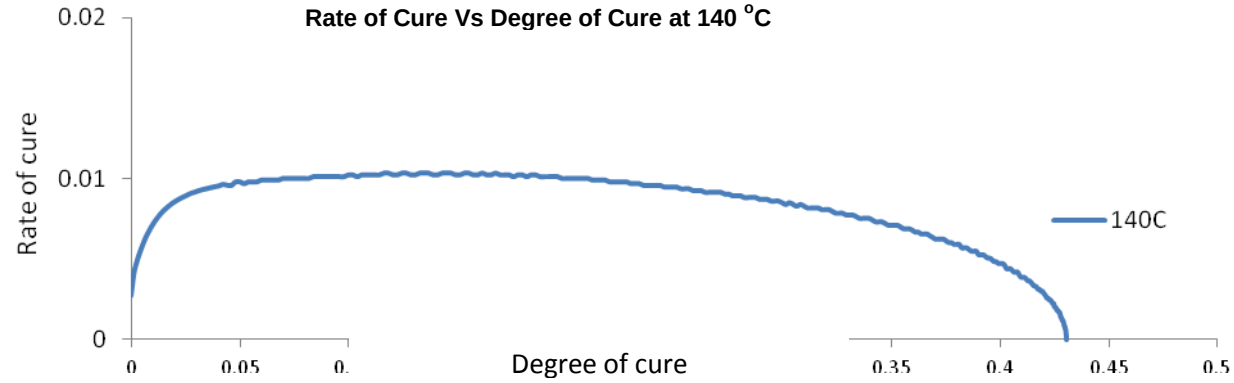

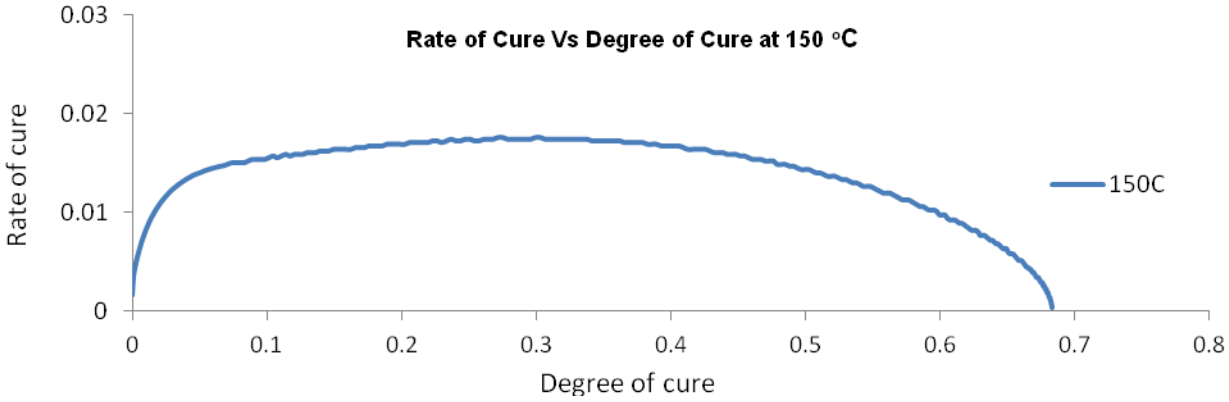

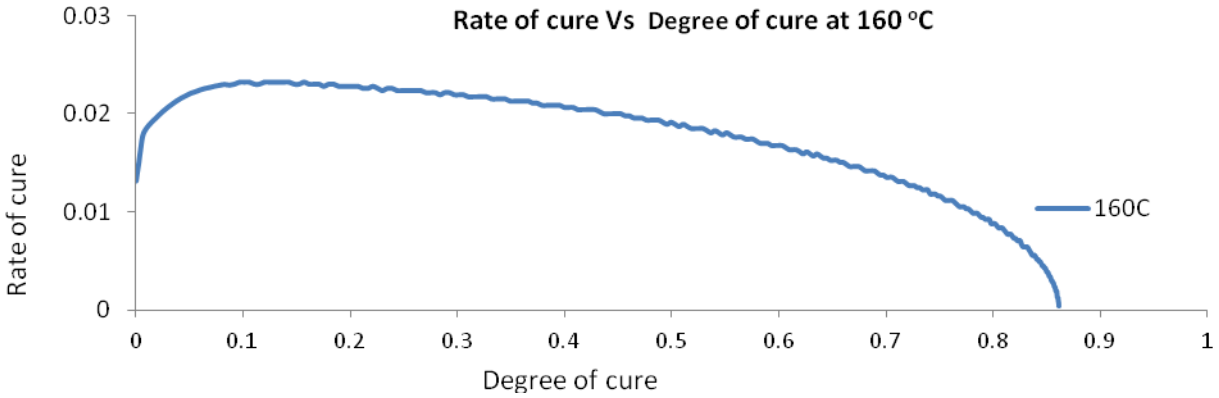

APPENDIX C (continued)

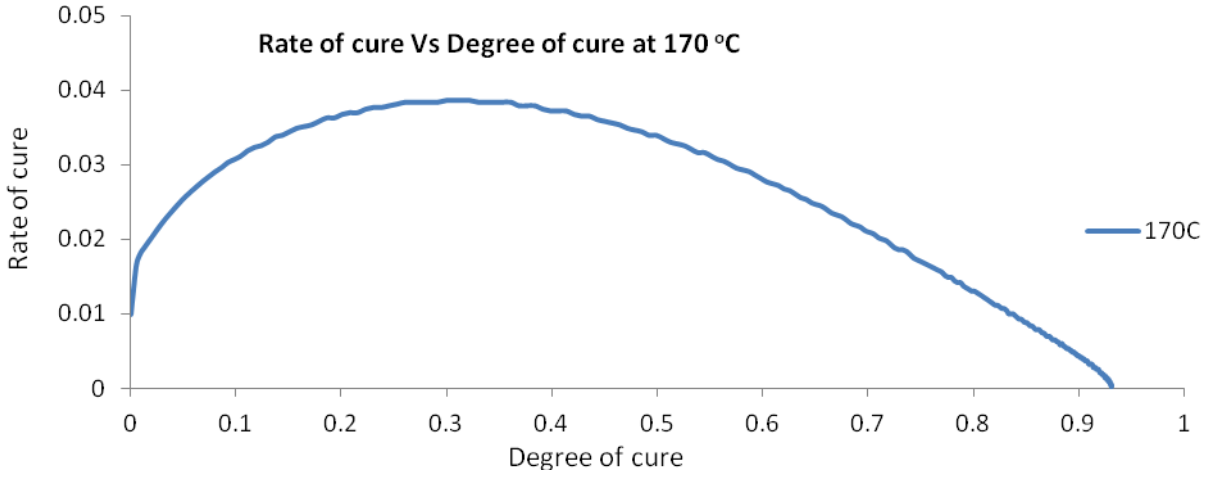

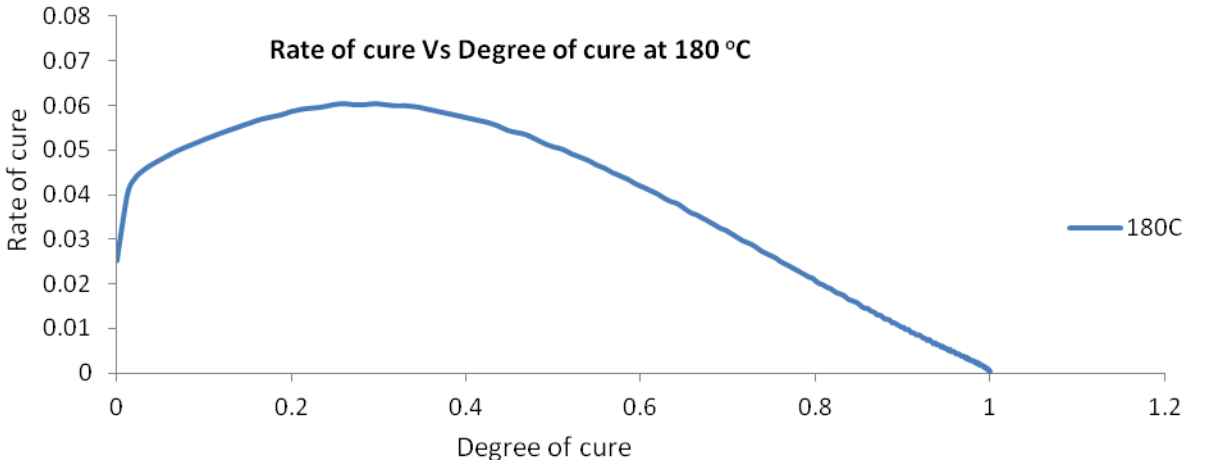

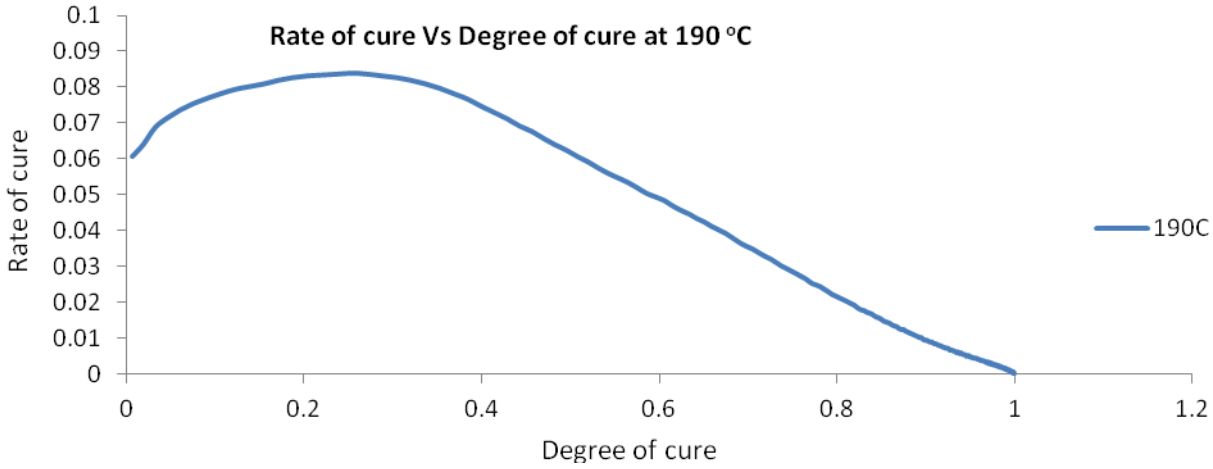

APPENDIX C (continued)

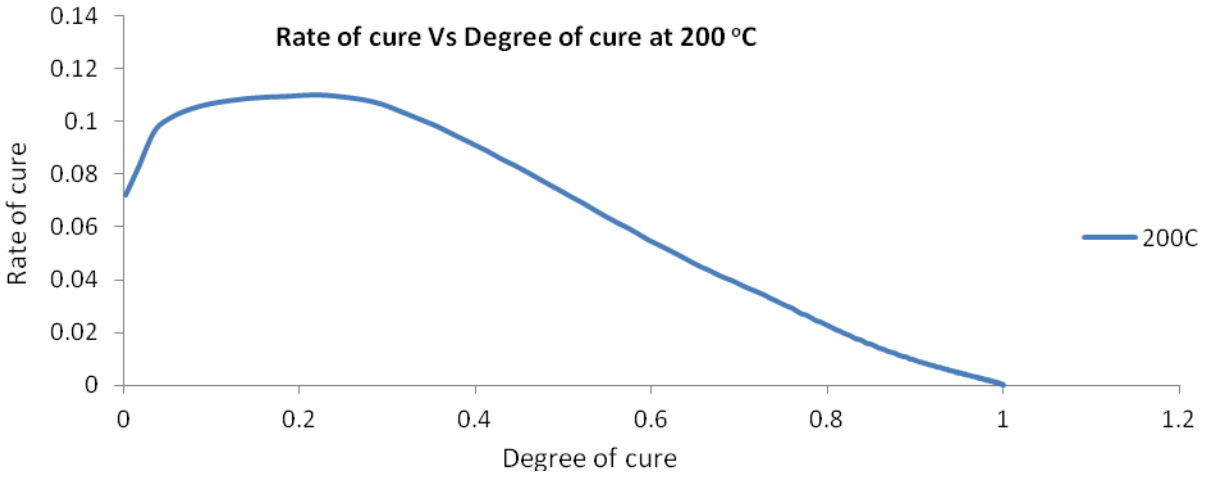

APPENDIX D

Rate of Cure vs. Degree of Cure at various temperatures for Nanopox F 400 resin cured with DDS curative under isothermal conditions in the DSC apparatus

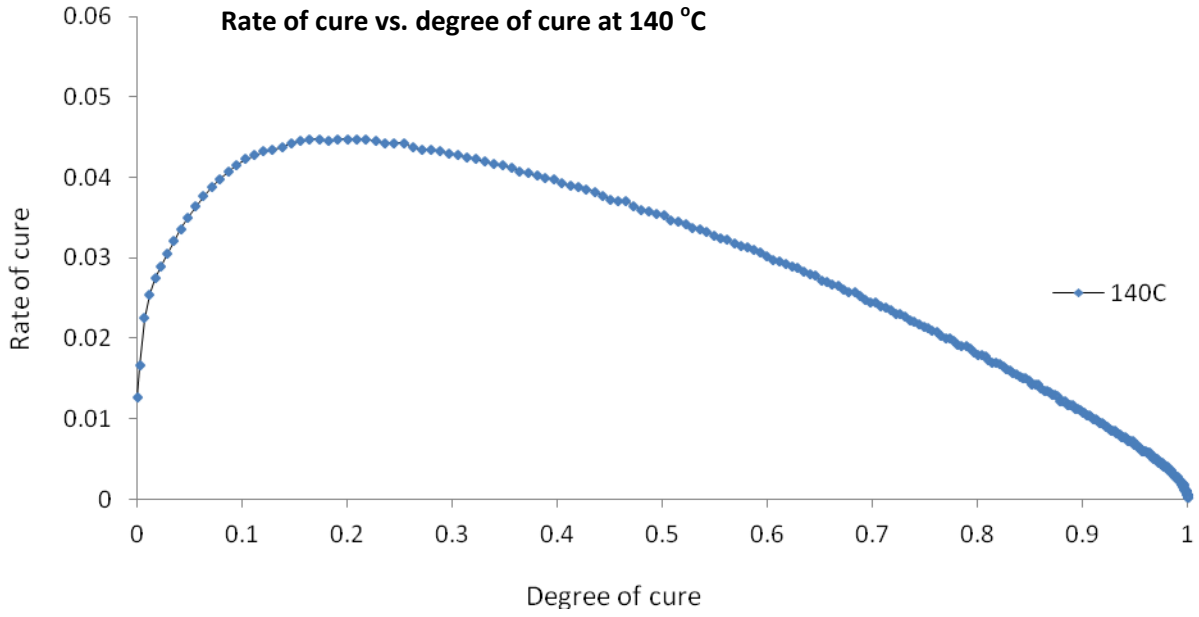

APPENDIX D (continued)

Rate of cure vs. degree of cure at 150 °C

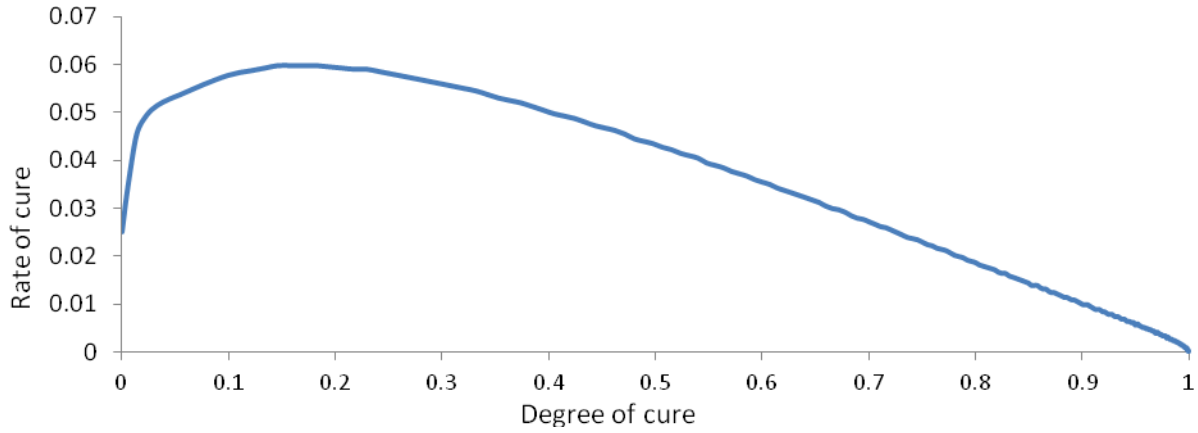

Rate of cure vs. degree of cure at 160 °C

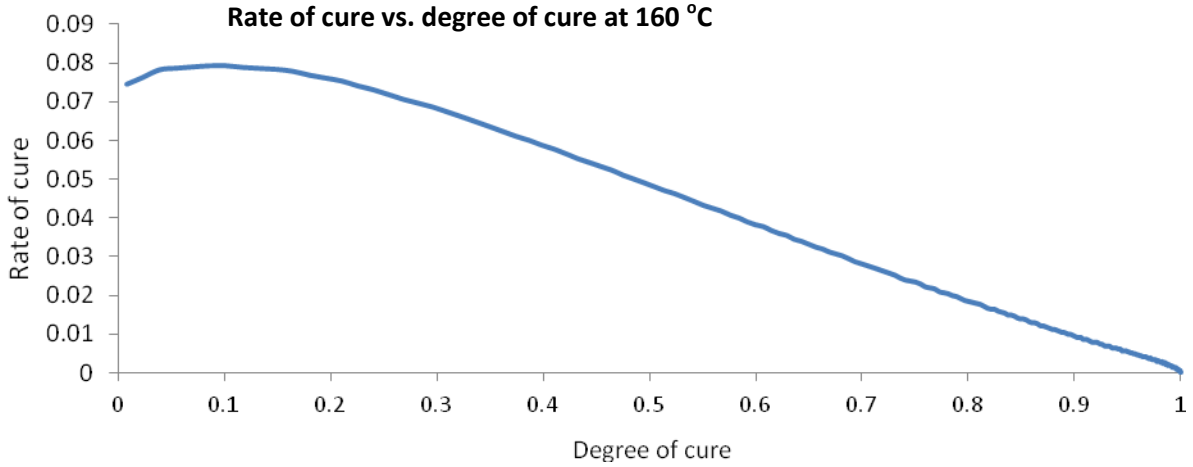

Rate of cure vs. degree of cure at 170 °C

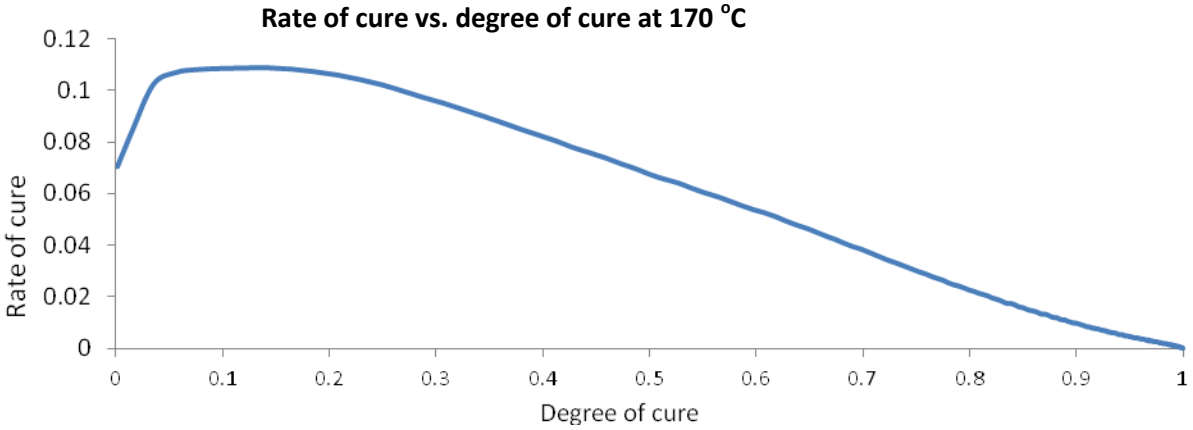

APPENDIX D (continued)

Rate of cure vs. degree of cure at 180 °C

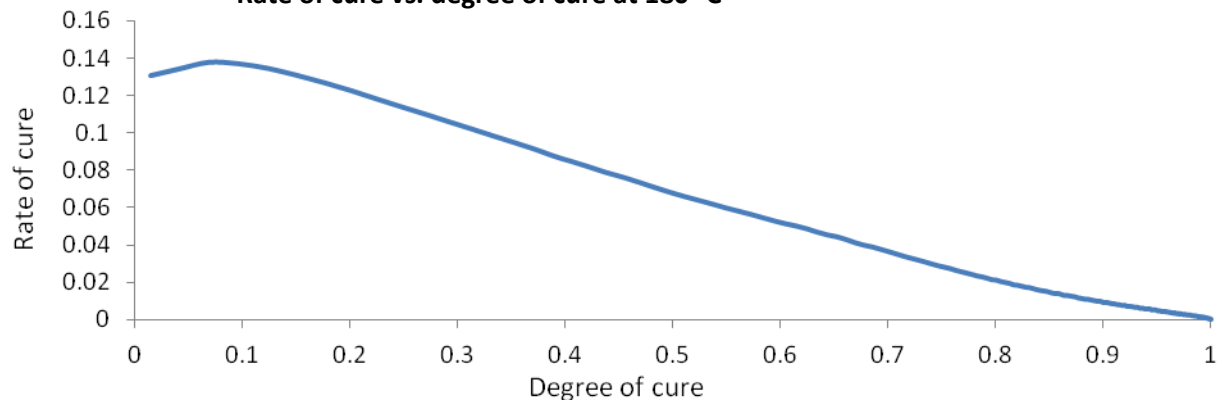

Rate of cure vs. degree of cure at 190 °C

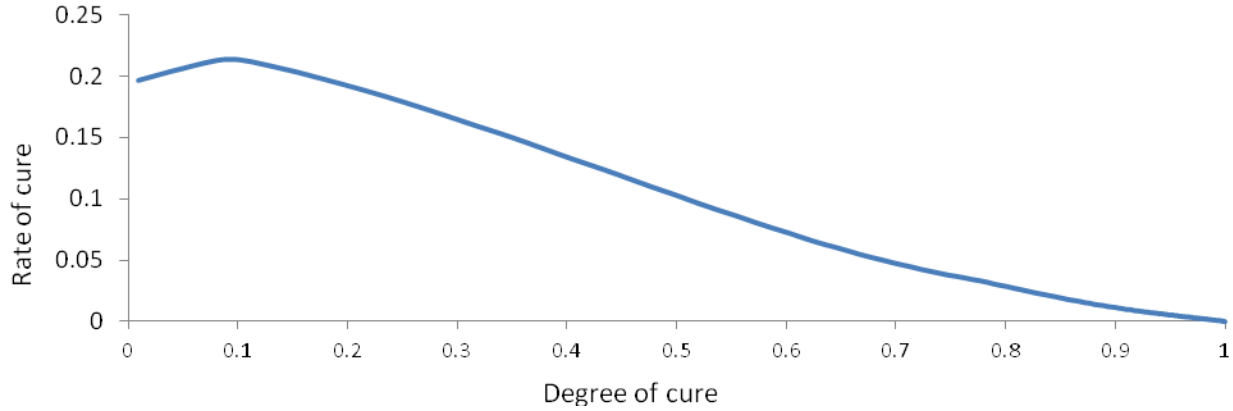

Rate of cure vs. degree of cure at 200 °C

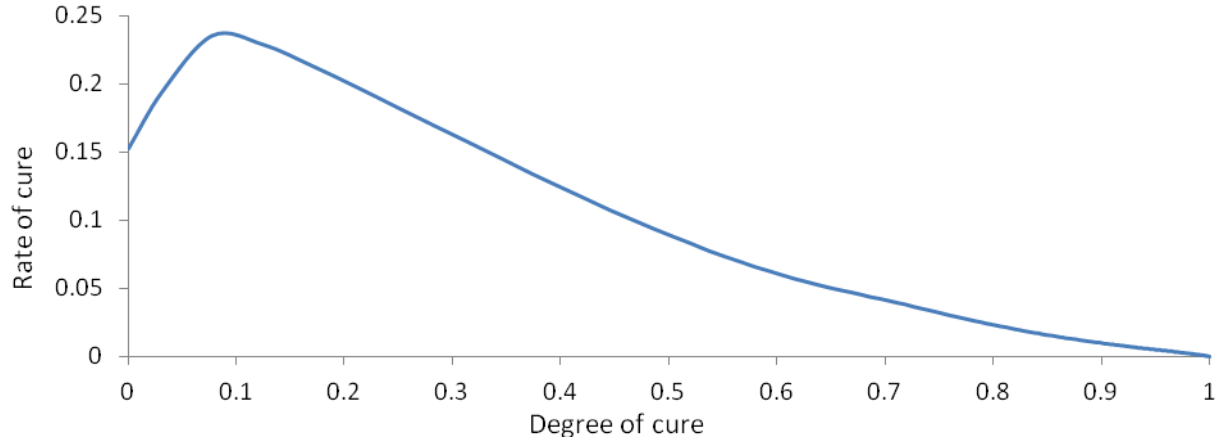

APPENDIX E

Summary of stress-strain plot at low strain for the control resin specimens cured with DDS at an N-H/epoxy molar ratio 0.9:1. (Sample specimens were stretched at a speed of 5 mm/min)

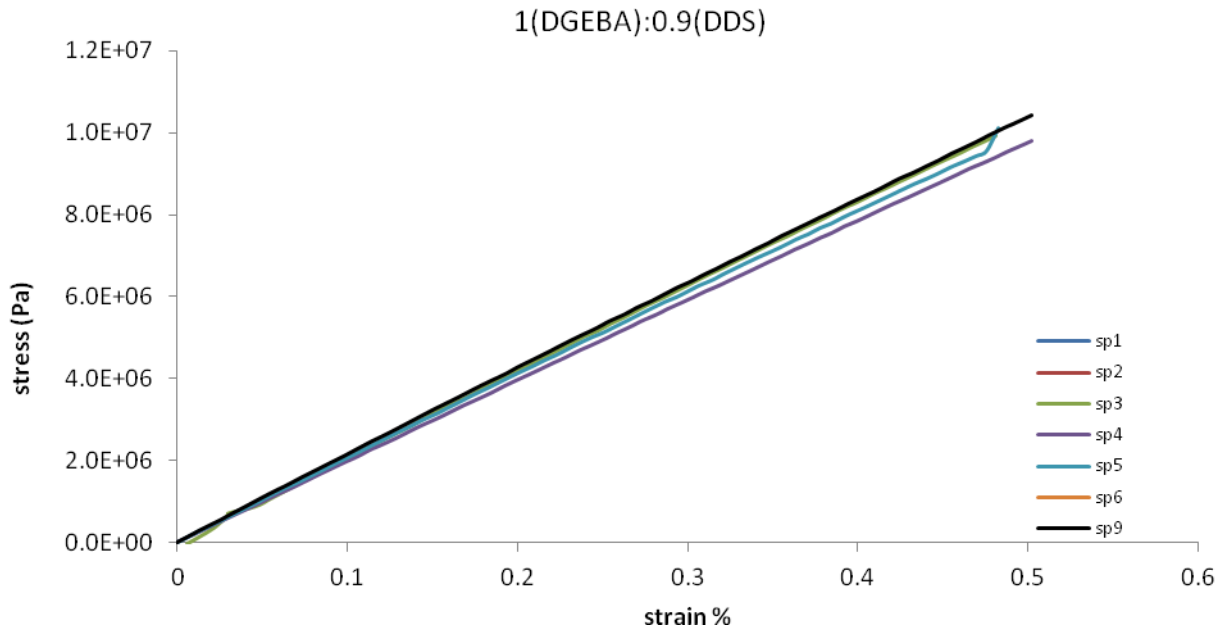

Summary of tensile testing for the control resin cured with DDS at an N-H/epoxy molar ratio 0.9:1

sample	Modulus, E (GPa)	Strain to failure, ε_u, (%)	Stress at break, σ_u (Mpa)
1	2.13	2.76	60.48
3	2.80	3.34	68.34
4	1.97	3.87	75.00
5	2.01	3.37	69.93
7	1.76	2.66	56.54
8	2.07	2.29	51.18
9	2.07	2.33	52.56
Ave	2.01	2.95	62.00
Std dev.	1.21	0.60	9.23
%RSD	5.98	20.20	14.88

APPENDIX E (continued)

Summary of stress-strain plot of the control resin specimens cured with DDS at an N-H/epoxy molar ratio 1:1. (Sample specimens were stretched at a speed of 5 mm/min)

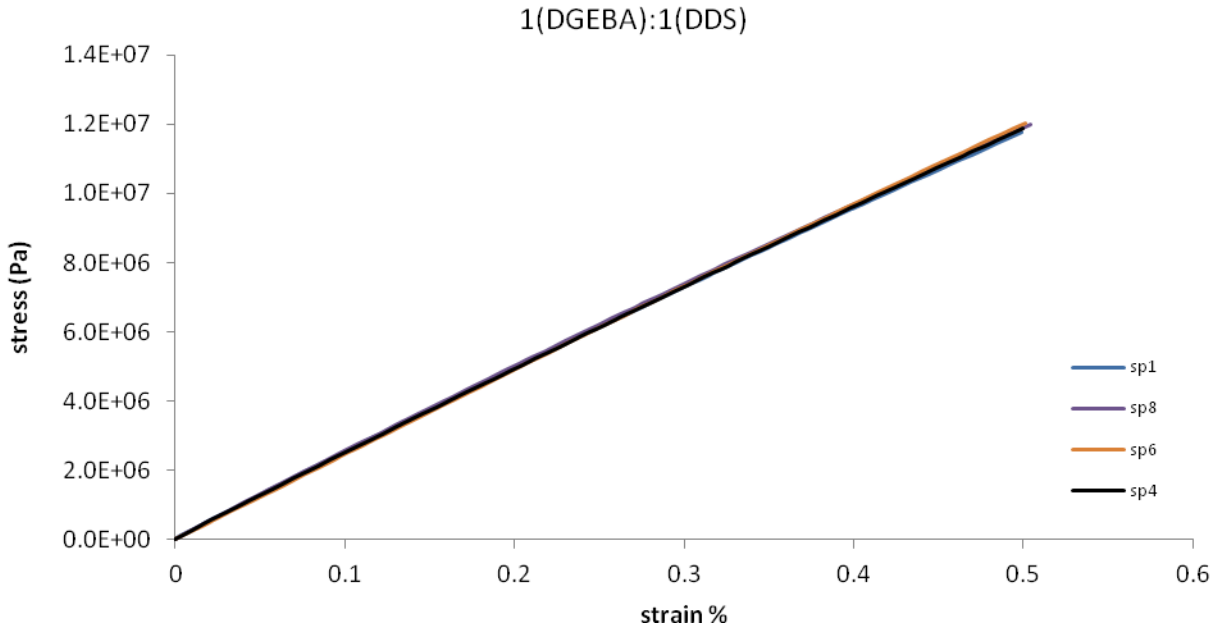

Summary of tensile testing for the control resin cured with DDS at an N-H/epoxy molar ratio 1:1

sample	Modulus, E (GPa)	Strain to failure, ε_u (%)	Stress at break, $\sigma_{u,}$(MPa)
1	2.34	5.58	72.62
4	2.37	4.99	73.71
6	2.40	5.75	72.89
8	2.40	5.96	59.19
Ave	2.38	5.57	69.60
Std dev.	0.30	0.42	6.96
%RSD	1.24	7.53	9.99

APPENDIX E (continued)

Summary of stress-strain plot of Nanopox F 400 resin specimens cured with DDS at an N-H/epoxy molar ratio 0.9:1 (Sample specimens were stretched at a speed of 5 mm/min)

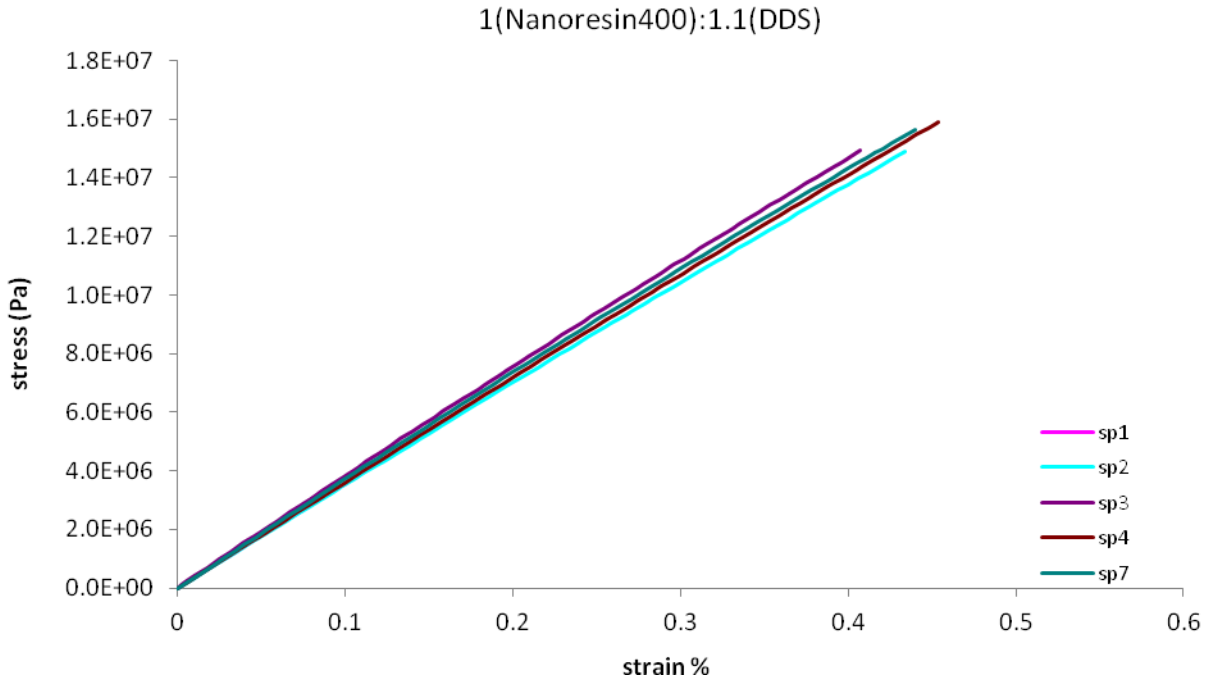

Summary of tensile testing for Nanopox F 400 resin cured with DDS at an N-H/epoxy molar ratio 0.9:1.

sample	Modulus, E (GPa)	strain to failure, ε_u (%)	stress at break, σ_u (MPa)
1	3.43	2.12	48.07
2	3.40	2.46	54.73
3	3.74	1.32	41.57
4	3.47	2.22	55.04
7	3.58	2.15	37.88
Ave	3.52	2.05	47.46
Std dev.	1.37	0.43	7.70
%RSD	3.89	20.98	16.22

APPENDIX E (continued)

Summary of stress-strain plot of Nanopox F 400 resin specimens cured with DDS curative at an N-H/epoxy molar ratio 1:1. (Sample specimens were stretched at a speed of 5 mm/min)

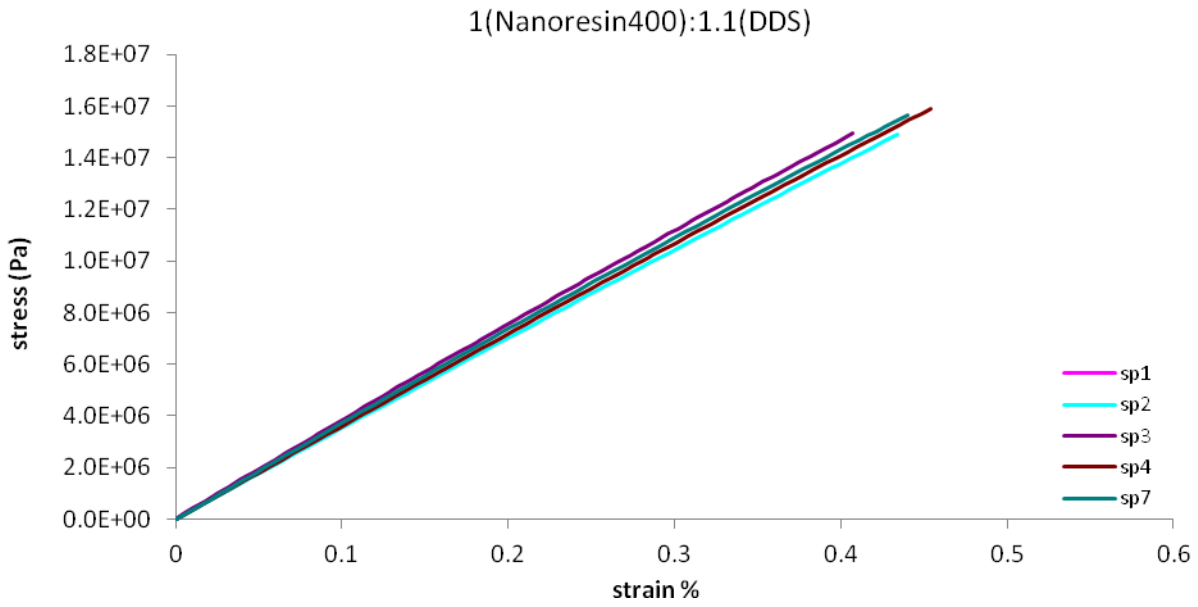

Summary of tensile testing for Nanopox F 400 resin cured with DDS at an N-H/epoxy molar ratio 1:1.

sample	Modulus, E (GPa)	strain to failure, ε_u (%)	Stress at break, σ_u (MPa)
1	3.691	2.03	58.49
6	3.705	2.06	54.05
7	4.094	2.13	64.87
8	4.056	1.72	48.20
9	3.611	2.26	57.85
Ave	3.831	2.04	56.69
Std dev.	2.25	0.20	6.14
%RSD	5.88	9.81	10.83